VACCINIA VIRUS BINDING AND INFECTION OF PRIMARY HUMAN LEUKOCYTES

Daniel James Byrd

Submitted to the faculty of the University Graduate School
in partial fulfillment of the requirements
for the degree
Doctor of Philosophy
in the Department of Microbiology and Immunology,
Indiana University

March 2014

Accepted by the Graduate Faculty, of Indiana University, in partial fulfillment of the requirements for the degree of Doctor of Philosophy.

_____
Andy Qigui Yu, Ph.D., Chair

_____
Randy R. Brutkiewicz, Ph.D.

Doctoral Committee

_____
Kenneth G. Cornetta, M.D.

January 13, 2014

_____
Mark H. Kaplan, Ph.D.

DEDICATION

I would like to dedicate this work to my family for their constant support, and for raising me to always stay curious.

ACKNOWLEDGEMENT

I would like to thank Dr. Andy Yu for taking me as his first graduate student at IU, and allowing me to have a high amount of freedom in my work although it led to many dead ends. I would also like to thank my committee members Dr. Randy Brutkiewitz, Dr. Kenneth Cornetta, and Dr. Mark Kaplan for donating your time and ideas helping me these past 5 years. You kept my goals realistic but also gave me plenty of room for creativity. Also, I would like to thank Dr. Janice Blum for her scientific guidance and career advice.

Thank you all for your invaluable service.

Daniel James Byrd

VACCINIA VIRUS BINDING AND INFECTION OF PRIMARY HUMAN LEUKOCYTES

Vaccinia virus (VV) is the prototypical member of the orthopoxvirus genus of the *Poxviridae* family, and is currently being evaluated as a vector for vaccine development and cancer cell-targeting therapy. Despite the importance of studying poxvirus effects on the human immune system, reports of the direct interactions between poxviruses and primary human leukocytes (PHLs) are limited. We studied the specific molecular events that determine the VV tropism for major PHL subsets including monocytes, B cells, neutrophils, NK cells, and T cells. We found that VV exhibited an extremely strong bias towards binding and infecting monocytes among PHLs. VV binding strongly co-localized with lipid rafts on the surface of these cell types, even when lipid rafts were relocated to the cell uropods upon cell polarization. In humans, monocytic and professional antigen-presenting cells (APCs) have so far only been reported to exhibit abortive infections with VV. We found that monocyte-derived macrophages (MDMs), including granulocyte macrophage colony-stimulating factor (GM-CSF)-polarized M1 and macrophage colony-stimulating factor (M-CSF)-polarized M2, were permissive to VV replication. The majority of virions produced in MDMs were extracellular enveloped virions (EEV). Visualization of infected MDMs revealed the formation of VV factories, actin tails, virion-associated branching structures and cell linkages, indicating that infected MDMs are able to initiate *de novo*

synthesis of viral DNA and promote virus release. Classical activation of MDMs by LPS plus IFN-γ stimulation caused no effect on VV replication, whereas alternative activation of MDMs by IL-10 or LPS plus IL-1β treatment significantly decreased VV production. The IL-10-mediated suppression of VV replication was largely due to STAT3 activation, as a STAT3 inhibitor restored virus production to levels observed without IL-10 stimulation. In conclusion, our data indicate that PHL subsets express and share VV protein receptors enriched in lipid rafts. We also demonstrate that primary human macrophages are permissive to VV replication. After infection, MDMs produced EEV for long-range dissemination and also form structures associated with virions which may contribute to cell-cell spread.

Andy Qigui Yu, Ph.D., Chair

TABLE OF CONTENTS

LIST OF TABLES

LIST OF FIGURES

LIST OF ABBREVIATIONS

Ab	Antibody
ActT	Activated T cell
AD	Atopic dermatitis
APC	Allophycocyanin
Akt	Protein kinase B
Arg1	Arginase 1
CCR5	C-C chemokine receptor type 5
CD	Cluster of differentiation
CEV	Cell-associated enveloped virus
CME	Crude membrane extract
CsCl	Cesium chloride
CTB	Cholera toxin subunit B
Cu	Cucurbitacin I
CXCR4	C-X-C chemokine receptor type 4
DC-SIGN	Dendritic Cell-Specific Intercellular adhesion molecule-3-Grabbing Non-integrin
DMSO	Dimethyl sulfoxide
DNA	Deoxyribonucleic acid
DRM	Detergent-resistant membrane
EEV	Extracellular enveloped virus
EGFP	Enhanced green fluorescent protein

ELISA	Enzyme-linked immunosorbent assay
ER	Endoplasmic reticulum
EV	Eczema vaccinatum
FACS	Fluorescence-activated cell sorting
FBS	Fetal bovine serum
FITC	Fluorescein isothyocyanate
fNLPNTL	*formyl*-L-norleucyl-L-leucyl-L-phenylalanyl-L-norleucyl-L-tyrosyl-L-lysine
GM-CSF	Granulocyte-macrophage colony-stimulating factor
GM1	Ganglioside M1
GPI	Glycosylphosphatidylinositol
HIV-1	Human immunodeficiency virus 1
HNL	Human neutrophil lipocalin
h	Hour(s)
hpi	Hours post-infection
HPV	Human papillomavirus
HRP	Horseradish peroxidase
HS	Heparan sulfate
HSV	Herpes simplex virus
ICAM-2	Intercellular adhesion molecule 2
ICS	Intracellular staining
IFN-γ	Interferon gamma
IgG	Immunoglobulin G

IL	Interleukin
IMV	Intracellular mature virus
JAK	Janus kinase
JNK	c-Jun N-terminal kinase
LPS	Lipopolysaccharide
mAb	Monoclonal antibody
MAPK	Mitogen-activated protein kinase
M-CSF	Monocyte colony-stimulating factor
MDM	Monocyte-derived macrophage
MERS-CoV	Middle East respiratory syndrome coronavirus
MFI	Mean fluorescence intensity
MOI	Multiplicity of infection
Mono	Monocyte
MV	Mature virus
NK cell	Natural Killer cell
ORF	Open reading frame
pAb	Polyclonal antibody
PBMC	Peripheral blood mononuclear cell(s)
PBS	Phosphate-buffered saline
PCR	Polymerase chain reaction
PE	Phycoerythrin
PerCP	Peridinin chlorophyll
PFA	Paraformaldehyde

PFU	Plaque-forming unit
PHL	Primary human leukocyte(s)
PI3K	Phosphatidylinositol (3) kinase
PKR	Protein kinase R
PMA	Phorbol 12-myristate 13-acetate
Pre	Pre-immune serum
ResT	Resting T cell
rh	Recombinant human
RNA	Ribonucleic acid
RPMI-1640	Roswell Park Memorial Institute 1640 medium
RT-PCR	Reverse transcription polymerase chain reaction
SAPK	Stress-activated protein kinase
SARS-CoV	Severe acute respiratory syndrome coronavirus
SDF-1	Stromal cell-derived factor 1
siRNA	Small interfering ribonucleic acid
Sup	Supernatant
STAT	Signal-transducer and activator of transcription
SV-40	Simian virus 40
W	Whole cells
WR	Western Reserve
YFP	Yellow fluorescent protein

Chapter I - Introduction

Virus tropism

Rapid advances in the last century have considerably reduced mortality due to infectious diseases. This was mainly achieved by scientific advancement in the treatment and control of infections leading to the introduction of antibiotics and vaccines. Despite such advances, emerging or re-emerging pathogens remain as a primary concern for global healthcare (1). The treatment of viral diseases has mostly depended on the development of vaccines and updated medical practices as the development of anti-viral drugs has progressed relatively slower than antibiotics. Most emerging pathogens of particular worry are viruses and include several virus families: bunyaviruses (hantavirus, Rift Valley), coronaviruses (SARS-CoV, MERS-CoV), filoviruses (Ebola, Marburg), flaviviruses (Dengue, hepatitis C, West Nile), poxviruses (monkeypox), and retroviruses (HIV-1) (1). The emergence of a virus as an agent of human disease usually involves the transfer from another species, called zoonosis. The possibility of viral zoonosis occurring is determined by the host tropism of the virus which can be described at the micro and macro levels.

Viral tropism can be viewed as having a three-tiered barrier: cellular specificity, tissue specificity, and the host response to infection (2). At the cellular level, virus replication for certain cell types of certain species can either be abortive, meaning failure to replicate, or permissive, meaning success in infection and replication. The permissiveness of a cell to virus infection can be examined

by success or failure at any stage of the virus life cycle, including binding, entry, capsid uncoating, nucleic acid replication, particle assembly, and release. Virus tropism at the level of tissues is influenced by cellular tropism, but is also determined by tissue-specific anti-viral responses. This level is largely dependent on the patterns of virus distribution and dissemination within an organism. Tropism at the level of whole organisms is largely influenced by the first two levels and is defined by the possible range of effects from viral pathogenesis, symptoms of disease, and the ability to infect other individuals. This level defines whether a whole species supports permissive or abortive infections. Certain species may also be reservoir hosts that can be infected, avoid any overt pathogenesis, but still lead to the infection of other individuals or support zoonosis. These three levels of viral tropism determine the permissiveness of a species to a virus, and can be used to describe in detail why a virus causes disease.

All viruses are obligate intracellular infectious agents and require specific host factors on the surface and within cells to replicate and spread to other cells. For viruses that infect large multicellular organisms, it is most likely that only particular cell types or tissues contain these necessary factors. In general, all viruses must bind to their receptors on the surface of target cells to initiate infection. Viruses must then induce the entry of the virus particles either by membrane fusion if it has a lipid envelope, or by some form of endocytosis for both enveloped and non-enveloped viruses. For example, the HIV-1 virus envelope protein gp120 requires the host T cell CD4 as a receptor, along with

CXCR4 or CCR5 as a co-receptor to be able to bind to cells and initiate fusion of the virus envelope with the host cell membrane. Often, membrane fusion occurs via the induction of low pH environments as with endosomes containing virus particles that are endocytosed. For example, the influenza envelope protein hemagglutinin (HA) binds to sialic acid (3) or DC-SIGN (Dendritic Cell-Specific Intercellular adhesion molecule-3-Grabbing Non-integrin) (4) on the host cell surface to induce endocytosis of the virus particle. As the vesicle containing influenza particles converts to an endosome, the pH drops which activates the fusion activity of HA, releasing the capsid into the cytoplasm. However, HIV-1 and other retroviruses rely on pH-independent route of entry. Once a virus enters the cell cytoplasm, the virus capsid degrades and specific intracellular host factors must be present to complete each stage of the virus life cycle. Virus replication often requires host polymerases, chromosomes, translational machinery, kinases, cytoskeletal structures, and motor proteins. Thus, virus-receptor interactions, induction of entry, and intracellular factors influence the susceptibility of cell types and can all therefore constitute interspecies barriers.

Poxvirus tropism

Poxviruses are a family of large, complex, enveloped DNA viruses that show a wide range of species specificities (2, 5), and are known to infect invertebrates and vertebrates including fish, reptiles, birds, and mammals. The sub-family *Chordopoxvirinae* specifically infects vertebrates and includes four genera that infect humans. One of the genera in this sub-family, *Orthopoxviridae*,

is mammal-specific. The orthopoxviruses all have approximately 200 genes, are morphologically indistinguishable, and include virus species such as variola major, vaccinia, cowpox, monkeypox, and camelpox. Variola virus is the causative agent of smallpox, a disease which has likely killed more people than any other pathogen in human history (2), with a mortality rate of around 30% (6). Vaccination against variola was undertaken beginning in the 18th century using the live or attenuated orthopoxvirus cowpox. Because of the extreme sequence similarity between orthopoxviruses and the relatively slow rate of mutation, cross-protection against many orthopoxviruses can be induced upon vaccination with another virus species from the genus. Vaccinia and cowpox were chosen as live vaccines for smallpox because of the relatively benign symptoms following percutaneous infection and the near certainty of acquired immunity developed against smallpox. In the 20th century, a global vaccination campaign using attenuated vaccinia strains led to the complete eradication of smallpox by 1979, ending millennia of terror from a disease which had killed hundreds of millions of people since its emergence before the beginning of human history (6). Thus, smallpox is eradicated, but many lessons can be learned from the disease related to fighting current outbreaks or preventing the emergence of new deadly pathogens.

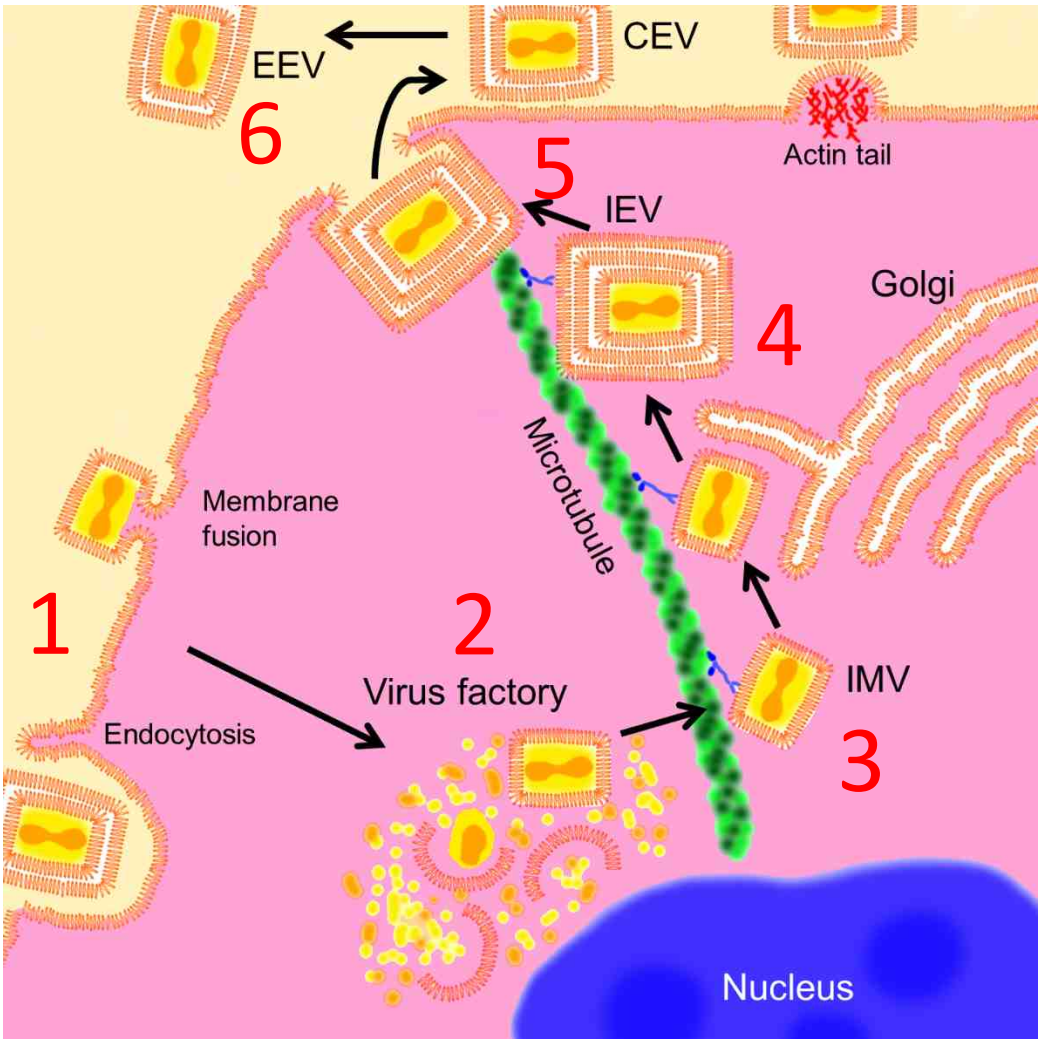

Fig. 1. Overview of poxvirus morphogenesis. General steps following the formation of a mature extracellular poxvirus virion. 1) Virus binding and envelope fusion. 2) Juxta-nuclear virus factory formation. 3) IMV formation and migration on microtubules. 4) Wrapping of trans Golgi membrane to form IEV. 5) Fusion of outer envelope to produce CEV. 6) Detachment from the cell surface to produce a free-floating EEV particle.

Cellular tropism for orthopoxviruses, like all viruses, can be examined by the success or failure at every stage of the virus life cycle in the cell (Fig. 1). Orthopoxviruses first bind to host cell receptors and initiate entry either by fusion to the cell surface, or endocytosis followed by fusion to the vesicle membrane. The virus capsid then degrades or “uncoats” and genes with early promoters are transcribed which mainly code for factors used in viral DNA replication. Poxviruses are unique among DNA-based viruses because they undergo DNA replication entirely in the cytoplasm rather than the nucleus. Eventually a “virus factory” forms where a section of the rough endoplasmic reticulum is converted into a structure for assembling virus particles (7). Virions first exist as single enveloped “intracellular mature virions” (IMV) and are transported along microtubules (8). Some IMVs are wrapped in a double membrane originating from the Golgi apparatus containing unique viral envelope proteins which is then referred to as the triple-enveloped “intracellular enveloped virion” (IEV) (8). Via microtubules, the IEV is brought to the cell surface membrane where the outer virus envelope fuses to the cell surface, thereby secreting a double-membraned virion out of the cell. The virion will then stay attached to the cell surface, called the “cell-associated virion” (CEV), until various mechanisms are used to release the virion from the cell (9, 10). CEVs often remain on the cell surface and are launched away from the cell via polymerization of intracellular actin to contact neighboring cells (11). The final, free-floating form is referred to as the “extracellular enveloped virus” (EEV), and is considered the main mediator for

long range infections within a host. These actin tails are formed via signaling from viral envelope proteins on the cell surface (10).

Despite the high sequence similarity of orthopoxviruses, stringent host species tropisms exist between the virus species, i.e., variola virus is a strict human-specific pathogen that causes smallpox in humans only (2), and myxoma virus is a rabbit-specific poxvirus that causes a lethal disease (myxomatosis) in rabbits only (2, 5). The genomes of most of the known orthopoxviruses have been sequenced, and while many genes are highly conserved between the different viral species and are essential for infection (12), divergent genes exist, called “host range genes,” and have been used to explain certain characteristics of the restrictive host tropisms. Host range genes were first identified in poxviruses by spontaneous deletions from viruses in culture, whereas many more were discovered later by targeted viral gene recombination. Most of these deletions or knockouts were tested in cell lines to show a loss of infectivity for certain cell types. The first host range genes for poxviruses were discovered from cultured vaccinia virus (VV) that developed spontaneous deletions in the K1L and C7L genes and, although able to transcribe some viral genes, these viruses lost the ability to replicate in human cells (13). Among many other host range genes, the best categorized are the E3L and K3L genes in VV. Double-stranded RNA (dsRNA) is a common product from viral infection in eukaryotic cells, and host immune responses have evolved to sense dsRNA to initiate innate immunity (14). In humans, dsRNA is first detected by PKR which activates the interferon response and induces apoptosis. Viruses have evolved many strategies to hide

dsRNA, and VV has developed ways to surround its dsRNA with E3L to directly block host PKR or create a decoy substrate with K3L to inhibit PKR (15). When E3L and K3L are deleted in VV, they show reduced rates of infectivity in different cells lines specific for cell lines from particular species (15).

Poxvirus binding

Despite the advances in understanding poxvirus cellular tropism using cells lines, much remains unknown concerning host species specificity. For instance, variola major is particularly deadly in humans and is thought to have never naturally crossed into another species. Meanwhile, the main host for the myxoma virus is the brush rabbit, where only mild symptoms are induced, but myxoma can also infect the European rabbit usually causing fatal disease. The precise molecular basis underlying the strict species barriers for poxviruses remains unclear which may reflect the lack of knowledge in many facets of the basic virology of poxviruses . In particular, no specific cellular receptor for any poxvirus has yet been identified; however, several ubiquitous carbohydrate-based molecules have been suggested as receptors for VV. The first discovered were heparin sulfate (HS) and chondroitin sulfate (CS). Both are complex, highly negatively charged unbranched polysaccharides called glycosaminoglycans (GAGs) that are associated with numerous membrane proteins, including collagen in the extracellular matrix. The VV envelope protein A27L and H3L, previously associated with virus entry, was found to bind cell surface HS, as soluble HS reduced VV binding to cells and virions were found to bind to HS-

coated beads (16). The VV envelope protein D8L binds to cell surface chondroitin sulfate in a similar manner (17). Apart from GAGs, VV was also found to bind to the ubiquitous extracellular matrix laminins, which are complexes of glycoproteins with many functional isotypes (18). However, different lines of evidence suggest that GAG-independent receptors exist for VV. The VV envelope protein L1R was shown to be crucial for entry into cell lines as anti-L1R antibodies blocked virus entry into cells and soluble L1R pretreatment could block entry (19). Interestingly, L1R was shown to bind to cells that were negative for GAGs (19). Additionally, recent work examining primary human leukocytes has strongly suggested a GAG-independent, protein-mediated poxvirus receptor on the surfaces of these cell types. Additional notions have been raised of the existence of potentially GAG-independent VV receptors as VV binding and entry in cell lines has been demonstrated to be highly dependent on specific areas of the cell membrane called lipid rafts.

The raft hypothesis

The cell membrane is composed of hundreds of types of lipids. The organization of the cell membrane was slowly elucidated in the last century, culminating in the development of the fluid mosaic model by Singer and Nicholson (20). From freeze-fracture electron microscopy, the cell membrane was found to be an ocean of lipids with proteins embedded either into the membrane or bound peripherally. The fluid mosaic model presented a picture of cell membranes as an equalizing solvent with no long term membrane

organization, rather than having a relatively permanent crystalline structure. However, through observations of epithelial cell layers it was found that cell membranes on the apical and basolateral cell surfaces had distinct lipid and protein components, and that transport of proteins into these different domains involved vesicles with different components which used special sorting systems (21). Apical domains on cells were found to be enriched in cholesterol, sphingolipids and sphingomyelin, whereas basolateral surfaces had more phosphatidylcholine (21). Observations of virus budding were also key in identifying the components of these membrane domains, where viruses such as influenza (22) that bud from the apical membrane tended to have sphingolipids and sphingomyelin, whereas viruses such as vesicular stomatis virus (23) that bud from the basolateral surfaces contained more phosphatidylcholine. Other than the apical surface of epithelial cells, smaller cholesterol and sphingolipid-rich regions on cells have also been identified such as caveolae which are small invaginations in the cell membrane important for certain types of endocytosis.

A further indication of the segregation of cell membrane domains is the behavior of glycosylphosphatidylinositol (GPI)-anchored membrane proteins. Rather than having a transmembrane domain like most surface membrane proteins, GPI-anchored proteins are peripherally bound to the membrane surface via a carbohydrate linkage with phosphatidylinositol. It was found that GPI-proteins specifically trafficked only to the apical side of epithelial cells (24), and as such, were found on viruses that bud from apical surfaces (25). The existence of unique membrane domains was further suggested by the differential

insolubility of cell membranes. Certain methods to extract cell membranes using non-ionic detergents were found to produce an insoluble material easily separable from detergent-soluble material by density gradients. Analysis of the material, called “detergent-resistant membrane” (DRM), found that it was enriched in components specific for the apical surface of epithelial cells, namely: sphingolipids, sphingomyelin, cholesterol, and GPI-anchored proteins (26, 27).

Thus, in slight opposition to the classic fluid mosaic model, a “raft hypothesis” has developed describing cell membranes as having separate domains that aggregate particular components which are critical for cellular membrane functions. Based on the above observations, an operational definition of membrane lipid rafts was proposed to be areas of the membrane that: 1) have high sphingolipids, sphingomyelin, cholesterol, and GPI-linked proteins; 2) can be specifically enriched with cold non-ionic detergent extractions; and 3) have functions that are inhibited via the disruption of cellular cholesterol. Rafts are thought to be involved in nearly every function associated with membrane structure, including: surface protein organization, cell motility, cell cycle control, antigen presentation, phagocytosis, nutrient uptake, and virus budding and entry. Many of the factors located specifically in DRMs, such as integrins (28) and IgE receptors (29), are known to become activated by cross-linking on the cell surface, a process that only happens once they enter the dense environment created by membrane rafts.

Lipid rafts and virus entry

Because lipid rafts play a major role in organizing the cell surface membrane, it is not surprising that rafts are found to be crucial for the success of the virus life cycle at various stages for several viruses. Numerous studies have found the importance of rafts in viral binding, entry, assembly, and budding, by showing the localization of viral components in rafts and by disrupting rafts to see inhibitions to virus infection (30). Cholesterol is crucial to maintain the organization of all lipid raft-associated structures, and removing it from the cell or inhibiting its production leads to the dissolution of lipid rafts on the cell surface, and thus, can be a useful tool to study the importance of rafts in various conditions. Removing cholesterol can be achieved by treating cells with cyclodextrin, a membrane-permeable small molecule that binds to cholesterol and pulls it out of the cell membrane. This condition can be rescued by adding cholesterol back into the cells using cholesterol-embedded liposomes. Cholesterol synthesis can also be inhibited with pharmacological methods such as with statins to study raft formation. Using these tools, intact lipid rafts were found to be essential for the entry of non-enveloped viruses: adenovirus, Coxsackievirus, echovirus, enterovirus, human papillomavirus (HPV), rotavirus, and simian virus 40 (SV40); as well as enveloped viruses: Ebola virus, Epstein Barr virus, Hepatitis C virus, herpes simplex virus-1, HIV-1, influenza, VV, and SARS.

Lipid rafts were found to be crucial for the entry of many viruses. Many routes of endocytosis for viruses in eukaryotic cells have been investigated, such

as clathrin-mediated entry, phagocytosis, and macropinocytosis, but a special route involving raft-enriched caveolae has also been identified. Caveolae are lipid rafts on the cell surface that form small invaginations and have a constant recycling of membrane components. The internalized membrane from caveolae form special compartments called “caveosomes” and can be specifically stained inside the cell to observe any associations with other factors. Viruses that specifically bind to rafts in caveolae can take advantage of this recycling system to enter the cell. This process is sensitive to cholesterol depletion, and is inhibited by the knockdown of dynamin-1, or caveolin-1, a raft-specific surface protein. SV-40, HPV, echovirus, coronaviruses, and other viruses are known to take advantage of caveolae-dependent endocytosis. Echovirus uses CD55, a GPI-anchored raft-enriched host protein as a cell receptor, whose binding induces caveolin and raft-dependent endocytosis (31, 32). Similarly, coronaviruses bind to raft-specific CD13 which induces caveolin-dependent endocytosis (33). However, virus receptors need not always be raft specific to induce this pathway. SV-40 binds to MHC-I on the cell surface which is not raft-specific, but the binding itself causes MHC-I to localize with caveolin-1 which then induces endocytosis (34, 35).

Caveolae are only a part of the ways lipid rafts are structured on the cell surface, and virus entry has been associated with rafts while also being caveolin-independent. The receptor for HIV-1 is CD4 along with co-receptors CCR5 or CXCR4. While CD4 usually exists inside lipid rafts, in T cells CCR5 and CXCR4 do not. It was found that for HIV-1 entry into macrophages, however, intact lipid

rafts and the raft-localization of CXCR4 is a requirement (36, 37). Lipid rafts not only play a role in entry, but also in virus budding. HIV-1 has evolved to take advantage of the ability of lipid rafts to form unique platforms too aggregate specific components by localizing envelope proteins in rafts along with other host components advantageous to the virus(25). Thus, when viral components are collected at the membrane surface, viral envelope proteins induce budding while taking with it host lipid raft proteins (38). Host lipid rafts contain the GPI-anchored proteins CD55 and CD59 which are crucial regulators of host complement activation that also resists the effects of the complement system on the HIV-1 particle (39). Although most studies of lipid rafts focus on their influence on the cell surface membrane, lipid raft and associated components recycle into the cell and form a unique membrane environment among intracellular organelles. This unique environment is also thought to be critical to intracellular virus assembly at certain stages (30).

Lipid rafts and poxviruses

It has been found that the VV envelope proteins A14, A17, and D8L localize to detergent-resistant fractions within 30 mins after the virus entry into HeLa cells (40). This indicates that VV entry may be related to lipid rafts as viral envelope proteins quickly enter host lipid rafts once the envelope has fused. The same study found that VV entry into HeLa cells was dependent on intact lipid rafts as cholesterol depletion with methyl-β-cyclodextrin (mβCD) greatly inhibited entry in a HS-independent manner (40). VV entry was also caveolin-independent

suggesting that the caveolae recycling pathway was not involved. Considering the raft-association with VV entry and the recent reports of VV receptors on primary human leukocytes, we hypothesized that unique protein receptors for VV may exist on primary human leukocytes enriched in lipid rafts.

Poxvirus replication and interactions with monocytic cells

Poxviruses infect a wide array of organs and tissues, but usually depend on infection of the skin and mucosal tissues for propagation and dissemination. In nature, variola virus has a strict human-specific tropism and non-human reservoirs of the virus have never been found. Variola virus transmission via inhalation is followed by infection and replication in epithelial cells of the oral and respiratory mucosa (41). The subsequent stages of infection involve viral infiltration of lymphoid organs accompanied by strong viremia and skin lesions. In an attempt to develop an animal model of smallpox, recent studies using high doses of variola virus to infect *Cynomolgus macaques* have demonstrated that infected animals develop systemic infection and hemorrhagic symptoms, therefore replicating smallpox disease in humans (42, 43). In infected macaques, variola virus could not be isolated from plasma, but was found to be associated with blood monocytes implicating that monocytes serve as an important means of virus transportation via viremia (42). Additionally, through immunofluorescent staining, infected monocytic cells in macaques were found carrying virus antigens into organs that later erupted in lesions (42). In the macaque infection model it was also found that virus trafficking via monocytic cells was correlated

with increased severity of disease (43). Given their importance in defense against invading pathogens, monocytic cells may act as a double-edged sword in variola virus infection by mediating both infection control and virus dissemination.

VV has a genome 95% homologous to variola virus (19) which reflects its extreme antigenic similarity. Similar to variola virus but without the overt pathogenesis, VV can produce a generalized infection which involves EEV viremia with subsequent infection of distant sites on the skin (8). Additionally, CEV can rapidly transfer between neighboring cells in culture via actin tails (11), but the precise routes of long-range dissemination via viremia are unknown. Visualizations of VV skin lesions in mice have shown that highly motile infected macrophages are adjacent to infected skin foci (44). Extraction and analysis of these macrophages have revealed that the cells are permissively infected, and are associated with 7% of the total VV in the lesion (44). Thus, macrophages have been exhibited in mammals as potential candidates for mediating long-range VV dissemination. Among studies of VV infection of primary human macrophages, one report has demonstrated that the infection is abortive, as the cells only support early stages of the VV infection cycle, including morphologic cytopathic effects, deactivation of host cell protein synthesis, and activation of early viral protein synthesis; but not infection in late stages, including synthesis of late viral proteins, replication of viral DNA, and production of infectious viral progeny (45). VV infection of primary human monocytes and dendritic cells (DCs) has also been demonstrated to be abortive *in vivo* and *in vitro* (46-52); here, viral DNA is only weakly replicated, no late genes are transcribed, and no actin tails or

viral factories form. Hence, it has been speculated that, in humans, VV cannot replicate in monocytic cells including monocytes, macrophages and DCs.

Summary of findings

In this report, the binding and infection of VV in *ex vivo* human leukocytes is profiled. Among all cell types observed, VV was able to bind to monocytes, B cells, activated T cells, and neutrophils, but not resting T cells. This binding was mediated by protein receptors on the cell surface which are enriched in lipid rafts for all susceptible cell types. Although a specific protein receptor has not been identified yet, a list of putative receptors was made via deductions from raft-associated proteins matched with expression data for each cell type. Only monocytic cells were able to express virus genes to a significant degree, and this observation holds true for *in vitro* monocyte-derived macrophages. Macrophages are observed *in vivo* as being a significant source of VV antigen staining. Previously, among primary human leukocytes, activated T cells were the only cell type known to support VV replication. This report reveals that *in vitro* monocyte derived macrophages are permissive to VV. This permissiveness persisted during many different macrophage activation states, but was sensitive to M2b (LPS plus IL-1β) and M2c (IL-10) activation.

Chapter II - Research Goals

Poxvirus binding and infection of leukocytes

Poxviruses are currently being tested as vaccine vectors for HIV-1 prevention (53) and as cancer cell-targeted therapies (54, 55). Despite the importance of studying poxvirus effects on the human immune system, reports of the direct interactions between poxviruses and PHLs are limited. When used as a vaccine vector, the efficacy of the vaccine depends on the dynamics of the immune response to the virus. Approaches to use poxviruses as cancer therapies have focused on the immunomodulation potential of the virus by engineering it to focus the immune response against tumors. Indeed, even though both of these therapies depend entirely on the immune system, there are few studies analyzing specific interactions of poxvirus with primary human cells. Greater knowledge of these interactions will no doubt aid in engineering poxviruses to provide improved immunogenicity and greater honing of the immune response against cancer cells.

Poxviruses infect a wide variety of cell lines in culture, leading to the presumption that specific receptors for these viruses may not be required, or that conserved and ubiquitous receptors may be widely distributed on the surface of diverse cell types (2). These conjectures may have impeded attempts to identify cellular receptors that mediate poxvirus binding and infection. However, recent reports have shown that VV and canarypox virus (ALVAC) do not indiscriminately infect all cell types of primary human hematopoietic cells they encounter, but

instead demonstrate an extremely strong preference for infection of monocyte-lineage cells among peripheral blood mononuclear cells (PBMCs) (56-58). Significantly, expression of VV receptor(s) can be induced *de novo* on primary human T cells upon T cell activation (56). As a consequence, activated T cells become susceptible to VV binding, infection, and replication. In contrast, resting T cells are not susceptible to VV binding or infection. These receptors are likely proteins because inhibitors of transcription (actinomycin D), protein synthesis (cycloheximide), and intracellular protein transport (brefeldin A) significantly reduce VV binding to activated primary human T cells, and also treatment of primary human monocytes or activated T cells with trypsin or pronase diminishes VV binding and infection (56).

Poxviruses not only bind to and infect monocytes but also use these cells to initiate a systematic infection. A recent report using high doses of variola virus, the most virulent member of the poxvirus family, to infect *Cynomolgus macaques* in an attempt to develop an animal model of smallpox has demonstrated that variola virus is disseminated by means of monocytic cell-associated viremia (42). This suggests that monocytes play a significant role in the initiation of systematic infection. Monocytes may use putative viral receptors to collect infectious variola virus particles and then disseminate them to uninfected cells and tissues, resulting in a generalized infection. However, the specific molecular events that determine poxvirus bias towards monocyte binding and infection remain unclear. In this work, we investigated the susceptibility of major subsets of primary human leukocytes (PHLs) to VV binding and infection. We show that PHL subsets

express and share protein VV receptors on the cytoplasmic membrane, and that VV receptors are induced *de novo* on certain but not all PHL subsets.

VV binding and lipid rafts

The finding that VV entry into HeLa cells in dependent on intact lipid rafts presents questions to other facets of VV infection. It is suggestive that since these specialized areas of the cell membrane are required for entry, they likely contain factors such as binding receptors to direct virions to these areas for entry to take place. Thus, we hypothesize that VV receptors are enriched in host cell surface lipid rafts. Primary human cells are, so far, the only cell types to demonstrate a clear distinction in the behaviors of VV binding in terms of *de novo* synthesis of a protein receptor. VV cannot bind to *ex vivo* human peripheral T cells other than in trace amounts, but upon T cell activation with anti-CD3 and anti-CD28 antibodies, the cells become highly susceptible to binding (56). Therefore, this system is advantageous in hunting for unique VV receptors, which have not been discovered to date, and is suitable to test our hypothesis that VV preferentially binds to factors in lipid rafts. In this study, we used cholera toxin subunit B (CTB) as a marker for membrane rafts. The cholera toxin binds to host cell surface ganglioside M1 (GM1), which is known to be a component of detergent-resistant membranes. CTB was found to be highly colocalized in all VV binding-susceptible leukocytes previously tested. We therefore proceeded to verify the presence of VV receptors in rafts by reshaping rafts to observe the VV binding response and by attempting to block with DRM-derived mouse serum.

VV replication in primary human macrophages

Macrophages are found in tissues throughout the body in most organs. These tissue macrophages are mainly derived from circulating monocytes, but are difficult to collect and study. To obtain macrophages, researchers have developed several approaches to differentiate primary blood monocytes by incubating them with (1) media containing human AB or fetal bovine serum (FBS) (59), (2) media containing FBS supplemented with GM-CSF or M-CSF (60, 61), or (3) conditional serum-free media with or without GM-CSF or M-CSF (62, 63). These different methods for MDM generation have not been systematically related to one another functionally or transcriptionally. GM-CSF-induced MDMs replicate some of the functions and transcriptional profiles of classically activated pro-inflammatory (M1) cells *in vivo*, whereas M-CSF-induced MDMs are more like alternatively activated anti-inflammatory (M2) macrophages (64). Gene expression profile studies of murine M2 cells have found some common expression of genes between M2 cells generated *in vitro* and M2 cells from *in vivo* disease models (65, 66). *In vitro* M1 and M2 macrophages largely mirror the functional phenotypes of macrophages *in vivo* in allergy, parasitic infections, and certain cancers (67), but other pathological conditions such as neurodegenerative diseases express unique macrophage phenotypes. In contrast, human AB serum-derived MDMs have so far not been related to particular states *in vivo.* Here we report that both M1- and M2-polarized macrophages are permissive for VV infection and replication, whereas human AB serum-derived MDMs could be infected, but were abortive as reported previously

(45). Infected M1 and M2 MDMs mainly produced EEV and exhibited virion-associated structures that may promote virus spread to neighboring cells. VV replication was found to be dependent on known poxvirus-associated signaling pathways, and the activation of STAT3 was strongly inhibitory to virus production.

These results provide critical information to the burgeoning fields of cancer-killing (oncolytic) virus therapy with VV. Recent successful clinical trials using VV engineered to be cancer cell-specific have demonstrated the potential for VV as an oncolytic agent, particularly as a platform for various immune therapies for cancer (68-71). M2 macrophages are considered a common presence in tumors and are associated with poor prognosis. These results demonstrate a preference for VV replication in M2 macrophages, and could assist in designing treatments and engineering poxviruses with special considerations for their effect on M1 vs. M2 macrophages. Macrophages may not only be a target for oncolytic therapy, but also as a delivery medium. Macrophage-based delivery of oncolytic adenovirus was previously demonstrated to be more effective at tumor reduction than virus alone (72). Our findings are also uniquely relevant for oncolytic VV therapy because the level of EEV in a tumor was highly correlated to effectiveness of treatment (73). We have observed that infected MDMs produce predominantly EEV after 2 days of infection. Therefore, this work highlights macrophages as highly relevant to VV oncolytic therapy whether in terms of residents in a tumor or vehicles for delivery.

This work also highlights the importance of macrophages in the design of vaccines using poxvirus vectors. The understanding of the dynamics of poxvirus-

infected foci is central in understanding the effectiveness of the immune response to poxvirus-mediated vaccine vectors. The high CD8 T cell response of poxvirus vaccines makes them particularly promising as a vaccine vector against viral diseases (74). Monocytic cells have been found to be an important part of vaccinia skin lesions in mice in controlling the infection as well as mediating virus transport out of infected foci (44). VV infected foci are surrounded by monocytic cells that are heavily stained with virus antigen. It was observed that monocytic cells uptake virus around the foci while CD8 cells target and kill infected monocytes (44). Thus, monocytic cells likely play an essential role in the immunogenicity of poxvirus-based vaccines.

Chapter III - Materials and methods

Cytokines, antibodies, and flow cytometric analysis

The following anti-human monoclonal antibodies (mAbs) or polyclonal Abs (pAbs) conjugated with fluorochrome were purchased from BD PharMingen (San Diego, CA): anti-CD3^{APC}, anti-CD4^{PerCP}, anti-CD8^{PE}, anti-CD14^{APC}, anti-CD19^{PE}, anti-CD56^{PE}, and matched-isotype control Abs conjugated with FITC, PE, PerCP, or APC. Anti-human neutrophil lipocalin (HNL) (pAbs) were purchased from Novus Biologicals (Littleton, CO) (cat. # NBP1-45682) and anti-human CD66b^{PE} Ab (clone B1.1/CD66) were purchased from BD Biosciences (San Diego, CA) (cat# 333412), respectively. Rabbit pAbs against full-length human Integrin β-1 (CD29) were purchased from Abnova (Taipei, Taiwan) (cat# H00003688-D01P) and rabbit pAbs against human amino acid transporter SLC3A2 (CD98) were purchased from Thermo Fisher Scientific (Pittsburgh, PA) (cat# PA5-21547). Isolated PHL subsets including monocytes, B cells, T cells, neutrophils, and NK cells were subjected to VV binding and surface staining with different combinations of Abs, followed by flow cytometric analysis (FACS) using a BD FACSCalibur (BD Biosciences, San Diego, CA). Data were analyzed using FlowJo software (TreeStar, San Carlos, CA). Appropriate isotype controls were used at the same molarity as the test Abs and control staining was performed during every FACS. The following mouse anti-human monoclonal antibodies (MAbs) conjugated with fluorochromes were purchased from BioLegend: anti-CD68 (clone Y1/82A) conjugated with Alexa Fluor 488, anti-CD163 (clone

GHI/61) conjugated with PE, and anti-CD86 (clone IT2.2) conjugated with APC. For intracellular staining (ICS) of STAT3 activation or caspase-3, cells were fixed with 2% paraformaldehyde (PFA), permeabilized with 0.1% saponin, and stained with mouse anti-human Stat3 phospho-Tyr705 (clone 4/P-STAT3) conjugated with Alexa Fluor 647 or rabbit anti-human caspase-3 (active form) conjugated with FITC (BD Biosciences). Staining for apoptosis and necrosis with Annexin V-FITC plus propidium iodide (PI) was performed using the Annexin-V-FLUOS Staining Kit (Roche, Mannheim, Germany) according to the manufacturer's instructions.

The following recombinant human cytokines for cell culture were purchased from EMD Millipore (Darmstadt, Germany): rhIL-1β, rhIL-10, and rhIFN-γ. Recombinant hM-CSF and rhGM-CSF (carrier-free) were purchased from BioLegend (San Diego, CA). Ultrapure lipopolysaccharide (LPS) derived from *Salmonella minnesota* R595 was purchased from InvivoGen (San Diego, CA).

VV enrichment, titration, and infection protocols

The primary VV strain used in this study was Western Reserve (WR). The EGFP reporter virus "VV-EGFP" is a WR strain containing a chimeric gene including the influenza virus nucleoprotein, the ovalbumin SIINFEKL peptide, and enhanced green fluorescence protein (EGFP) that localizes to the nucleus (75). Both VV WR and VV-EGFP were obtained from Dr. Jonathan Yewdell (NIH, Bethesda, MD). vA5L-YFP is a recombinant WR VV constructed with the viral

core protein A5L fused to yellow fluorescence protein (YFP) suitable for visualizing individual virions (76) and obtained from Dr. Bernard Moss (NIH, Bethesda, MD). All viral stocks were generated and titrated in chicken embryo fibroblasts (Charles River Laboratories, Wilmington, MA) or the monkey kidney cell line CV-1 (ATCC, Manassas, VA) in complete RPMI-1640 (RPMI-1640 medium supplemented with 10% FBS, 2 mM L-glutamine, 100 U/ml penicillin, and 100 U/ml streptomycin). After 3 days of infection, cells were lysed in a dounce homogenizer. Culture supernatants and cell lysates were then subjected to ultracentrifugation at 25,000 g for 80 min through a 36% sucrose cushion. Pellets were resuspended and subjected to virus purification by ultracentrifugation through a 24 - 40% sucrose gradient as previously described (77). Viral titers were determined by a virus plaque assay. Briefly, CV-1 cells were grown in 6-well plates to 90% confluency and overlaid with various dilutions of purified virus. After 1 h of incubation, cells were washed and overlaid with complete RPMI-1640 containing 1.5% carboxylmethylcellulose to prevent *de novo* EEV plaque formation. After 2-3 days of culture, cells were washed and stained with a 0.01% crystal violet with 15% ethanol solution and then washed so that plaques could be counted to calculate virus plaque-forming units (pfu).

For infections involving the virus plaque assay and CsCl gradient separation, primary macrophages in 12- or 6-well plates (50,000 or 300,000 cells per well, respectively) were incubated with VV WR at a multiplicity of infection (MOI) of 5 for 1 h, washed three times with PBS and cultured for 2 days in complete RPMI-1640. Culture supernatants and cells were harvested at various

time points. Cells were lysed by three rounds of freezing and thawing, followed by sonication in a cup horn sonicator. Cell lysates and supernatants were either mixed together or analyzed separately for determination of virus titers. VV-EGFP was used to monitor viral gene expression in MDMs, except that these cells were cultured for a short period (6 h) in order to analyze for EGFP expression. At 6 h of culture, cells were fixed with 2% PFA and EGFP-positive cells were quantitated using FACS. For VV binding assays, primary MDMs were chilled to 4°C and incubated with vA5L-YFP at an MOI of 5 on ice for 1 h with gentle mixing. Cells were washed three times with ice-cold PBS, fixed with 2% PFA, and YFP-positive cells were quantitated using FACS.

Preparation of human PBMCs

Whole-blood samples or leukapheresis products were obtained from healthy blood donors with written consent obtained from each participant. Investigational protocols were approved by Institutional Review Boards for Human Research at the Indiana University School of Medicine (Indianapolis, IN). To isolate peripheral blood mononuclear cells (PBMCs), whole blood or leukapheresis products were separated by Ficoll-Hypaque (Amersham Pharmacia Biotech AB, Uppsala, Sweden) gradients. Monocytes, B cells, and NK cells were then enriched by negative isolation using Ab-conjugated magnetic beads in the Monocyte, B cell, and NK cell Negative Isolation Kits (Dynal, Oslo, Norway). Resting T cells were isolated from the PBMCs using the Pan T Cell Isolation Kit II (Miltenyi Biotec, Auburn, CA), which yielded >95% purity of $CD3^+$ T

cells. $CD3^+$ T cells were activated by incubating with anti-CD3/anti-CD28 Ab-coated magnetic beads (Life Technologies, Carlsbad, CA), and cultured in complete RPMI 1640 medium. The resulting cell preparations contained more than 95% of the desired cell types assessed by CD14, CD3, CD4, CD8, CD19, or CD56 staining and FACS. Neutrophils were isolated from whole blood from healthy donors by density gradient separation in Lympholyte-Poly solution (Cedarlane Labs, Hornby, ON) to isolate polymorphonuclear cells, followed by treatment with water to lyse red blood cells. Neutrophil purity was >98% as determined by flow cytometric analysis of HNL^+CD66b^+ cells.

To differentiate cells into macrophages, isolated monocytes were cultured in complete RPMI-1640 media supplemented with either 50 ng/ml of rhGM-CSF or 50 ng/ml of rhM-CSF, or in RPMI-1640 containing 10% human AB serum (Gemini Bio Products, West Sacramento, CA). Culture media were changed every 3 days. Macrophages were considered fully differentiated after 7 days of culture as determined by morphology. T cells were separated from PBMCs and subjected to activation using the Dynabeads Human T Cell Expander kit (Life Technologies, Carlsbad, CA) according to the manufacturer's instructions. T cells were allowed to incubate with anti-CD3 and anti-CD28-coated beads for 72 h before use in experiments.

HIV-1 infection of cell lines

The latently HIV-1-infected cell line U1 was activated with 10 nM PMA to allow for virus production. After 2 days, supernatants were collected from cells

and centrifuged at 100,000g to pellet the virions. The pellet was resuspended, dispersed with a cup horn sonicator, and used to infect the monocytic cell lines THP-1 and U937. After 3 weeks of culturing, the infected cell lines were compared to uninfected controls for the presence of integrated viral DNA using PCR. Also, the downregulation of CCR5 was detected by surface staining with a PE-conjugated antibody against human CCR5 followed by FACS analysis. A VV binding assay was then performed on the HIV-1 infected and uninfected cell lines.

Polarization of primary human leukocyte subsets

Individual PHL subsets were treated with various agents at 37°C to induce membrane polarization and lipid raft relocation. Briefly, isolated monocytes were incubated with 100 ng/mL of GM-CSF (BioVision, Milpitas, CA) for 24 h (78), B cells were incubated with 100 ng/mL of SDF-1 (Biolegend) on rhICAM-2 (fc)-coated coverslips for 30 min (79), activated T cells adhered to anti-CD44 coated coverslips for 30 min (80, 81), and neutrophils were treated with 10 nM of the bacterial peptide fNLPNTL (Bachem, Torrence, CA) for 5 min (82). After treatment, all cell types were fixed with 2% PFA, and subjected to VV binding and analyzed by fluorescence microscopy.

Immunosera raised against cell membrane extracts or whole cells

All animal experimentation was conducted following the NIH guidelines for housing and care of laboratory animals and performed in accordance with

Indiana University Institutional regulation after review and approval by the institutional Animal Care and Use Committee at Indiana University. Female BALB/c mice, 6-8 weeks of age, from the Jackson Laboratory (Bar Harbor, ME) were subjected to *intraperitoneal* (*i.p.*) immunization. Mice were divided into nine groups with 3 mice per group, and then subjected to immunization with: (1) detergent-resistant membranes (DRMs), (2) crude membrane extracts (CMEs), or (3) whole cells. These immunogens were prepared from either $40x10^6$ monocytes, resting T cells, or activated T cells from the same blood donors. DRMs and CMEs were prepared from each type of these cells as previously described (83). Briefly, $40x10^6$ cells were lysed in 1% Triton X-100/PBS plus 1x Protease Inhibitor Cocktail (Fisher Scientific, Pittsburgh, PA) at 4˚C for 1 h. Lysates were clarified by centrifugation at 1,000 x g for 10 min, and the resulting supernatants were mixed with 45% sucrose in PBS which was then added to the bottom of an ultracentrifuge tube. Equal volumes of 35% and 5% sucrose/PBS were sequentially added to the tube to create discontinuous gradients. The tube was centrifuged at 166,000 x g for 18 h at 4°C in an Optima LE-80K ultracentrifuge (Beckman Coulter, Brea, CA). The light-scattering band near ~20% sucrose (DRMs) was harvested, diluted in PBS containing 1x Protease Inhibitor Cocktail, and then centrifuged at 166,000 x g at for 2 h at 4°C. The DRM pellet was homogenized in PBS using a Dounce homogenizer. For CME preparation, $40x10^6$ cells of each subset in PBS with 1x Protease Inhibitor Cocktail were disrupted with a Dounce homogenizer. After clarification, the resulting supernatant was centrifuged at 120,000 x g, and the pellet was

resuspended in PBS. Primary immunizations were followed by two immunization boosts on day 14 and day 28. Two weeks after the last immunization boost, animals were anesthetized with isoflurane and harvested from the retro-orbital sinus for serum collection.

To evaluate the immunization efficacy, an ELISA assay was developed to titrate Abs against human CD55, a common glycosylphosphatidylinositol (GPI)-anchored protein in cell lipid rafts (84). Briefly, microplates were coated with recombinant CD55 protein at 0.1 ug/mL (R&D Systems, Minneapolis, MN). After washing and blocking with 5% FBS/PBS, plates were incubated with serially diluted immunosera, followed by the addition of anti-mouse IgG mAb conjugated with horseradish peroxidase (HRP). Pooled pre-immunization mouse sera were used as negative controls. Absorption was read at a wavelength of 450 nm in a plate spectrophotometer (BioTek, Winooski, VT).

Knockdown of CD29 and CD98 in HeLa cells and T cells

Dharmacon Smartpool Accell siRNA constructs against human CD29 and CD98 were purchased from Thermo Fisher Scientific (Pittsburgh, PA). These siRNA constructs were transfected into cells using the Amaxa Nucleofector system (Lonza, Basel, Switzerland) according to the manufacturer's instructions. Briefly, 150 - 300 nM of each siRNA mixture was used per 5 x 10^6 activated T cells or 1 x 10^6 HeLa cells. Transfected cells were cultured for 48 h, and then subjected to Western blot or FACS using rabbit pAbs against human CD29 or CD98 to analyze knockdown of human CD29 or CD98. These cells were also

subjected to VV binding and infection to determine the effects of CD29 and CD98 on VV binding and entry.

Pretreatment of cells with polyclonal antibodies specific for host membrane proteins

Whole PBMCs were incubated with various pAbs against human membrane proteins of interest in an attempt to block VV binding. PBMCs were pretreated for 30 mins on ice with the following antibodies: rabbit pAbs against CCR2 purchased from Proteintech Group (Chicago, IL) (cat# 16153-1-AP); mouse anti-CD11a (clone G43-25B) purchased from BD Biosciences; rabbit pAbs against integrin beta-1 (CD29) purchased from Abnova (Taipei, Taiwan) (cat# H00003688-D01P); goat pAbs against integrin beta-2 purchased from Santa Cruz Biotechnology (Dallas, TX) (cat# sc-6624); mouse anti-CD33 (clone P67.6) purchased from BD Biosciences; CD52; rabbit pAbs against SLC3A2 (CD98) purchased from Thermo Fisher Scientific (Pittsburgh, PA) (cat# PA5-21547); mouse anti-CD169 (clone 7-239) purchased from AbD Serotech (Cardiff, UK). After washing, cells were resuspended in complete RPMI and subjected to VV binding assays. After PFA fixation, cells were analyzed with FACS for the mean fluorescent intensity (MFI) of YFP while gating on either myeloid or lymphocyte- specific morphologies.

Macrophage activation and RT-PCR transcriptional profiling

Monocyte-derived macrophages (MDMs) were activated using different cytokine combinations. First, isolated blood monocytes were cultured in complete RPMI-1640 supplemented with either 50 ng/ml of rhGM-CSF or 50 ng/ml of rhM-CSF. After 7 days of differentiation, GM-CSF-induced MDMs (M1) were stimulated with 10 ng/ml of LPS plus 50 ng/ml of rhIFN-γ. M-CSF-induced MDMs (M2) were activated with either 10 ng/ml of rhIL-4 (M2a), 10 ng/ml of LPS plus 10 ng/ml of rhIL-1β (M2b), or 10 ng/ml of rhIL-10 (M2c). Cells were cultured for 24 h. For inhibition of JAK2/STAT3 during M2c activation, 1-5 μM of cucurbitacin I (JSI-124, Sigma-Aldrich, St. Louis, MO) was added along with rhIL-10. For RT-PCR analysis of activation-associated genes, cells were washed three times in PBS and subjected to RNA extraction using the RNeasy Mini kit (Qiagen, Hilden, Germany) according to the manufacturer's instructions. RNA was subjected to cDNA synthesis using the Superscript III First Strand synthesis kit (Life Technologies, Carlsbad, CA) according to the manufacturer's instructions. Real-time RT-PCR was performed using the RT^2 SYBR Green/ROX FAST mastermix (Qiagen, Hilden, Germany) with primers against M1 or M2 specific genes, including: IL-6 forward, 5'-GAGGATACCATCCCAACAGACC-3' and IL-6 reverse, 5'-AAGTGCATCATCGTTGTTCATACA-3'; IL-10 forward, 5'-GCCTAACATGCTTCGAGA-3' and IL-10 reverse, 5'-TGATGTCTGGGTCTTGGTTC-3'; CD163 forward, 5'-CCAGTCCCAAACACTGTC-3' and CD163 reverse, 5'-TTCTGGAATGGTAG GCCTTG-3'; Arg1 forward, 5'-CAGAAGAATGGAAGAGTCAG-3' and Arg1

reverse, 5'-CAGATATGCAGGGAGTCACC-3'; and β-actin forward, 5'-CTCGACACCAGGGCGTTAG-3 and β-actin reverse, 5'-CCACTCCATGCTCGATAGAT-3' (Life Technologies, Carlsbad, CA). Expression data by the cycle threshold (Ct) value was compared to actin expression and analyzed using $2^{-\Delta\Delta CT}$ as previously described (85). For infection of activated cells, M1 or M2-polarized cells were infected with VV WR at an MOI of 5 for 3 h. Cells were washed extensively in PBS and then cultured in media containing the activation cytokines.

CsCl density-gradient ultracentrifugation for VV separation

Virus-containing supernatants and cell pellets were harvested from $5x10^7$ VV-infected M2 macrophages. To separate and analyze mature vs. enveloped virus particles, the virus was purified from cell lysates via 24 - 40% discontinuous sucrose gradients. Purified virus was added to CsCl gradients made with 2 ml of 1.30 g/ml overlaid with 3 ml of 1.25 g/ml, followed by 4 ml of 1.20 g/ml in a 12 ml tube as previously described (86, 87) and centrifuged in an Optima LE-80K ultracentrifuge with an SW-41 rotor (Beckman Coulter, Brea, CA) at 20°C for 2 h at 120,000 g (32,000 rpm). Fractions (0.5 ml each) were harvested from the top of each gradient, and subjected to virus collection by ultracentrifugation at 21,000 g (15,000 rpm) for 30 min in a tabletop microcentrifuge. Virus pellets were resuspended in 100 µl of PBS and sonicated in a cup horn sonicator. The absorbance of each fraction was measured at 260 nm and the number of virion

particles estimated using the follow formula: numbers of virus particles = A260 * $1.2x10^{10}$.

Signaling pathway inhibition in human primary macrophages

M2-polarized MDMs were infected with VV WR at an MOI of 5 for 3 h. Cells were washed three times with PBS, and incubated in complete RPMI 1640 medium with 5 - 40 μM of the Akt inhibitor LY294002, 1 - 100 μM of the ERK inhibitor PD98059, or 1 - 10 μM of the JNK inhibitor SP600125. After incubation for 24 – 48 h, cells and supernatants were harvested and virus titers determined using the virus plaque assay. Cell lysates were also analyzed for the level of kinase inhibition using the "Pathscan Phospho-SAPK/JNK (Thr185/Tyr185)," "Pathscan Phospho-Akt1," and "Pathscan Phospho-p44 MAPK" sandwich ELISA kits (Cell Signaling Technology, Danvers, MA) according to the manufacturer's instructions. Within the same kits, antibodies against SAP/JNK, Akt, and Erk (Cell Signaling Technology) were used to detect levels of unphosphorylated targets.

Confocal microscopy

PHLs were infected with vA5L-YFP VV at an MOI of 5 and fixed at various intervals. To detect extracellular virions, cells were incubated with the rabbit polyclonal antiserum NR-631 against the VV WR-encoded L1R protein (obtained through the NIH Biodefense and Emerging Infections Research Resources Repository, NIAID, NIH) followed by a secondary antibody staining of donkey anti-rabbit IgG (H+L) conjugated to Alexa Fluor 546 (Life Technologies, Carlsbad,

CA). An aliquot of the same infected cells were fixed with 2% PFA, permeabilized with 0.1% saponin, and incubated with phalloidin conjugated to Alexa Fluor 546 (Life Technologies, Carlsbad, CA) for F-actin staining. For lipid raft staining, cells were incubated with cholera toxin subunit B (CTB) conjugated with Alexa Fluor 647 (Life Technologies, Carlsbad, CA) at 4°C for 20 min to stain ganglioside M1 (GM1). For CTB-patching, cells were treated with a 1:100 dilution of goat anti-CTB pAbs (Millipore, Darmstadt, Germany) in 2% FBS/PBS for 30 min on ice, and then incubated at 37^{o}C for 20 min as previously described (88). Cells were then mounted onto glass slides using ProLong Gold Antifade reagent (Life Technologies, Carlsbad, CA) containing 4′,6-diamidino-2-phenylindole (DAPI) dye for DNA staining. Slides were viewed using an Olympus FV1000-MPE confocal/multiphoton microscope fitted with a 60X water objective. Images were processed using ImageJ version 1.47 software (NIH, Bethesda, MD).

Statistical analysis

Data obtained from two groups were analyzed using Student's *t* test, whereas data obtained from three groups or more were analyzed using Tukey's *post hoc* analysis of variance (ANOVA) test. *V*alues of $p<0.05$ were considered statistically significant.

Chapter IV - Results

VV differentially binds to PHL subsets

The majority of studies investigating the entry of VV into host cells have focused on single-enveloped VV IMV particles because they are the most abundant (>98%) and maintain their membrane integrity after freezer storage (8, 89). Double-enveloped virus forms like EEV and CEV not only have different binding behaviors for cell lines, they are difficult to maintain since they cannot be stored for long periods. The IMV particles of vA5L-YFP or EGFP-VV were therefore used in this study. Isolated monocytes, B cells, neutrophils, resting T cells, and NK cells were incubated with vA5L-YFP particles at binding conditions (4^{o}C for 30 min) to study VV binding profiles for these PHL subsets. At an MOI of 10, vA5L-YFP bound to 76 ± 10% of monocytes, 71 ± 9% of B cells, 28 ± 2% of neutrophils, 3 ± 2% resting T cells and 2 ± 2% of NK cells (Fig. 2A, 2B). These values were the results of the mean ± standard deviation (SD) from six healthy blood donors. VV binding to monocytes, B cells, and neutrophils was not affected by soluble heparan sulfate (HS) at 10 μg/mL (Fig. 2A, 2B), an optimal concentration that completely blocks VV non-specific binding to HS glycosaminoglycan (GAG) side chains of cell surface proteoglycans of BSC40 cell line (90). In contrast, HS at 10 μg/mL eliminated the trace amount of VV binding to resting T cells and NK cells (Fig. 2A, 2B), suggesting that binding to these cells is GAG-dependent. VV binding to monocytes, B cells and neutrophils was markedly reduced by trypsin treatment (Fig. 2A, 2B).

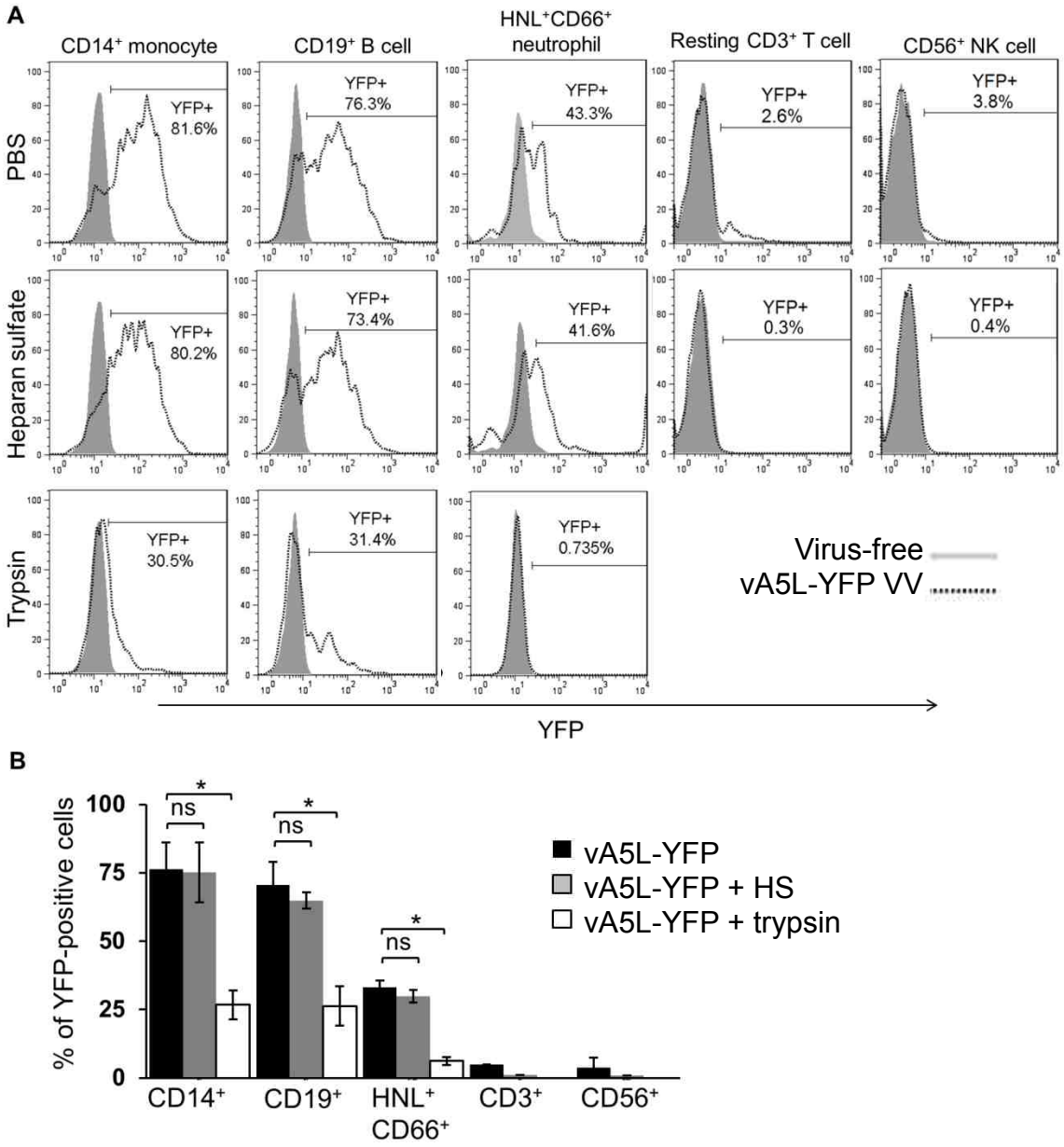

Fig. 2. VV differentially binds to PHLs. (A) Major PHL subsets including monocytes, B cells, neutrophils, resting T cells and NK cells were untreated or treated with trypsin or HS, and then subjected to vA5L-YFP binding at an MOI of 10. VV binding was measured by YFP intensity using flow cytometric analysis. (B) Pooled data represented mean ± SD of VV binding (% of YFP-positive cells) to PHL subsets from 6 blood donors. * $p<0.05$, ** $p<0.01$.

We investigated whether T cells activated with anti-CD3 and anti-CD28 antibodies become sensitive to VV binding to confirm that VV receptor(s) can be induced *de novo* upon T cell activation (56). As was previously reported, we found that cells became susceptible to binding upon activation which increased with time (Fig. 3A, 3B). Similar to the result with monocytes, B cells, and neutrophils, VV binding to activated T cells was markedly reduced by treatment with trypsin, but not soluble HS (Fig. 3B). In contrast, activated NK cells remain non-permissive to VV binding (Fig. 3C). These results indicate that VV binding to monocytes, B cells, neutrophils, and activated T cells is mediated by protein VV receptors independent of HS GAGs, and that these receptors are induced upon activation of T cells, but not with NK cells (Fig. 3D).

To visualize VV binding at the single cell level, purified monocytes, resting T cells, activated T cells and TA3 cells with vA5L-YFP paticles were incubated at binding conditions, and visualized with confocal microscopy to examine VV binding. At an MOI of 10, vA5L-YFP bound to monocytes at ~39 virions per cell (mean from 100 cells counted) (Fig. 4A, 4B), whereas VV binding was considerably lower in resting T cells (0.05 virions per cell, mean from 100 cells counted). vA5L-YFP did not bind to TA3 cells that were previously shown not to bind with VV (77, 91). After activation with anti-CD3/anti-CD28 Abs-coated magnetic beads for 3 days, activated T cells became sensitive to VV binding with a similar binding degree to that of monocytes (Fig. 4A, 4B).

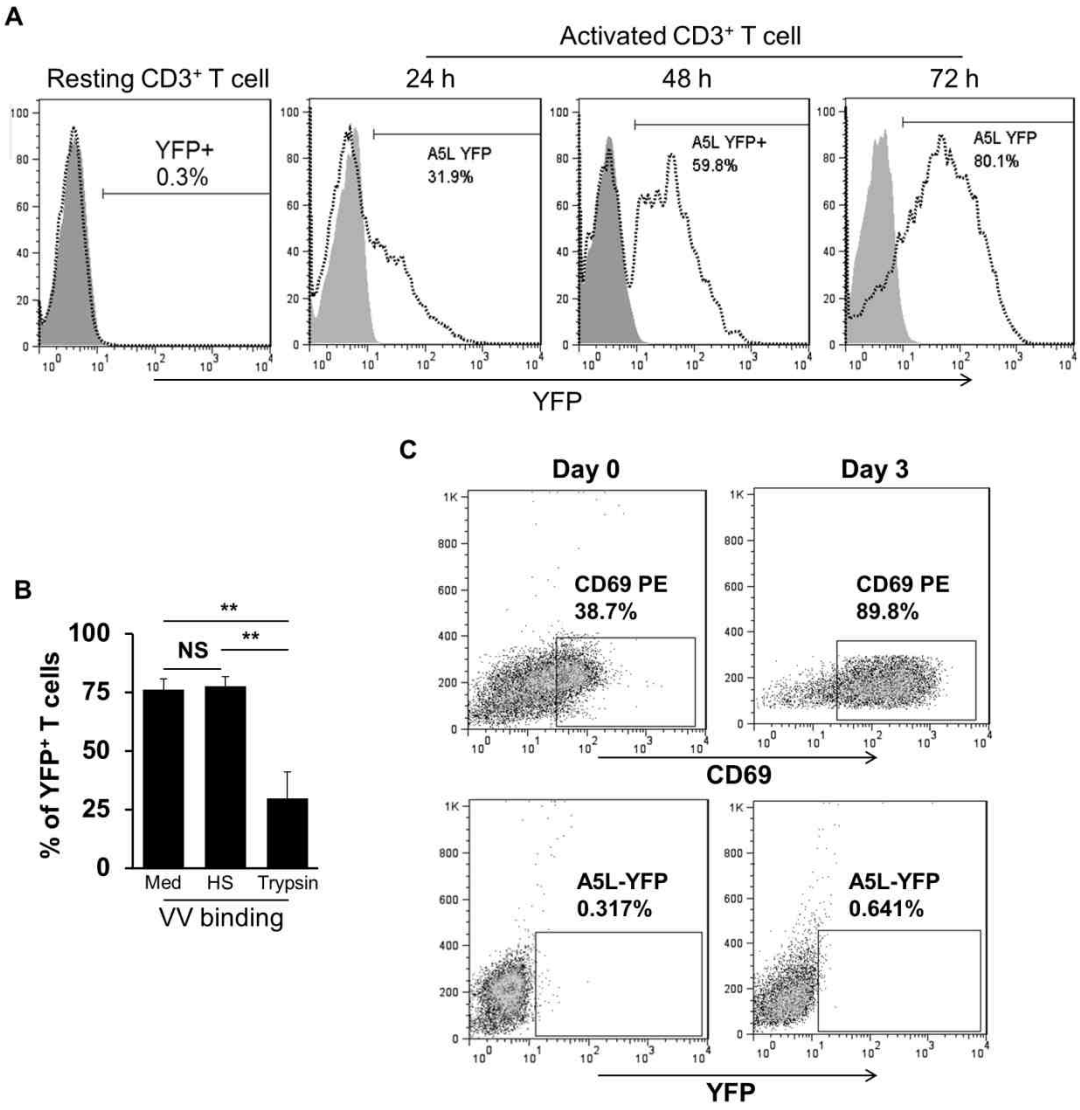

Fig. 3. T cell activation induces VV binding susceptibility. (A, B) The kinetics of VV binding to T cells activated with anti-CD3 and anti-CD28 antibodies (n=6) during a 0 – 72 h activation period. (C) VV binding to activated T cells on day 3 of activation with trypsin or HS pretreatment. (D) Isolated NK cells were activated with IL-2 for 3 days, stained for surface CD69 and subjected to VV binding assay. * $p<0.05$, ** $p<0.01$.

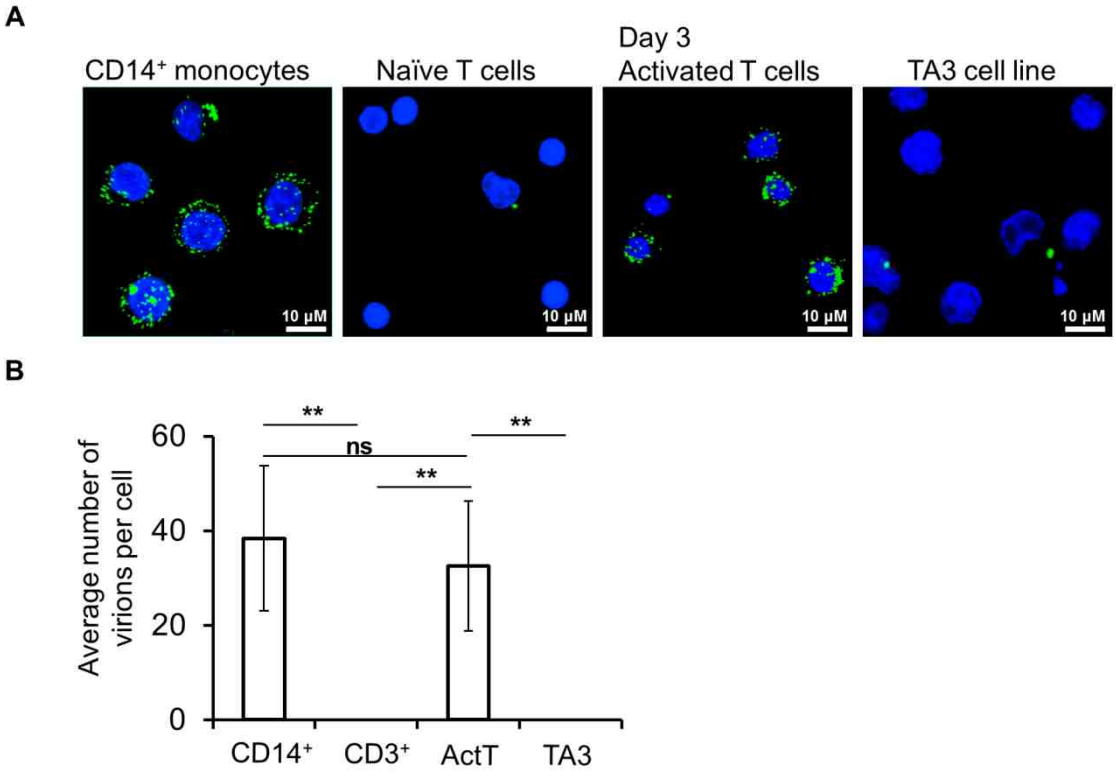

Fig. 4. T cell activation increases the number of attached virions. (A) Representational confocal microscope analysis of VV binding assay performed on monocytes, resting T cells, T cells activated with anti-CD3 and anti-CD28 antibodies, and the TA3 cell line at the single cell level. (B) Virions per cell count from a pool of 100 cells for donor represented as the mean ± SD (n=6) of VV binding to monocytes, resting T cells, T cells activated with anti-CD3 and anti-CD28 antibodies, and TA3 cells. ** $p<0.01$.

VV infection varies among PHL subsets

To determine whether VV binding was correlated to VV reporter gene expression, we infected PHL subsets with EGFP-VV at an MOI of 10 for various length of time. EGFP-VV is a VV WR strain with an EGFP reporter gene under a VV early/late promoter. We confirmed that VV preferentially infected monocytes with 65 ± 8% (n=6) cells becoming EGFP-positive 6 h post-infection, whereas 15 ± 5% (n=6) of activated T cells were EGFP-positive 24 h post-infection (Fig. 5A, 5B). In contrast, only 4 ± 2% (n=6) of B cells were infected, whereas neutrophils and resting T cells resisted VV infection as only trace amounts of these cells were EGFP-positive 24 h post-infection (Fig. 5A, 5B). VV infection of monocytes and activated T cells was significantly reduced by trypsin treatment, but not soluble HS (Fig. 5A, 5B). This result demonstrates the disparity between the degree of VV binding and viral gene expression in primary leukocytes. Particularly, although B cell and activated T cells are highly susceptible to VV binding, gene expression is relatively low. This may be explained by a rate-limiting factor in a post-binding step such as entry and uncoating. Further analysis of monocyte subpopulations revealed that the vast majority of virus was bound to "classical" $CD14^{high}$ $CD16^{-}$ monocytes and were sensitive to VV infection when compared to "patrolling" $CD14^{low}CD16^{+}$ monocytes (Fig. 6A, 6B). Thus, VV binding to primary human leukocytes is selective for certain cell types, and does not correlate with VV gene expression.

Two previous studies have demonstrated that VV-infected primary human monocytes do not produce either viral late-gene products or viral DNA copies,

indicating that VV undergoes abortive infection in primary human monocytes (56, 92). Our data together with these results indicate that: (1) monocytes are the most sensitive PHL subset to VV binding and infection, but the infection is abortive; (2) B cells and neutrophils are sensitive to VV binding, albeit to different degrees, but non-permissive to VV infection; (3) NK cells (both resting and activated states) and resting T cells resist VV binding and infection; and (4) from our findings and others (56), activated T cells are the only cell type among *ex vivo* PHLs to permit VV to complete the whole cycle of binding, infection and replication (56).

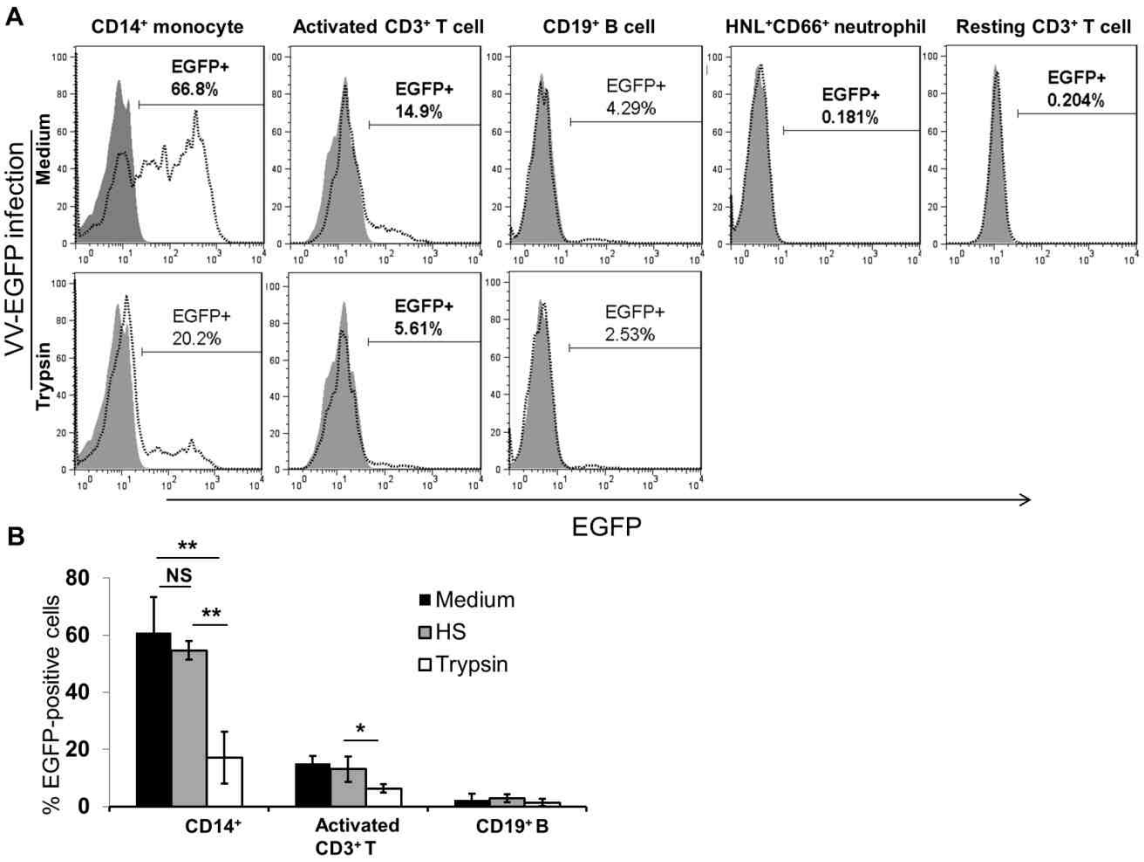

Fig. 5. VV reporter gene expression was mainly detected in monocytes. (A) Profiles of PHL subset expression of VV reporter gene EGFP and the effects of trypsin treatment. (B) Pooled data represent the mean ± SD of VV infected (% of EGFP-positive) cells to PHL subsets from 6 blood donors. * $p<0.05$, ** $p<0.01$.

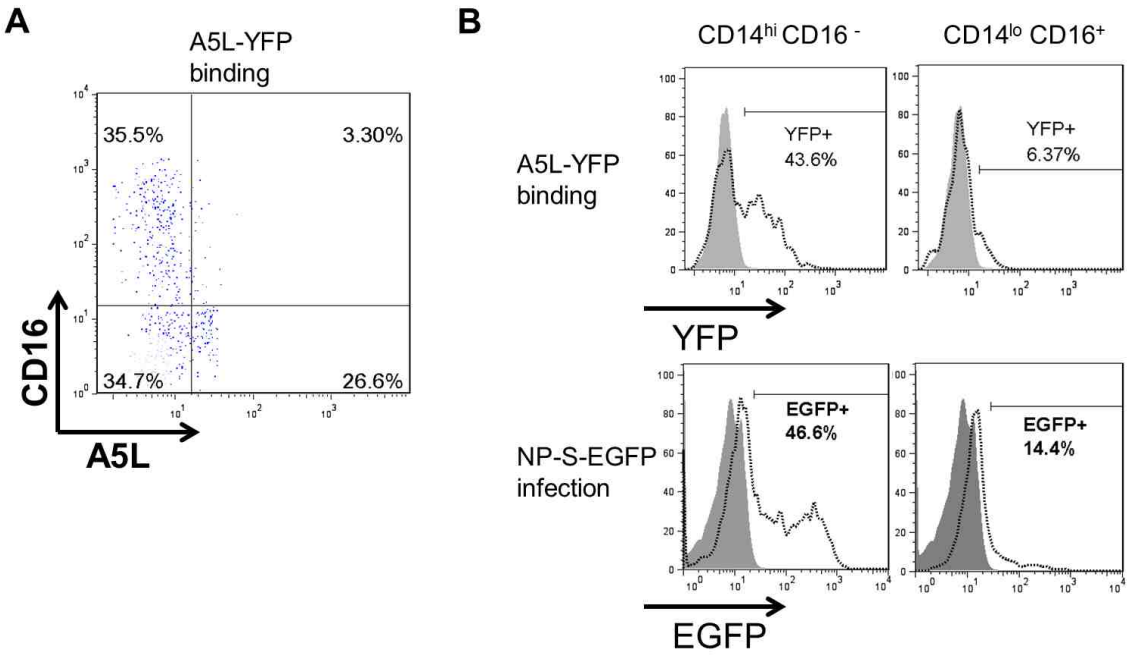

Fig. 6. VV preferentially binds and infects CD14^{high}, CD16^{-} monocytes. Isolated monocytes were subjected to the VV binding assay with vA5L-YFP or infected with VV-EGFP to test for VV gene expression and then stained for surface CD14 and CD16. (A) FACS plot of CD16 staining vs A5L expression corresponding to VV binding. (B) VV binding assay with vA5L-YFP or infection assay with VV-EGFP gated on CD14^{high} CD16^{-} or CD14^{low} CD16^{+} monocytes.

Profile of VV binding and infection of monocyte-derived cell lines

In light of the results showing that monocytes have among the highest degree of VV binding and are also the only cell type to express a VV reporter gene to a significant degree, VV binding and infection of monocytic cell lines was investigated. We used the human acute monocytic leukemia cell line THP-1, the pro-monocytic histiocytic lymphoma cell line U937, and the U1 cell line which is a HIV-1-infected clone from U937 with a latent infection phenotype. Using the VV binding assay at 5 MOI, U937 cells were by far the most susceptible to VV binding with 92.3 ± 5% YFP positive cells, followed by THP-1 with 30.8 ± 2%, and U1 with 35.1% ± 7% (Fig. 7A). In contrast, the degree of EGFP reporter gene expression for U937 was 24.5% ± 2% EGFP-positive, 48.7% ± 2% for THP-1, and 2.3% ± 1% for U1 (Fig. 7B). Similar to primary leukocytes that are susceptible to VV binding, no direct correlation was seen with VV binding and infection between the cell types. However, this result reveals a clear distinction in VV binding and infection of U937 compared to U1 which is suggestive that HIV-1 infection of U937 resulted in a down regulation of potential VV receptors.

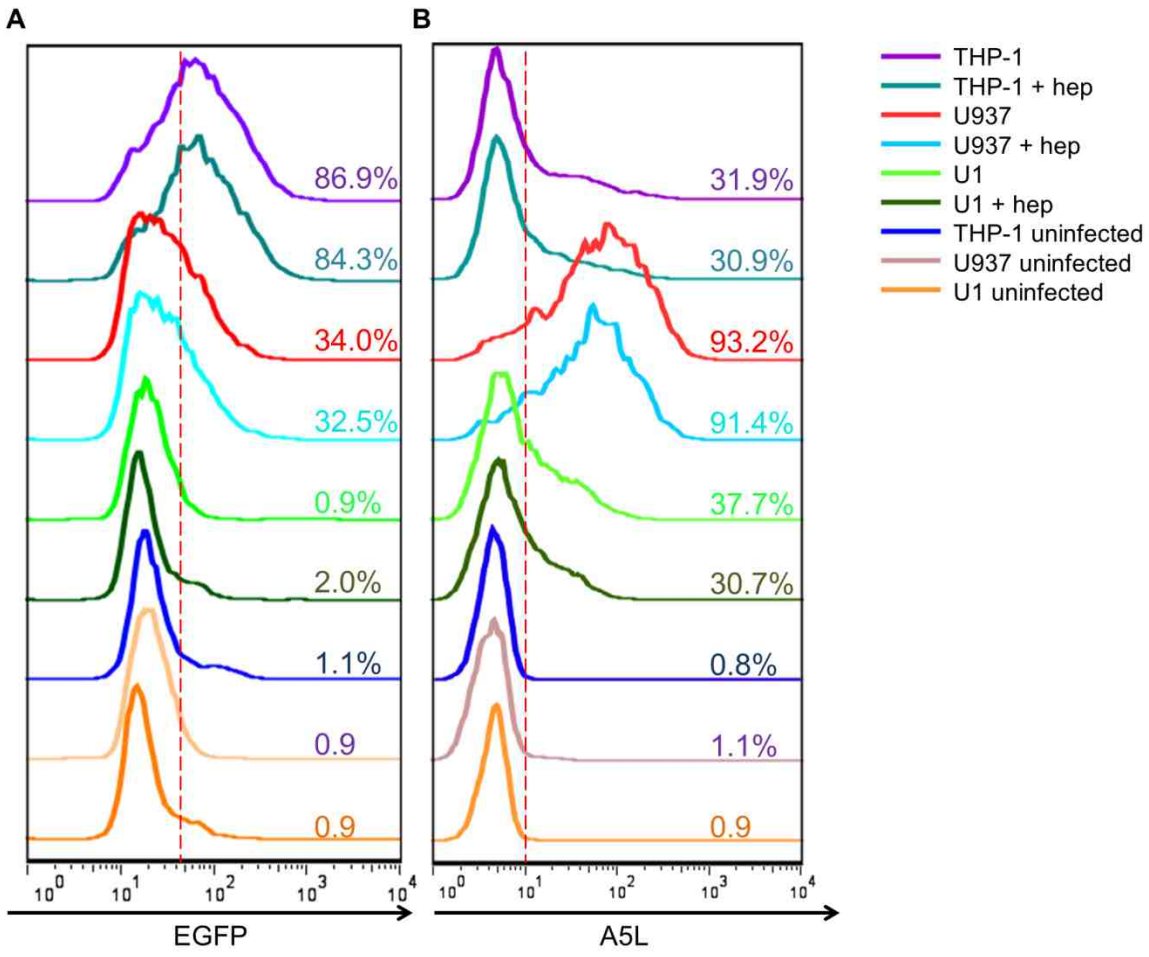

Fig. 7. VV binding to monocytic cell lines. VV binding with A5L-YFP or infection with VV-EGFP were performed on the indicated monocytic cell lines. VV reporter gene expression (A) and virus binding (B) representative FACS plot histograms for EGFP or YFP fluorescence.

Effect of HIV infection on VV binding and infection

It was observed in this study that the HIV-1-infected cell line U1 had a significantly reduced degree of VV binding and infection relative to its HIV-1 uninfected parent cell U937. To test the effects of HIV-1 infection on VV binding and infection, U937 and THP-1 cells were infected with HIV-1 derived from U1. U1 cells were activated with PMA and the culture supernatant was collected after 3 days of activation. The supernatant was ultracentrifuged to collect HIV-1 virions, resuspended, and incubated with U937. After 1 month in culture to allow for latent infection of cells, HIV-1 infection was detected via PCR amplification of the HIV-1 *gag* gene to measure the level of HIV-1 DNA integration. HIV-1-infected THP-1 and U937 cells were positive for *gag* integration whereas uninfected cells were negative (Fig. 8A). HIV-1 infection is known to downregulate surface expression of CCR5. Staining of CCR5 with FACS revealed that HIV-1 infected THP-1 and U937 had significantly reduced CCR5 surface expression (Fig. 8B). Thus, HIV-1 infected monocytic cells lines test positive for HIV-1 integration and the effects of host surface protein downregulation. It was revealed using the VV binding assay on the HIV-1 infected or uninfected U937 that HIV-1 infection significantly lowers the degree of VV binding (Fig. 9). HIV-1 infection, however, had no measureable effect on VV binding to THP-1 (Fig. 9), although the degree of binding to THP-1 was already similar to that of U1 (Fig. 8A). This reduction in VV binding is similar to the initial comparison between U937 vs. U1. Thus, HIV-1 infection of monocytic cell lines causes a downregulation of VV surface receptors.

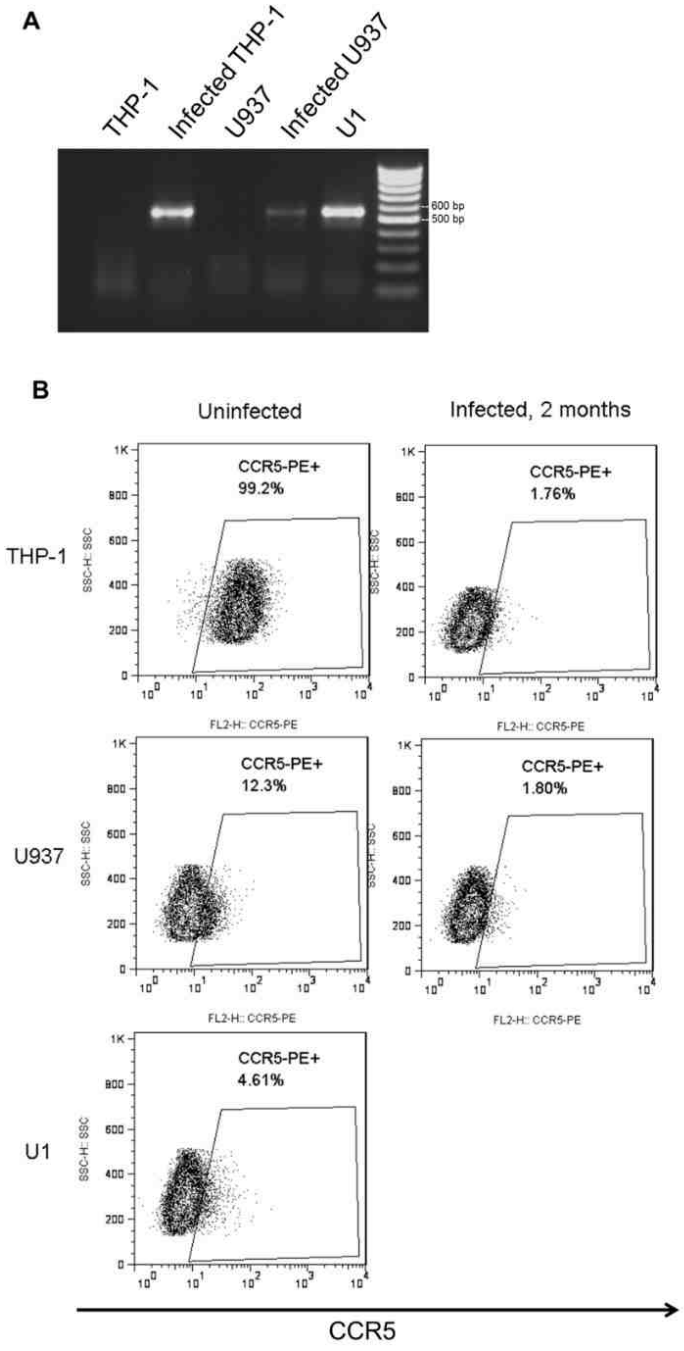

Fig. 8. Infection of monocytic cell lines with U1-derived HIV-1. Monocytic cell lines were infected with HIV-1 derived from the U1 cell line. (A) HIV-1 integration was examined by PCR by amplifying *gag* and detected using agarose gel electrophoresis (amplicon = 570 bp). (B) Representative FACS scatter plots of CCR5 surface expression of HIV-1 infected or uninfected monocytic cell lines.

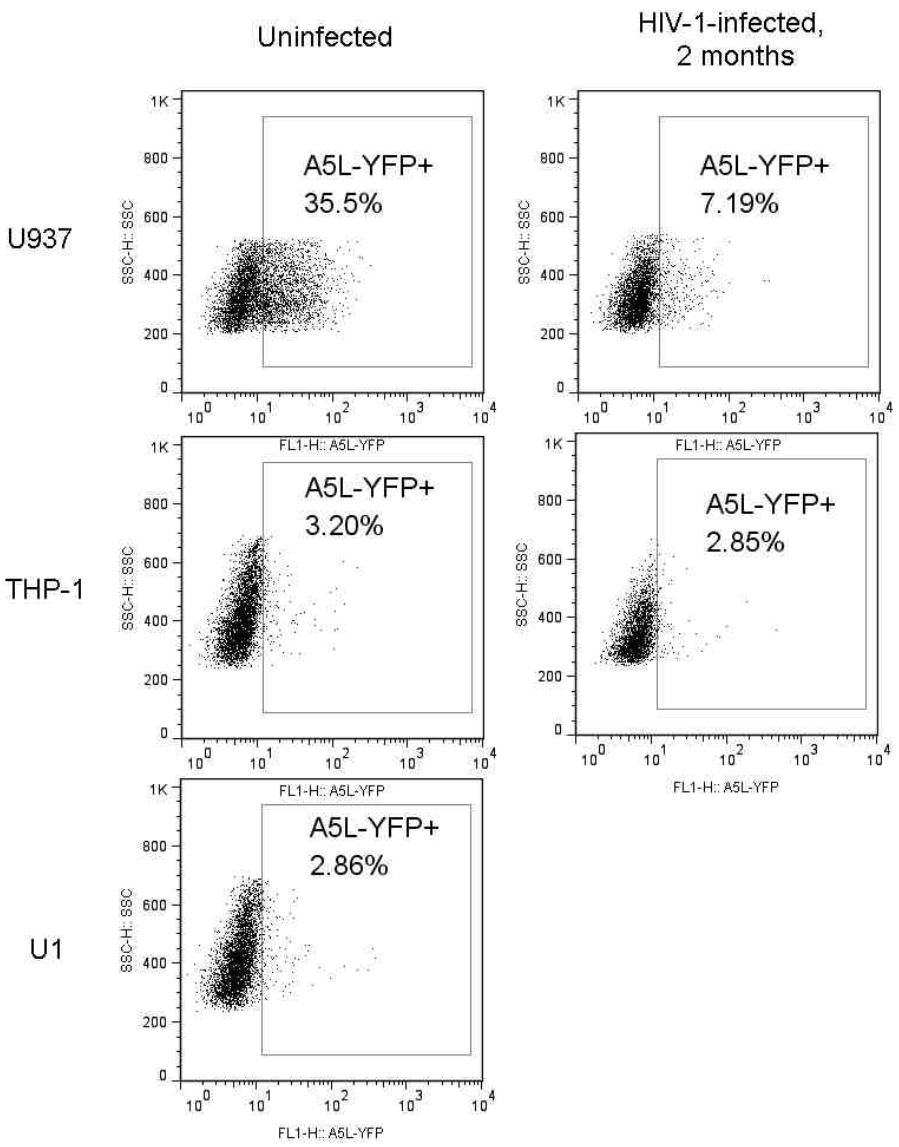

Fig. 9. HIV-1 infected monocytic cell lines become resistant to VV binding. vA5L-YFP VV binding assay of HIV-1 infected monocytic cell lines with representative FACS scatter plots.

VV strongly binds to lipid rafts on the surfaces of all susceptible PHL subsets

Because lipid rafts play a critical role in VV entry into cell lines (40, 88), and entry is inhibited by treatment of HeLa cells with methyl-β-cyclodextrin (mβCD) (40), potential VV receptors were tested for enrichment in lipid rafts on primary human cells. We searched for the colocalization of VV binding with CTB-stained lipid rafts on the surfaces of all susceptible PHL subsets. Visualization of lipid rafts in cell lines is often performed by “patching” which involves staining rafts with CTB and subsequently staining with anti-CTB pAb antibodies to aggregate rafts together on the cell surface. Colocalization of VV with lipid rafts on PHL subsets including monocytes, B cells, neutrophils, and activated T cells was observed in both patched and unpatched states, whereas CXCR4 on monocytes, neutrophils, and activated T cells, and CD19 on B cells did not colocalize with VV binding (Fig. 10A, 11A, 12A, 13A). Colocalization of CTB staining with VV A5L was measured as the percentage of pixels of A5L staining overlapping with CTB (Fig. 10B, 11B, 12B, 13B) and was always significantly higher than CXCR4 or CD19. CXCR4 and CD19 are not localized in surface lipid rafts in these cell types. This result strongly suggests that VV preferentially binds to surface lipid rafts in all *ex vivo* primary human leukocytes to which VV is known to be susceptible to bind.

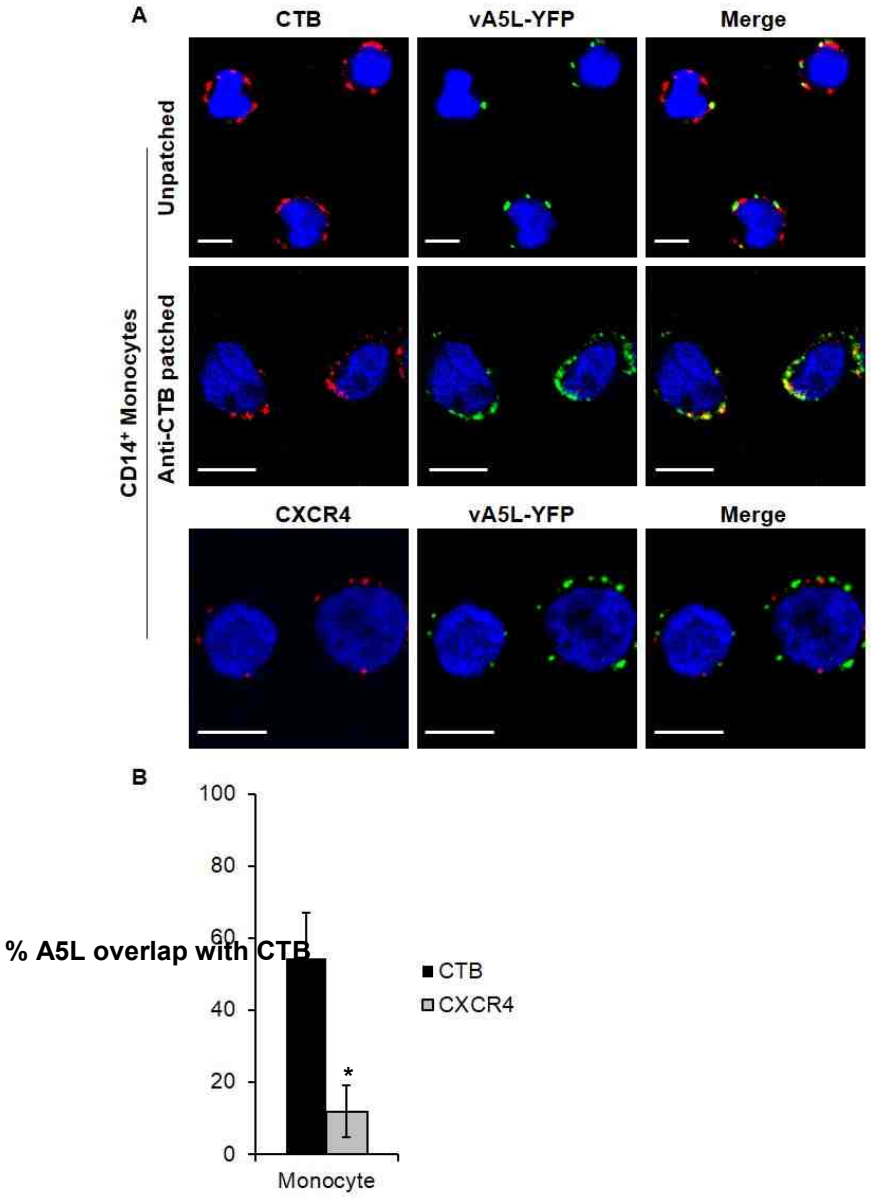

Fig. 10. VV binds to lipid rafts on monocytes. Isolated monocytes were subjected to staining with CTB conjugated with Alexafluor 647 (red), or anti-CXCR4 Ab conjugated with Alexafluor 647 (red) followed by patching with anti-CTB. Monocytes were then incubated with vA5L-YFP (green) at an MOI of 10 under binding conditions, fixed with 2% PFA, and adhered to poly-l-lysine coated coverslips. Scale bars represent 10 μM. (B) Colocalization analysis in the CTB-patched images of the percentage of A5L overlap with CTB or CXCR4. * $p<0.05$.

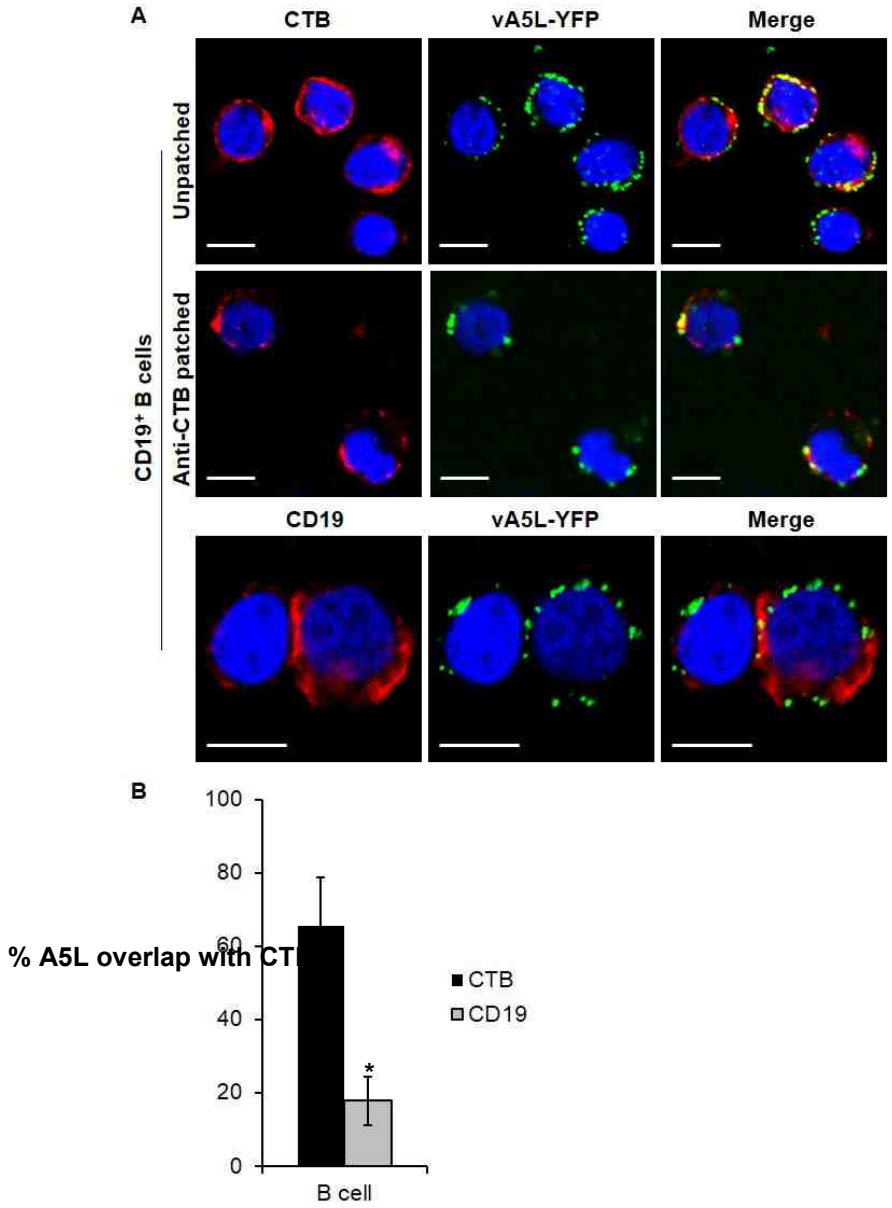

Fig. 11. VV binds to lipid rafts on B cells. Isolated B cells were subjected to staining with CTB conjugated with Alexafluor 647 (red), or anti-CD19 Ab conjugated with Alexafluor 647 (red) followed by patching with anti-CTB. B cells were then incubated with vA5L-YFP (green) at an MOI of 10 under binding conditions, fixed with 2% PFA, and adhered to poly-l-lysine coated coverslips. Scale bars represent 10 μM. (B) Colocalization analysis in the CTB-patched images of the percentage of A5L overlap with CTB or CXCR4. * $p<0.05$.

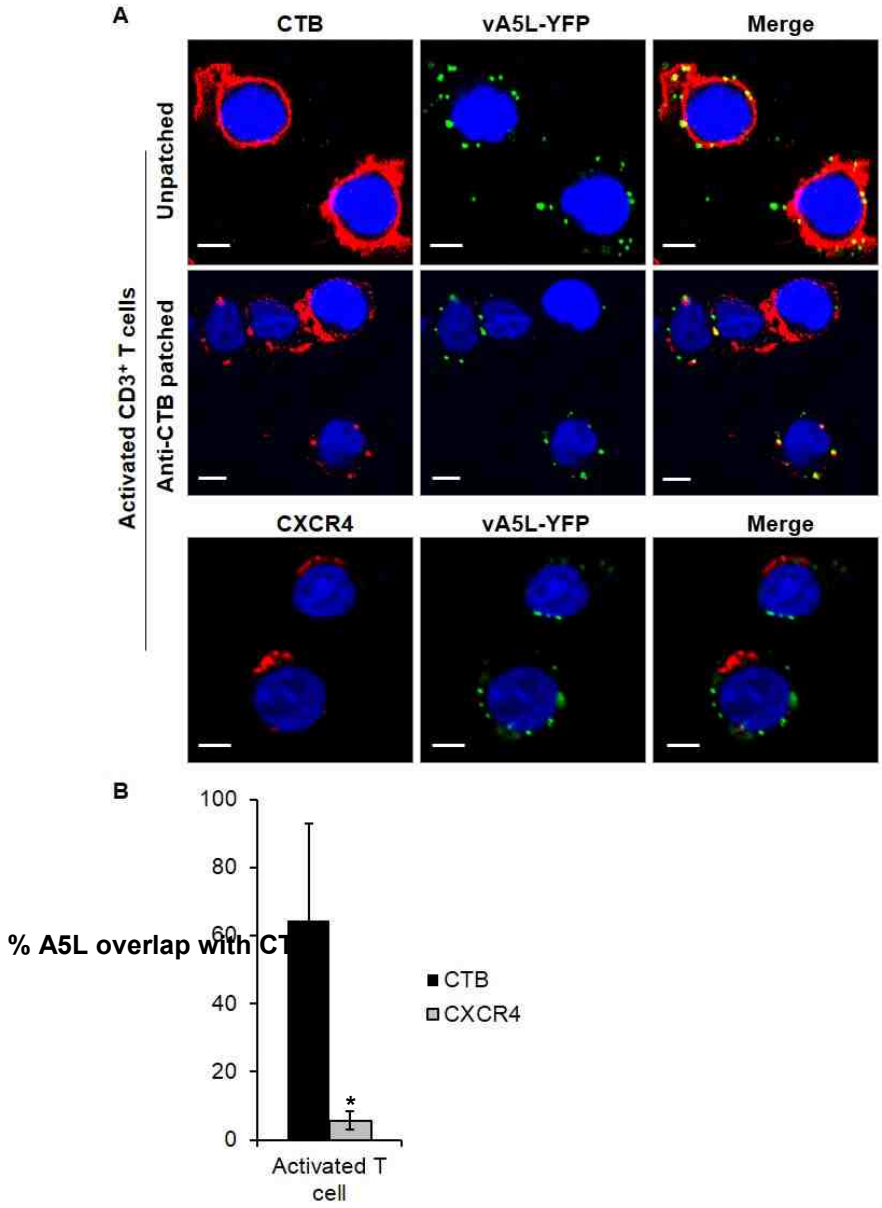

Fig. 12. VV binds to lipid rafts on activated T cells. Activated T cells were subjected to staining with CTB conjugated with Alexafluor 647 (red), or anti-CXCR4 Ab conjugated with Alexafluor 647 (red) followed by patching with anti-CTB. T cells were then i incubated with vA5L-YFP (green) at an MOI of 10 under binding conditions, fixed with 2% PFA, and adhered to poly-l-lysine coated coverslips. Scale bars represent 10 μM. (B) Colocalization analysis in the CTB-patched images of the percentage of A5L overlap with CTB or CXCR4. * $p<0.05$.

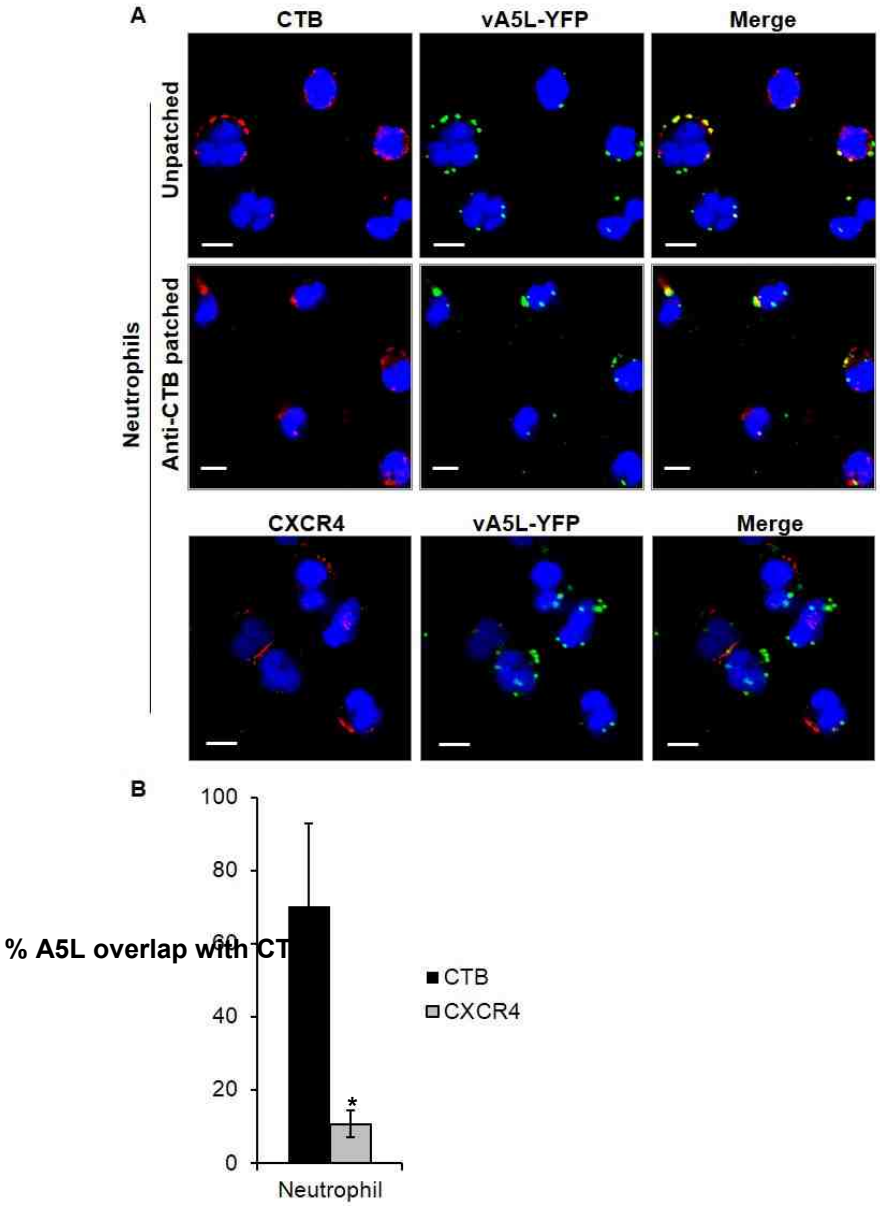

Fig. 13. VV binds to lipid rafts on neutrophils. Neutrophils were subjected to staining with CTB conjugated with Alexafluor 647 (red), or anti-CXCR4 Ab conjugated with Alexafluor 647 (red) followed by patching with anti-CTB. Neutrophils were then incubated with vA5L-YFP (green) at an MOI of 10 under binding conditions, fixed with 2% PFA, and adhered to poly-l-lysine coated coverslips. Scale bars represent 10 μM. (B) Colocalization analysis in the CTB-patched images of the percentage of A5L overlap with CTB or CXCR4. * $p<0.05$.

VV binds to lipid rafts enriched in uropods of polarized leukocytes

To further analyze the association of VV binding with lipid rafts, we polarized monocytes, B cells, neutrophils and activated T cells, and then conducted lipid raft staining and VV binding. During PHL migration and/or polarization *in vivo* and *in vitro*, GM1-stained lipid rafts and raft components move to the uropod ends of cells (93-96). Many surface proteins also move in and out of lipid rafts during the polarization process to fulfill certain physiological roles, e.g., as adhesion proteins move to the leading edge to regulate attachment and migration, cell communication proteins localize to the raft-enriched uropod (97). Thus, this assay not only provides another way to demonstrate the colocalization of VV with lipid rafts, but also presents a unique characteristic about the location of putative VV receptors during cell migration and polarization. As previously reported, GM-CSF, SDF-1, bacterial peptide fNLPNTL, and anti-CD44-coated coverslips effectively induced polarization of monocytes (93), B cells (96), neutrophils (95), and activated T cells (81), respectively, as 80 ± 8% (n=6) of monocytes, 65 ± 6% (n=6) of B cells, 75% ± 11% (n=6) of neutrophils, and 35% ± 4% (n=6) of activated T cells displayed elongated cell shapes and uropod formation. In all polarized cell types, vA5L-YFP strongly colocalized with CTB-stained lipid rafts enriched in polarized cell uropods (Fig. 14, 15, 16, 17, 18, 19). In contrast, VV did not colocalize with F-actin molecules in lamellipodia in the leading edge of polarized cells. If monocytes were continually cultured for 3 days in GM-CSF-containing complete RPMI 1640 (Fig. 15) to represent cell differentiation or 7 days (Fig. 16) to represent fully differentiated macrophages, the cells also

maintained a polarized phenotype with bound VV strongly colocalized with lipid rafts in the uropods. These results indicate that VV receptors are strongly associated with lipid rafts in PHL subsets in both *ex vivo* and polarized states.

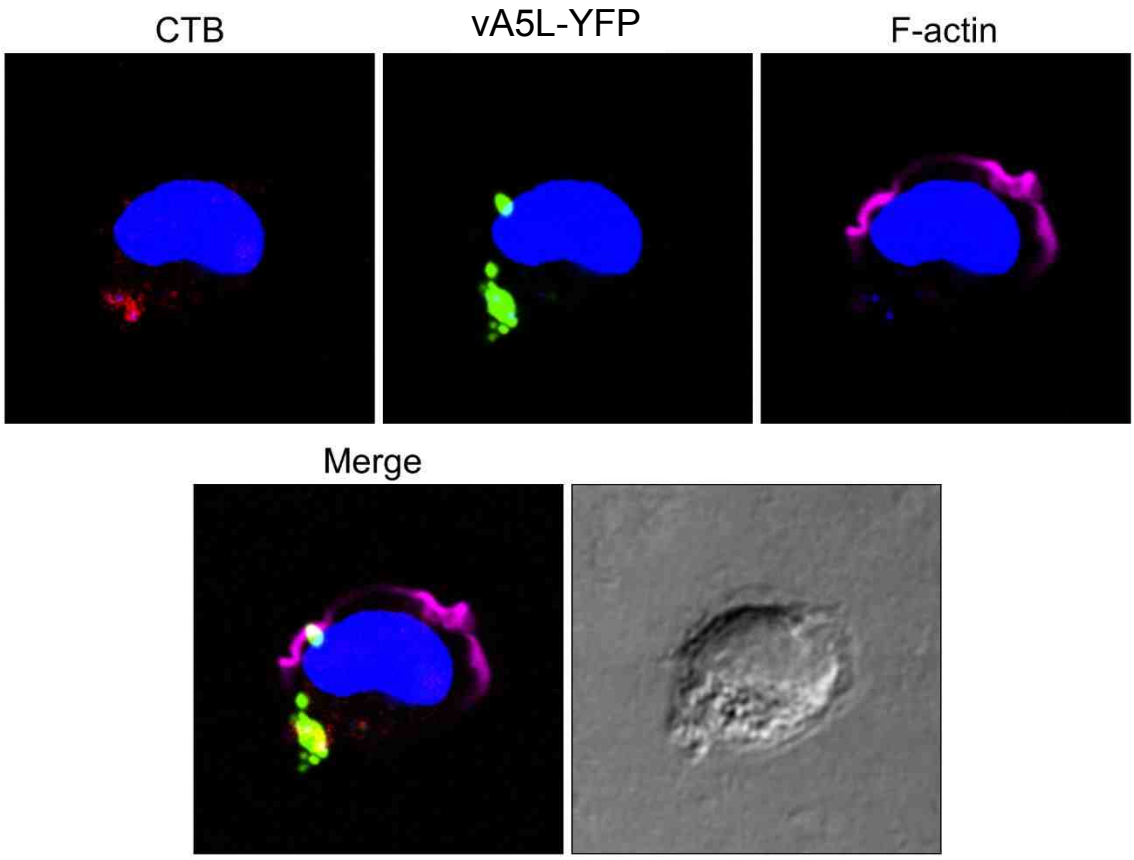

Fig. 14. VV binds to the uropods of polarized monocytes. VV binding to lipid rafts enriched in uropods of polarized monocytes. Cells were treated with GM-CSF to induce cell polarization. Polarized cells were subsequently fixed with 2% PFA and stained with CTB conjugated with Alexafluor 647 (red), phalloidin conjugated with Alexa Fluor 546 to stain actin filaments (violet) and DAPI (blue). Cells were then subjected to VV binding with vA5L-YFP (green) and confocal microscopy analysis.

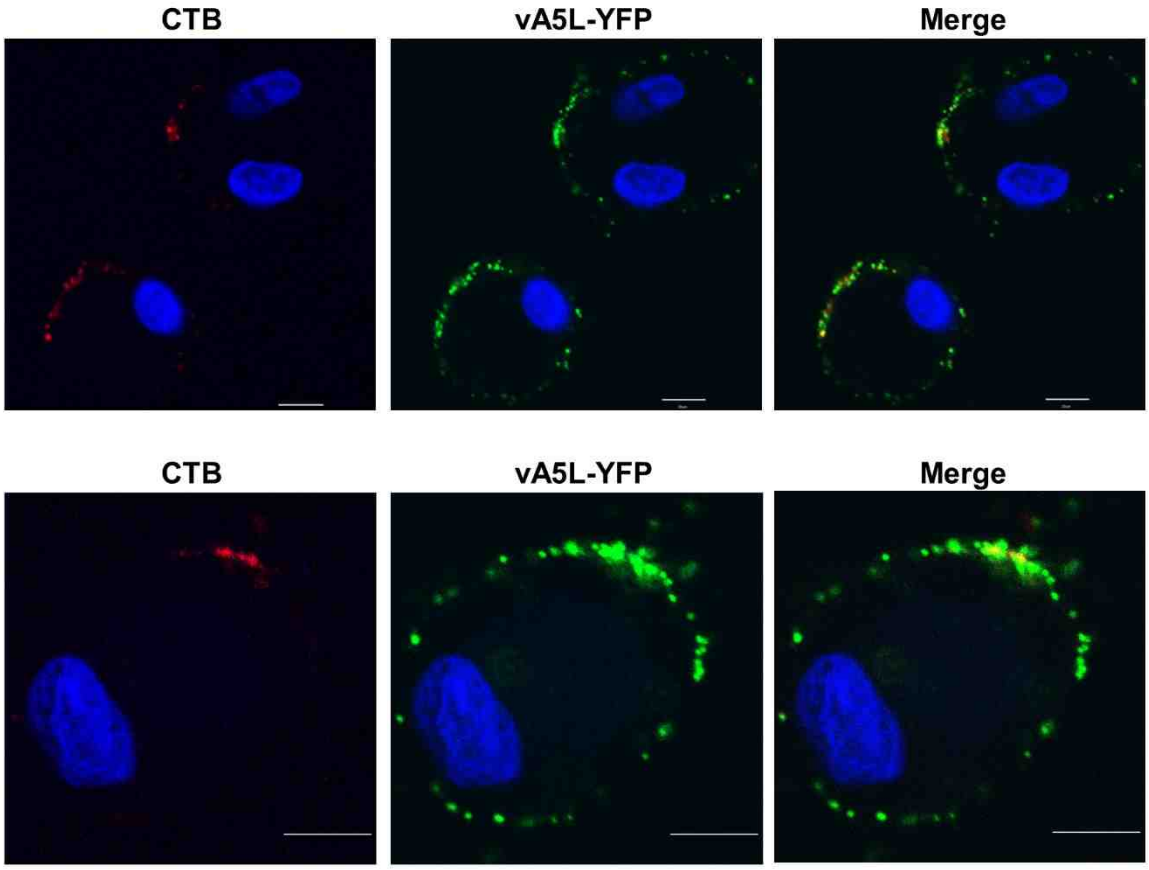

Fig. 15. VV binds to the uropods of polarized differentiating monocytes. VV binding to lipid rafts enriched in uropods of polarized differentiating monocytes. Cells were treated with GM-CSF to induce cell polarization for 3 days. Polarized cells were subsequently fixed with 2% PFA and stained with CTB conjugated with Alexafluor 647 (red), phalloidin conjugated with Alexa Fluor 546 to stain actin filaments (violet) and DAPI (blue). Cells were then subjected to VV binding with vA5L-YFP (green) and confocal microscopy analysis.

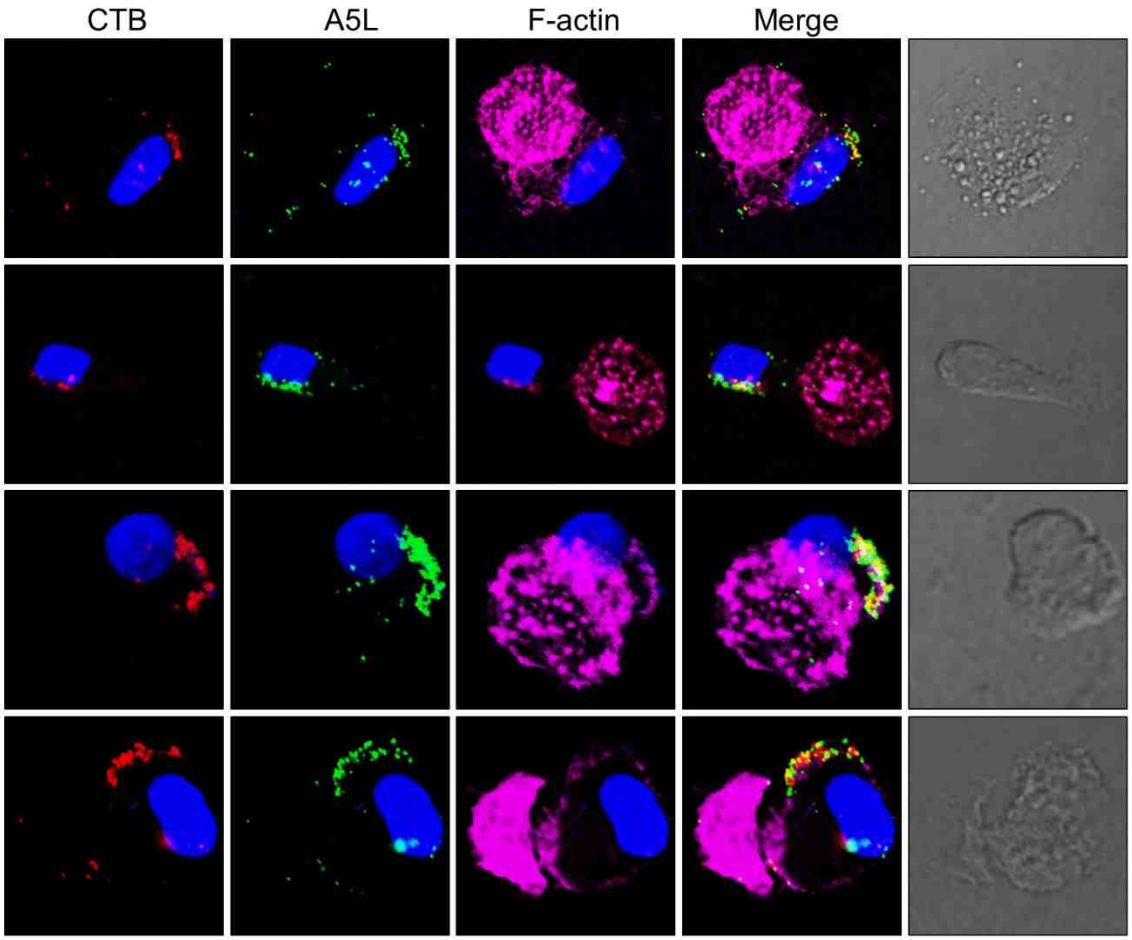

Fig. 16. VV binds to the uropods of macrophages. VV binding to lipid rafts enriched in uropods of polarized monocyte-derived macrophages. Polarized cells were subsequently fixed with 2% PFA and stained with CTB conjugated with Alexafluor 647 (red), phalloidin conjugated with Alexa Fluor 546 to stain actin filaments (violet) and DAPI (blue). Cells were then subjected to VV binding with vA5L-YFP (green) and confocal microscopy analysis.

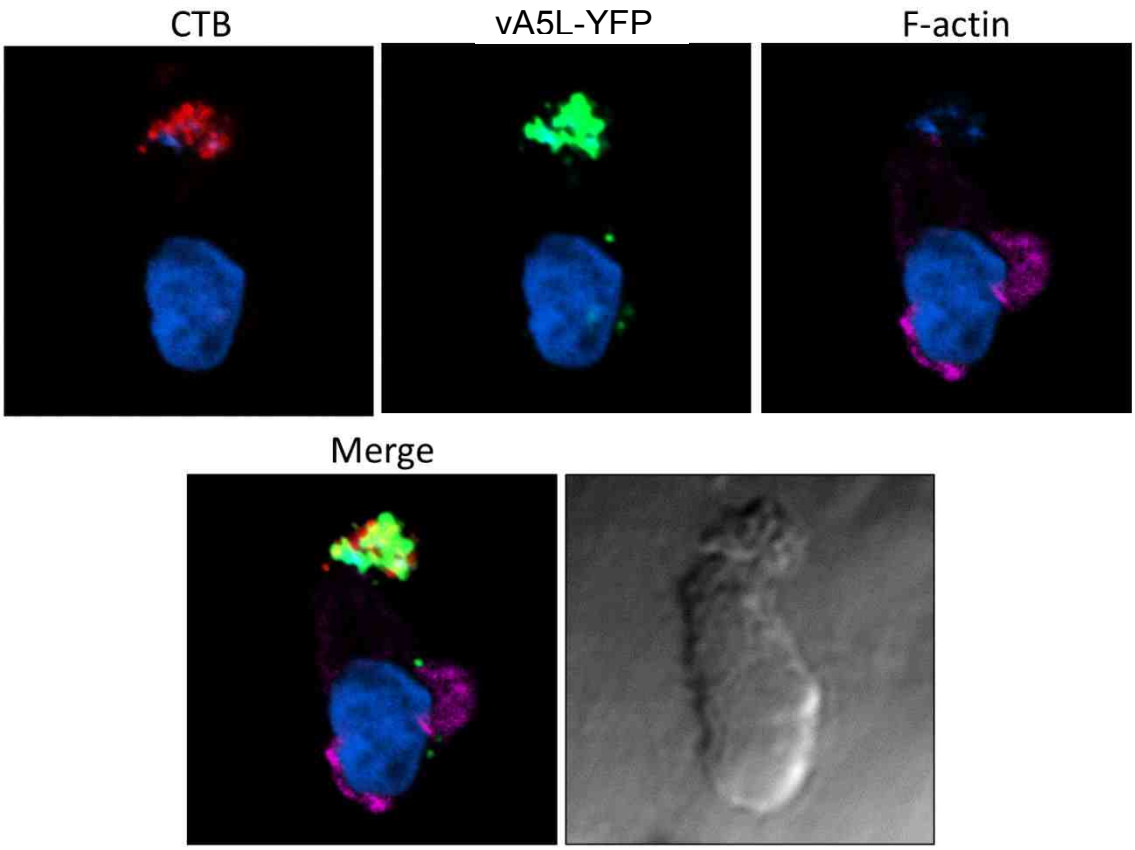

Fig. 17. VV binds to the uropods of polarized B cells. VV binding to lipid rafts enriched in uropods of polarized B cells. Cells were treated with SDF-1 to induce cell polarization. Polarized cells were subsequently fixed with 2% PFA and stained with CTB conjugated with Alexafluor 647 (red), phalloidin conjugated with Alexa Fluor 546 to stain actin filaments (pink), and DAPI (blue). Cells were then subjected to VV binding with vA5L-YFP (green), and confocal microscopy analysis.

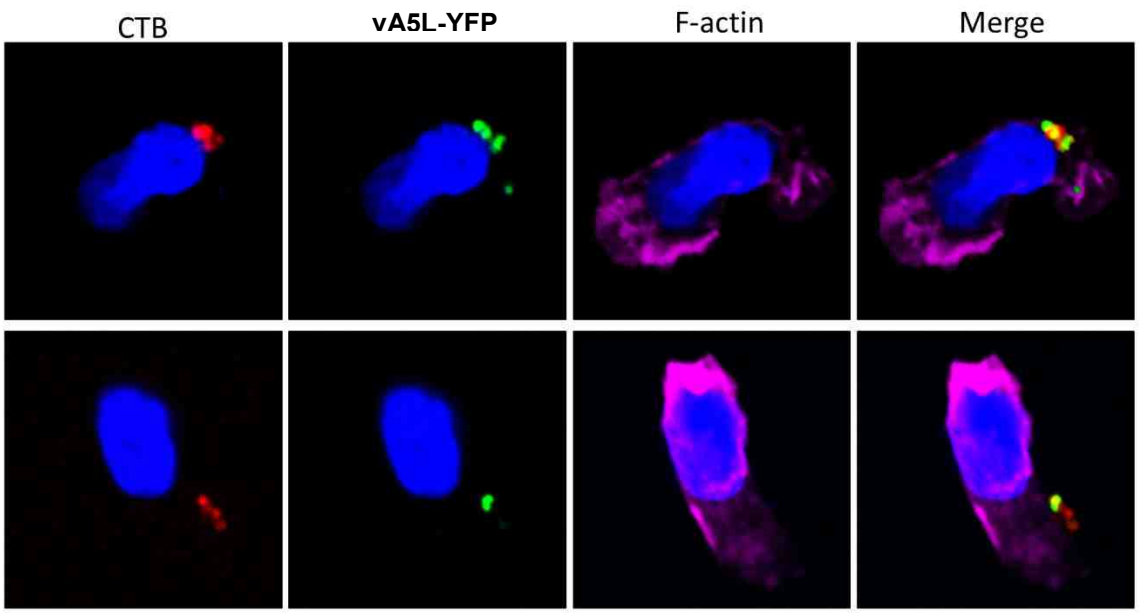

Fig. 18. VV binds to the uropods of polarized activated T cells. VV binding to lipid rafts enriched in uropods of polarized day 3 activated T cells. Cells were allowed to adhere to anti-CD44-coated plates to induce cell polarization. Polarized cells were subsequently fixed with 2% PFA and stained with CTB conjugated with Alexafluor 647 (red), phalloidin conjugated with Alexa Fluor 546 to stain actin filaments (pink), and DAPI (blue). Cells were then subjected to VV binding with vA5L-YFP (green), and confocal microscopy analysis.

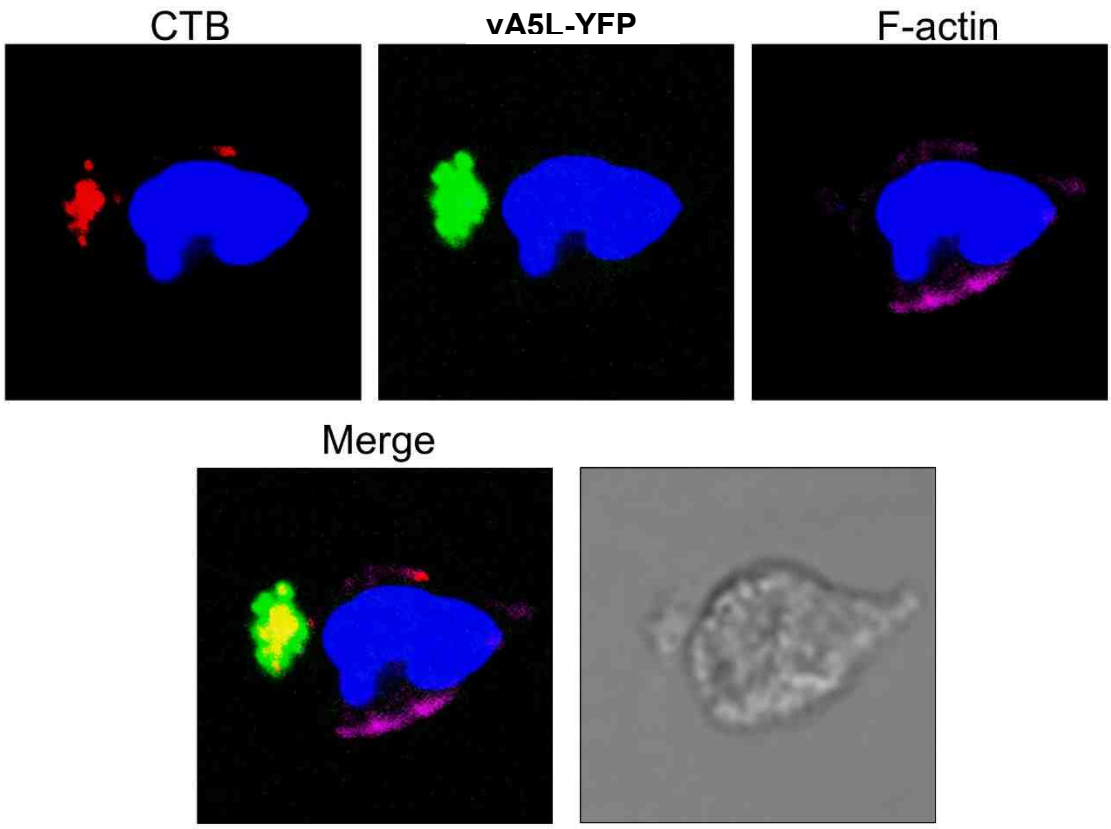

Fig. 19. VV binds to the uropods of polarized neutrophils. VV binding to lipid rafts enriched in uropods of polarized day 3 activated T cells. Cells were treated with bacterial peptide fNLPNTL to induce cell polarization. Polarized cells were subsequently fixed with 2% PFA and stained with CTB conjugated with Alexafluor 647 (red), phalloidin conjugated with Alexa Fluor 546 to stain actin filaments (pink), and DAPI (blue). Cells were then subjected to VV binding with vA5L-YFP (green), and confocal microscopy analysis.

Immunosera raised against DRMs strongly block VV binding

Because VV receptors are strongly associated with lipid rafts in PHLs and are likely proteins or protein modifications, we hypothesized that mouse immunization with DRMs from susceptible PHL subsets would be able to induce Abs that would block VV binding. To this end, we immunized BALB/c mice with DRMs fractionated from monocytes, activated T cells, or resting T cells. Immunosera against DRMs from resting T cells would not block VV binding as resting T cells do not express VV-binding receptors. Immunosera against whole cells or CMEs from monocytes, activated T cells, or resting T cells were also raised to be used as VV-blocking comparisons as a previous study has reported that immunosera against whole monocytes or activated T cells effectively blocked VV binding to activated T cells (56). We found that all immunogens from all cell types effectively elicited pAbs against the CD55 protein (Fig. 20). Because CD55 is associated with lipid rafts, DRMs from all cell types induced the highest titers of anti-CD55 Abs when compared with immunogens of whole cells or CMEs (Fig. 20). Immunosera raised against DRMs, whole cells, or CMEs from monocytes or activated T cells effectively blocked VV binding to monocytes, B cells, and activated T cells (Fig. 21). In contrast, immunosera raised against DRMs, whole cells, or CMEs from resting T cells did not affect VV binding to any of these cell types, which is similar to the results observed from pre-immunization sera. Anti-DRM immunosera exhibited the strongest blockage activity, followed by immunosera against CMEs and then whole cells (Fig. 21). None of the immunosera generated exhibited blocking activity against VV binding to

neutrophils. This result may suggest that VV binds to neutrophils using different receptors than on monocytes and T cells. The inability of immunosera to block VV binding on neutrophils may also be explained by the low basal level of VV binding which may limit the experimental resolution. Concordant with the monocyte binding result, infection of monocytes was drastically reduced when cells were pretreated with anti-DRM immunosera, and to a lesser extent by anti-CME immunosera, but not by immunosera against DRMs or CMEs from resting T cells (Fig. 22A). Notably, anti-DRM immunosera did not affect endocytosis of latex beads (Fig. 22B), whereas cytochalasin D, a known endocytosis inhibitor, effectively blocked endocytosis of latex beads (Fig. 22B). Thus, immunosera raised against DRMs from monocytes or activated T cells effectively blocked VV binding to and infection of VV-susceptible PHL subsets. The blocking activity is significantly higher than that mediated by immunosera raised against CMEs or whole cells. These results suggest that VV receptors are enriched in DRMs, and these receptors are shared by the virus-susceptible subsets of PHLs.

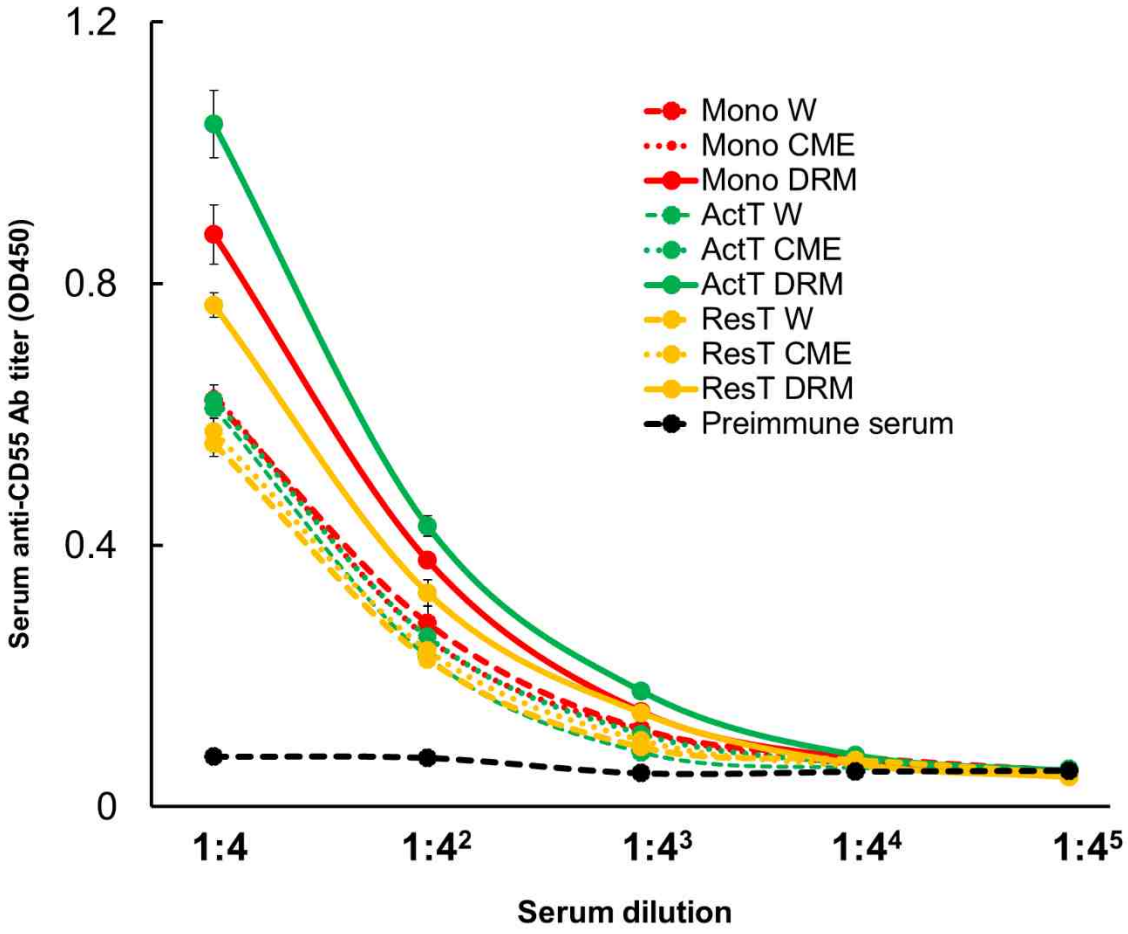

Fig. 20. Immunosera derived from DRM is more reactive against raft-specific CD55. Titers of anti-human CD55 Abs in immunosera raised against DRMs, CMEs, or whole cells from monocytes, resting T cells or activated T cells were determined using an ELISA assay. Mono W, whole monocytes; Mono CME, monocyte crude membrane extracts (CMEs); Mono DRM, monocyte detergent-resistant membranes (DRMs); ActT W, whole activated T cells on day 3 of activation; ActT CEM, activated T cell CMEs, ActT DRM, activated T cell DRMs, ResT W, whole resting T cells, ResT CME, resting T cell CMEs, ResT DRM, resting T cell DRMs, Pre, preimmune serum.

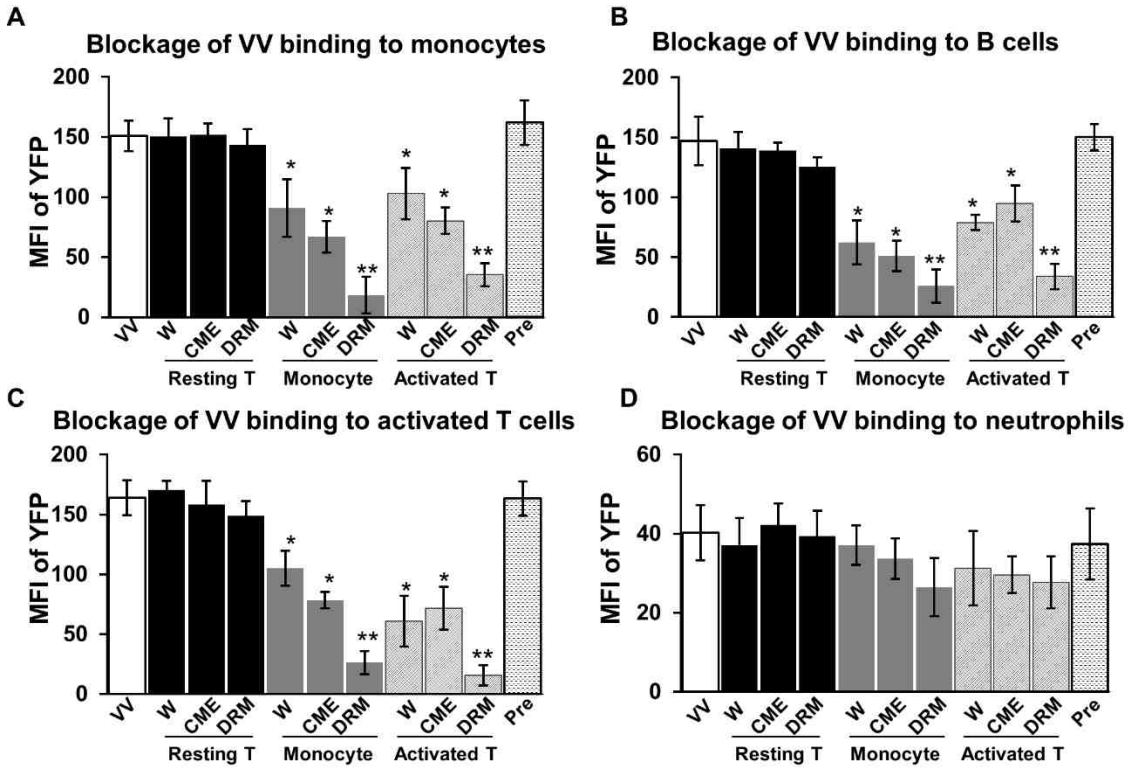

Fig. 21. Blockage of VV binding with immunosera against DRM. Diluted immunosera at 1:10 in PBS were used to block VV binding to monocytes (A), B cells (B), activated T cells (C), and neutrophils (D). The mean fluorescence intensity (MFI) of YFP represents VV binding intensity to PHL subsets of 6 blood donors. Mono, monocytes; ActT, activated T cells on day 3 of activation; ResT, resting T cells; W, whole cells; CME, crude membrane extracts; DRM, detergent-resistant membrane; Pre, preimmune serum. *p<0.05, and **p<0.01.

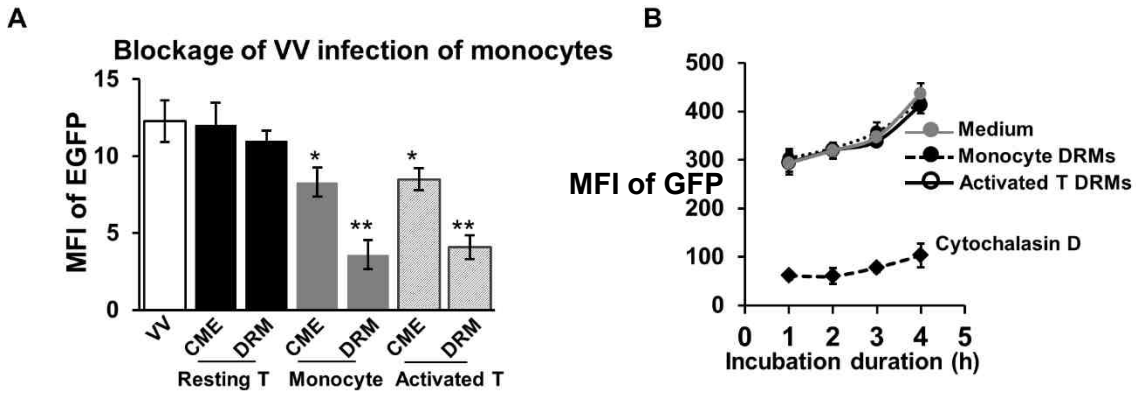

Fig. 22. Blockage of monocyte infection with immunosera against DRM. (A) Diluted immunosera at 1:10 in PBS were used to block VV infection of monocytes. (B) Effects of diluted immunosera at 1:10 in PBS and cytochalasin D on monocyte endocytosis of latex beads. The MFI of EGFP represents VV infection intensity to PHL subsets of six blood donors. CME, Crude membrane extract; DRM, detergent-resistant membrane. *p<0.05, and **p<0.01.

Immunosera depleted with VV-susceptible PHL subsets lose blocking activity against VV binding

To further test whether monocytes, activated T cells, and B cells share VV receptors, we pre-incubated anti-DRM immunosera with monocytes or activated T cells to deplete Abs in these immunosera. We found that anti-DRM immunosera depleted with either monocytes or activated T cells, but not resting T cells, profoundly reduced activity in blocking VV binding to all cell types examined including monocytes (Fig. 23A), B cells (Fig. 23B), and activated T cells (Fig. 23C). PHL subsets from six healthy donors were used in the Ab depletion. These results further indicate that VV receptors are enriched in lipid rafts and are protein or protein-mediated, and that efforts to identify poxvirus receptors. Thus, the study of interactions of individual poxvirus proteins with viral receptors should be focused on DRMs instead of soluble membrane proteins extracted from target cells by non-ionic detergent lysis methods.

This conclusion adds to the knowledge of characteristics of VV receptors on PHLs, where: (1) receptors are mainly expressed on monocytes, B cells, and neutrophils in peripheral blood; (2) receptors are expressed *de novo* following T cell activation; (3) receptors are upregulated on $CD16^-$ monocytes versus $CD16^+$; (4) receptors are lipid raft-associated. Using these criteria, a list of putative VV receptors was made using mass spectrometry or RNA-seq data from previous studies (Table 1). Proteins were selected based on their presence in monocyte detergent-resistant membranes (98), the upregulation on $CD16^-$ vs. $CD16^+$

monocytes (99) , and the upregulation on activated T cells vs. naïve T cells (100).

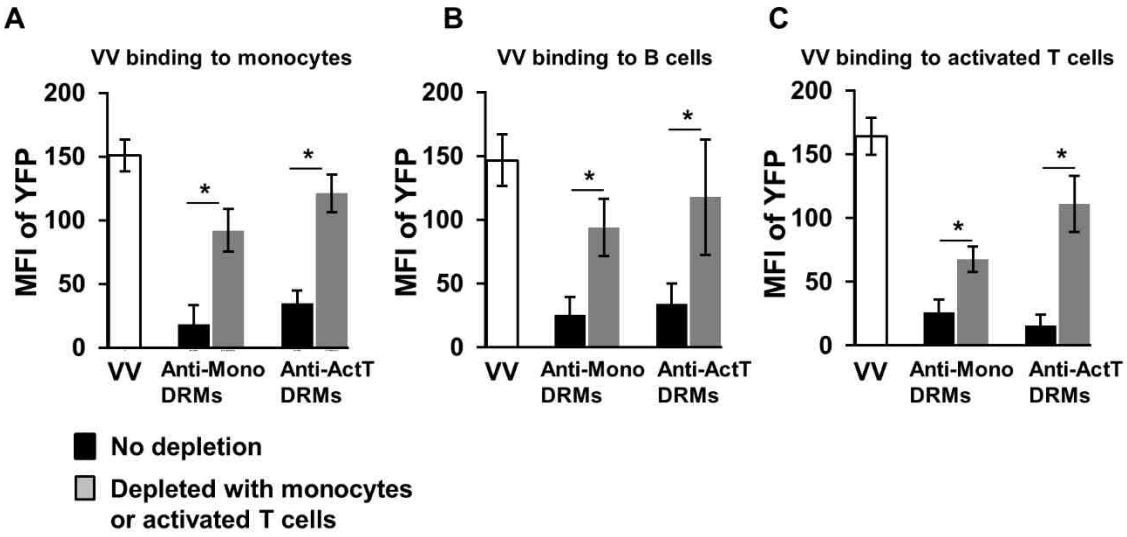

Fig. 23. Immunosera depleted with VV-susceptible PHLs subsets reduced their blocking activity against VV binding. Immunosera raised against DRMs from monocytes were diluted 1:10 in PBS, and then were treated with activated T cells ($40x10^6$); alternatively, immunosera raised against DRMs from activated T cells were treated with monocytes ($40x10^6$) to deplete Abs. Ab-depleted immunosera were then used to block VV binding to monocytes (A), B cells (B), and activated T cells (C). The MFI of YFP represent VV binding to PHL subsets of six blood donors. Data were compared using Tukey's ANOVA assay. Anti-M DRMs, immunosera raised against DRMs of monocytes were incubated with activated T cells to deplete Abs; Anti-Act T DRMs, immunosera raised against DRMs of activated T cells were incubated with monocytes to deplete Abs; *p<0.05.

Table 1. Partial list of lipid raft-associated proteins expressed on different PHL subsets.

Raft-associated proteins	Monocytes	Upregulated on CD16- monocytes	Activated T cells	B cells
Alpha enolase	x	x	x	x
Annexin VI	x	x	x	x
ATP1A1	x		x	x
Carboxypeptidase M	x	x		
Catenin, alpha 1	x		x	x
CAP1	x	x	x	x
***CCR5**	x	x	x	
CD11b	x	x	x	x
***CD18**	x		x	x
CD1d	x	x		x
***CD9**	x	x	x	x
***CD29**	x		x	x
***CD33**	x	x		
CD36	x	x		
CD44	x	x	x	x
***CD98**	x		x	x
CXCR1	x	x	x	
Flotillin 1	x	x	x	x
Flotillin 2	x		x	x
Galectin-9	x		x	
IL-13Rα1	x	x	x	x
Lamp 2	x		x	x
LDLR	x		x	x
Syntaxin 7	x		x	x

A list of putative VV receptors was made using mass spectrometry or RNA-seq data from previous studies. Proteins were selected based on the presence in monocyte detergent-resistant membranes (98), the upregulation on $CD16^-$ vs. $CD16^+$ monocytes (99) , and the upregulation on activated T cells vs. naïve T cells (100). ***Boldface** indicates that the protein was further investigated in this chapter. x, protein is expressed on the cell type surface.

Lipid raft-associated proteins CD29 and CD98 are not directly involved in VV binding

The lipid raft-associated proteins CD29 and CD98 in HeLa cells and mouse embryonic fibroblasts (MEFs) were demonstrated to play a critical role in VV entry into these cells, as knockdown or knockout of these proteins significantly reduce VV entry (101, 102). In addition, VV entry into GD25 cells (a mouse cell line that is deficient in CD29 expression) was less efficient than entry into GD25β1A cells (GD25 cells expressing human CD29) (101). We then wanted to determine whether these two lipid raft-associated proteins also play a role in VV binding, entry, and infection in PHLs. We found that knockdown of either CD29 or CD98 in HeLa cells (Fig. 24A) or activated T cells (Fig. 24B) did not affect VV binding to these cells (Fig. 24C, 24D). However, knockdown of CD29 or CD98 in HeLa cells reduced EGFP-VV infection, as MFI of EGFP was significantly reduced in HeLa cells transfected with siRNA constructs against human CD29 or CD98 (Fig. 24C), this result is consistent with the previous reports (101, 102). In contrast, knockdown of CD29 or CD98 in activated T cells had no effect on VV infection (Fig. 24D). In fact, CD29 expression on the surface of HeLa cells pre- or post-knockdown of CD29 had no correlation with VV binding, as both the CD29-negative and CD29-positive population did not show any difference in VV binding (Fig. 24E).

These results are in agreement with previous reports showing that CD29 and CD98 are important for VV infection in HeLa cells through mediating VV entry, but these two proteins have no effect on VV binding, entry, and infection of

primary human T cells, although they are highly expressed on activated T cells. Notably, VV binding and CD29 expression were highly correlated on activated T cells (Fig. 24E). VV binding was also previously shown to correlate with T cell activation markers CD25 and CD69 (56). The apparent correlation with VV binding and CD29 cannot be used to suggest CD29 as a VV receptor because CD29 is also expressed on naïve cells (103) and level of expression correlates with T cell activation (104), as well as with CD25 and CD69 (103).

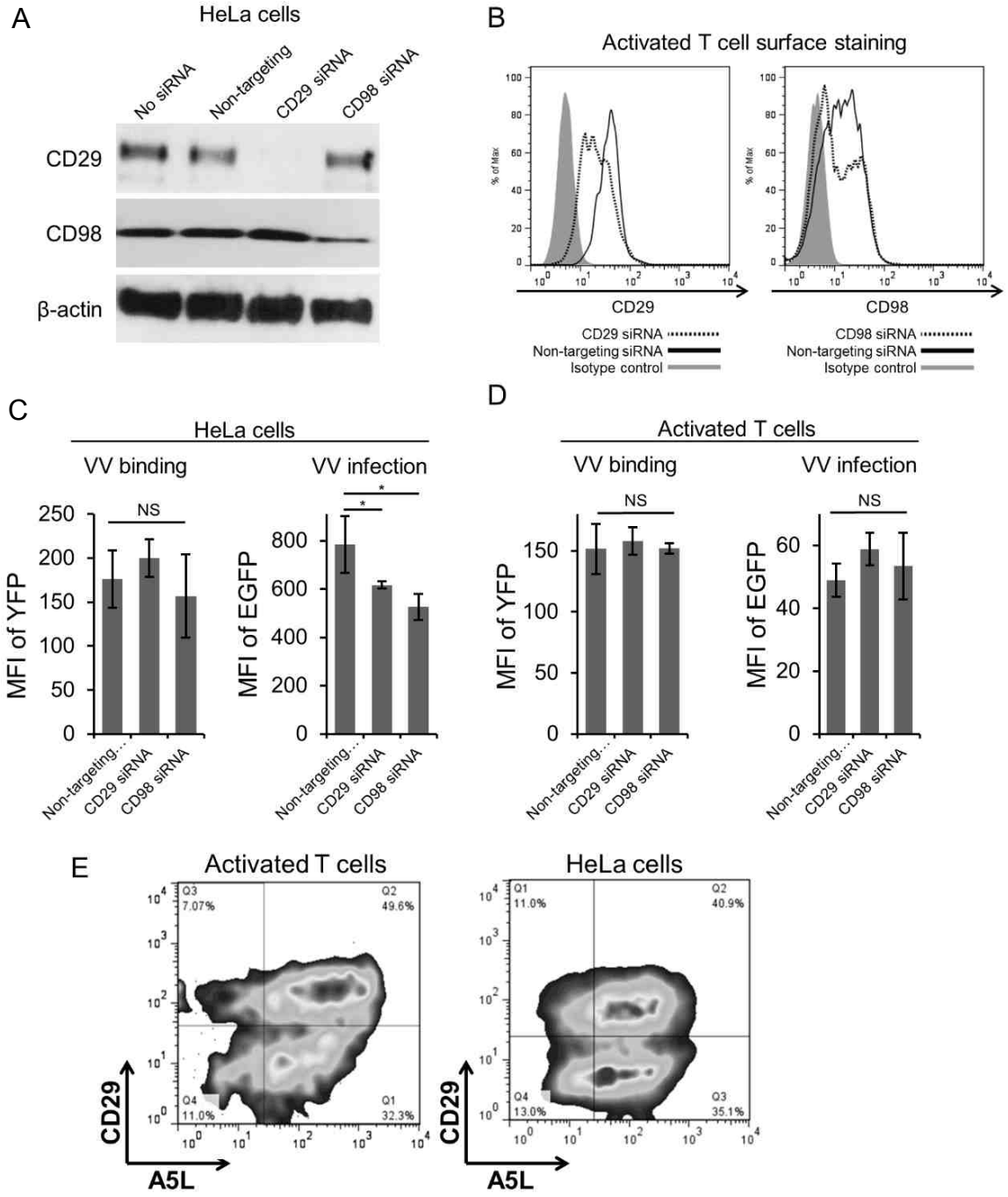
A
HeLa cells
No siRNA
Non-targeting
CD29 siRNA
CD98 siRNA
CD29
CD98
β-actin
B
Activated T cell surface staining
% of Max
CD29
CD98
CD29 siRNA
Non-targeting siRNA
Isotype control
CD98 siRNA
Non-targeting siRNA
Isotype control
C
HeLa cells
VV binding
VV infection
MFI of YFP
MFI of EGFP
NS
*
*
Non-targeting...
CD29 siRNA
CD98 siRNA
D
Activated T cells
VV binding
VV infection
MFI of YFP
MFI of EGFP
NS
NS
Non-targeting...
CD29 siRNA
CD98 siRNA
E
Activated T cells
HeLa cells
Q3
7.07%
Q2
49.6%
Q4
11.0%
Q1
32.3%
Q1
11.0%
Q2
40.9%
Q4
13.0%
Q3
35.1%
CD29
A5L

Fig. 24. Knockdown of the raft-associated factors CD29 and CD98 has no direct effect on VV binding. HeLa cells and primary human activated T cells were transfected with siRNA against CD29 and CD98 and the level of knockdown was measured by Western blot on HeLa cells (A) and surface expression by FACS on activated T cells (B). A VV binding assay with vA5L-YFP and infection assay with VV-EGFP were performed on HeLa (C) and activated T cells (D) to observe the effects on infection after siRNA knockdown. (E) A flow cytometry plot of HeLa cell CD29 surface staining versus vA5L-YFP showing the relationship between CD29 expression and VV binding. *p<0.05. NS, not significant.

Polyclonal antibody blockage of specific host surface proteins

Our data suggested several interesting candidates for protein VV receptors (Table 1). To test the potential binding of VV to particular protein species, we attempted to block VV binding by first pretreating cells with pAbs raised against full-length or extracellular domains of human membrane proteins of interest. Panels of pAbs included targets with surface expression patterns matching patterns of VV binding to PHL subsets, including: lipid raft-associated proteins CD9, CD33, CCR2, CCR5; adhesion molecules Integrin αL, integrin β1, CD169; and GPI-anchored proteins CD14, CD52, CD55, and CD59. None of the pAbs tested demonstrated aberrant VV binding measured by FACS (Fig. 25).

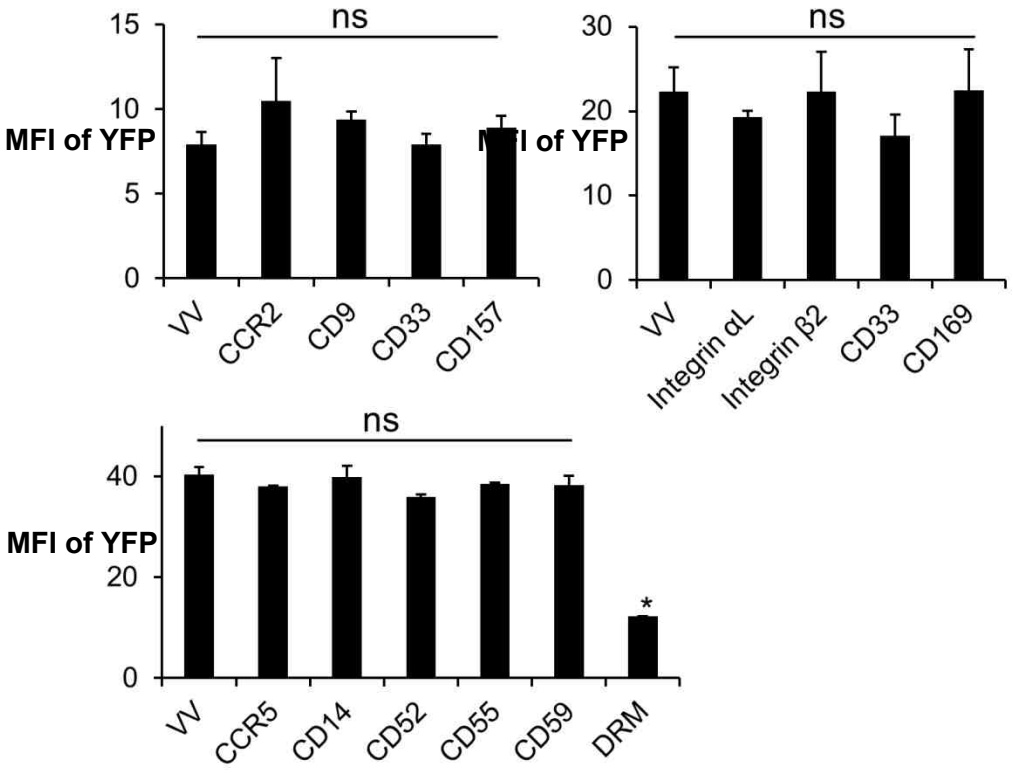

Fig. 25. Polyclonal antibody blockage against lipid raft-related surface proteins. Lipid raft-related human proteins of interest were targeted by pAb treatment to block VV binding. In three separate experiments, primary human monocytes were treated with different panels of pAbs and subjected to a VV binding assay with vA5L-YFP. Degree of binding was related by measuring the MFI of YFP. *p>0.05. VV, vaccinia virus; DRM, detergent-resistant membrane; ns, not significant.

M1- and M2-polarized macrophages are permissive to VV replication

It was previously reported that VV exhibits an abortive infection in primary human MDMs derived from peripheral blood monocytes by culturing them in media containing 10% human AB serum (45). We infected human AB serum-derived MDMs with VV WR at an MOI of 5 for 3 h to 48 h and found that VV did not replicate as virus plaque numbers did not increase (Fig. 26A), thus corroborating this prior report (45). Compared to MDMs generated with human AB serum, it is known that supplementation of media with GM-CSF or M-CSF generates M1- or M2-polarized cells, respectively, and promotes cell survival (105). After deriving MDMs with these cytokines, both M1 and M2-polarized MDMs expressed the low-density lipoprotein (LDL)-binding glycoprotein CD68, a common macrophage marker, whereas only M-CSF-polarized cells markedly expressed the scavenger receptor CD163, a surface marker for M2 MDMs (Fig. 26B). In contrast to MDMs derived from human AB serum, GM-CSF and M-CSF-derived MDMs were permissive to VV (Fig. 26C). At an MOI of 5, GM-CSF-polarized cells produced 11.3 ± 2.1 PFU per cell at 24 h and 15.3 ± 1.2 PFU per cell at 48 h. M-CSF-polarized cells produced 24.5 ± 2.3 PFU per cell at 24 h and 31.7 ± 3.1 PFU per cell at 48 h. In comparison, HeLa cells, a human epithelial carcinoma cell line widely used for VV infection and replication, produced 44.0 ± 6.0 PFU per cell at 24 h and 56.7 ± 5.5 virions per cell at 48 h. Primary T cells activated with anti-CD3 and anti-CD28 antibodies were also productive as previously reported (56), but only produced 1.8 ± 0.8 PFU per cell at 24 h and 3.3 ± 1.5 PFU per cell at 48 h (Fig. 26C). Thus, VV efficiently replicates in primary

human M1 and M2 cells, relatively less efficiently in activated T cells, but does not replicate in human AB serum-derived MDMs.

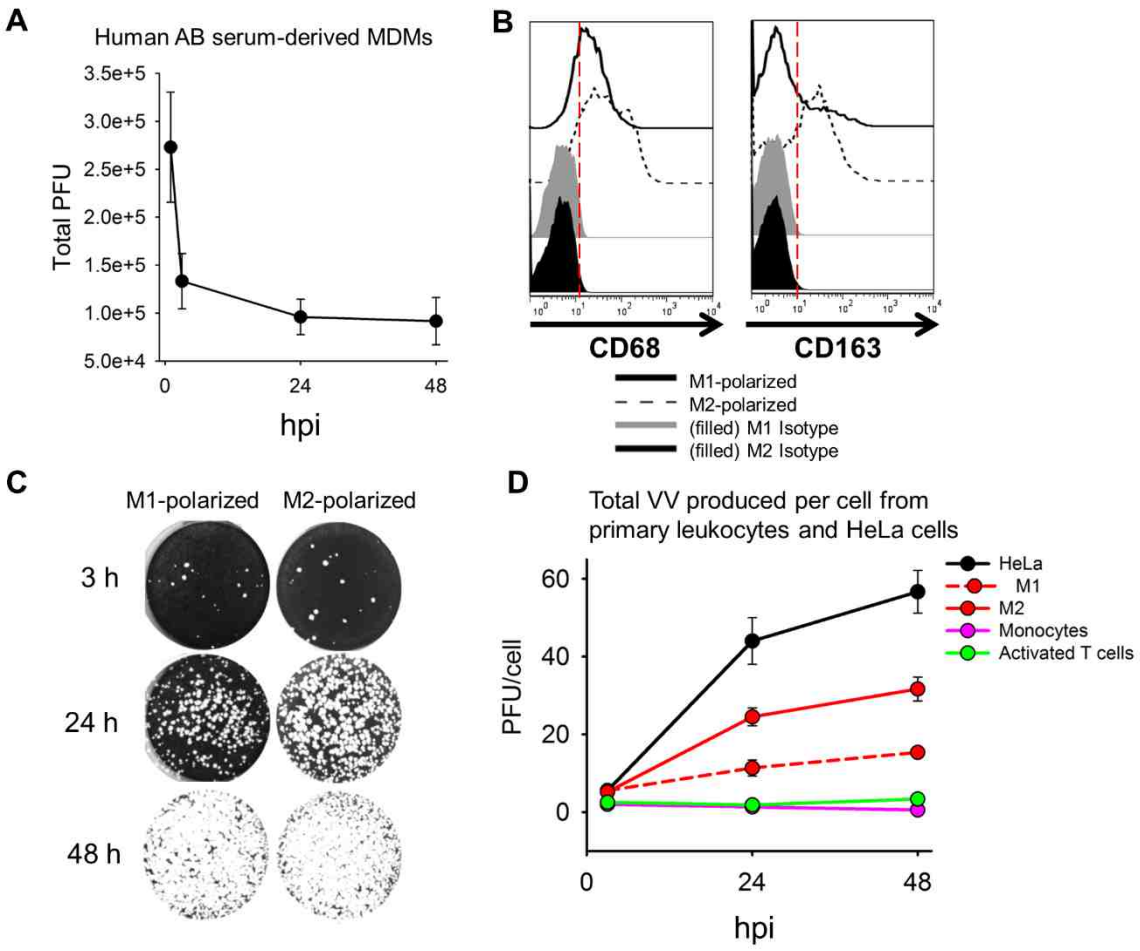

Fig. 26. VV replicates in GM-CSF or M-CSF-derived MDMs. MDMs derived from human serum AB (A) or with GM-CSF or M-CSF (C) were infected with 5 MOI of VV WR and virus was extracted from cell lysates at 3, 24, and 48 h of post infection. (B) CSF-derived MDMs were surface stained for the human macrophage marker CD68, and the M2-specific marker CD163 and analyzed by FACS. (D) The viral titers produced per cell of a variety of primary macrophages and HeLa cells were compared by infecting cells at 5 MOI and determined by plaque assays on the cell lysates at 3, 24, and 48 h of post-infection. All data are representative of cells derived from five blood donors. hpi, hours post-infection.

To understand whether the different degrees of VV replication in the three types of MDMs (M1, M2, and human AB serum-derived MDMs) are directly related to the efficacy of virus binding and infection, MDMs were infected with VV-EGFP, a VV WR containing an EGFP reporter gene regulated under a VV early/late promoter, for a short period (< 6 h), or incubated with vA5L-YFP under binding conditions (on ice for 30 min). EGFP-positive or YFP-positive cells were quantified by FACS. No significant differences in either early infection or virus binding were observed among these three MDM types (Fig. 27), suggesting that VV binding and early infection is comparable among human AB serum, GM-CSF, and M-CSF-derived cells. VV infection was previously reported to induce apoptosis in the murine macrophage cell line J774.G8 (106). To investigate the fates of VV infection in primary human cells, apoptosis was monitored by intracellular staining of active caspase-3. No significant levels of caspase-3-positive MDMs were detected and did not increase within two days of infection (Fig. 28A). This result is in contrast to uninfected primary human monocytes that are known to undergo spontaneous apoptosis in culture (107). Additionally, infected MDMs were stained with PI to detect necrotic cells and no increase in PI-positive cells was observed (Fig. 28B). This result is concordant with observations that cell numbers were never significantly decreased throughout the two-day infection and no nucelosomal units or apoptotic bodies were observed throughout extensive viewing with confocal microscopy. It is notable that detection of surface phosphatidylserine with annexin-V was not an appropriate assay for this experiment, as VV was found to contain phosphatidylserine in the

virion outer membrane (108, 109). We found that most cells were positive for annexin-V staining after virus binding and throughout the infection (data not shown). Therefore, MDMs derived from human AB serum, GM-CSF, or M-CSF treatment have a similar degree of early infection and binding, and do not undergo apoptosis within 2 days of infection.

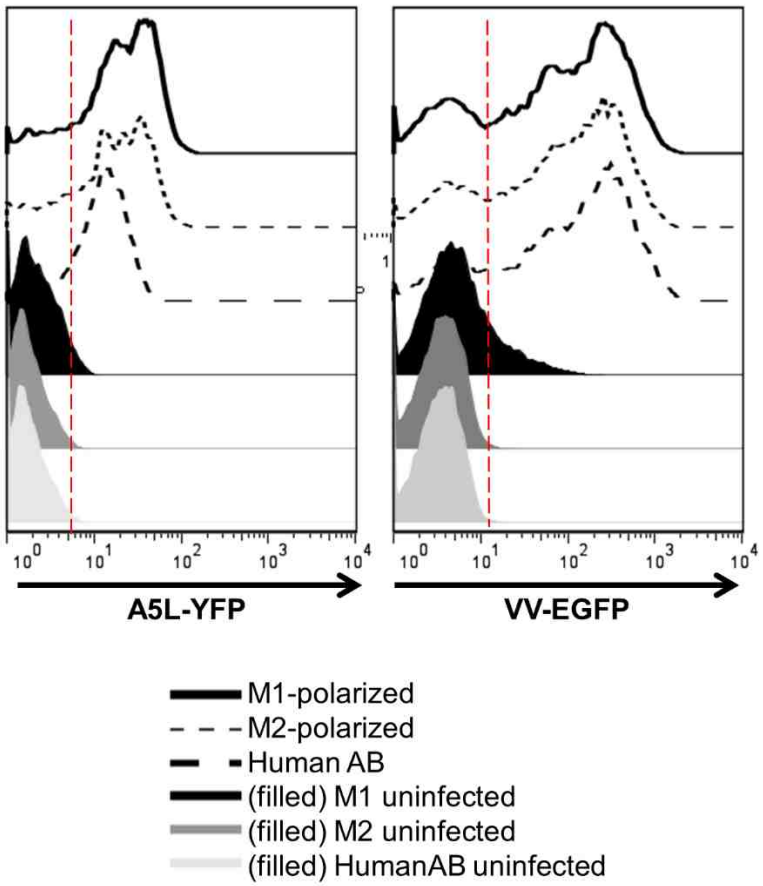

Fig. 27. VV binding and infection of human serum- and CSF-derived MDMs. The degrees of VV binding to and early infection of MDM subtypes were determined by FACS. MDM subtypes were incubated with vA5L-YFP at an MOI of 5 on ice for 30 min or with VV-EGFP at an MOI of 5 for 6 h and then subjected to FACS to determine the efficacy of VV binding and early infection. All data are representative of cells derived from five blood donors.

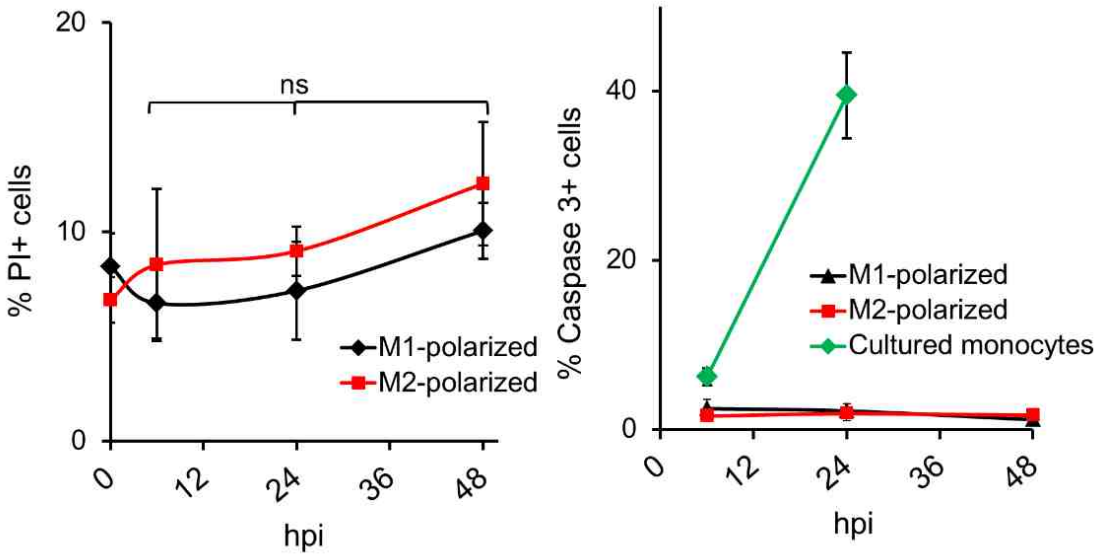

Fig. 28. VV infection does not induce apoptosis in MDMs. Necrosis and apoptosis of infected monocytes and MDMs were detected using PI staining and intracellular caspase-3 staining at 6 h, 24 h, and 48h post-infection. All data are representative of cells derived from five blood donors. hpi, hours post-infection; ns, not significant.

Virus factories, actin tails, and branching structures are formed in VV-infected macrophages

Since we found that primary macrophages are permissive to VV, we sought to find VV-associated structures previously discovered in infected cell lines. The first structure we searched for was actin tails. Virions attached to the cell surface induce intracellular signaling along with VV early proteins to induce the polymerization of actin to extend the membrane under the attached virions to thrust them far away from the main cell body (110). These actin tails are strongly associated with cell-to-cell spread of VV (11). Additionally, between 2 – 6 h post-infection, perinuclear regions in the cell where poxvirus DNA replication takes place become wrapped with membrane from the endoplasmic reticulum (ER) (7). These regions become the main sites of poxvirus assembly and are referred to as virus factories (7). Although virus factories and actin tails are well documented in VV-infected cell lines, they could not be detected in infected primary DCs (51). To further investigate the cellular effects of VV infection and replication in MDMs, we searched for the presence of these common structures associated with VV-infected cell lines. At various stages of vA5L-YFP infection, monocytes or M2-polarized MDMs were visualized using confocal microscopy. In addition, F-actin was stained with phalloidin conjugated to the fluorophore Alexafluor 647 to observe actin dynamics throughout the infection. In agreement with the results obtained from the virus plaque assay, primary monocytes showed no visible increase in VV particles after 24 h infection (Fig. 29). In contrast, VV replication in MDMs was apparent as cell-associated virions increased (Fig. 29).

Characteristically, VV infection in cell lines such as HeLa cell leads to the formation of perinuclear virus factories that co-opt a section of the ER for VV DNA replication and initial virus assembly (7). After 24 h infection, perinuclear VV factory structures with high levels of L1 expression were observed in M2-polarized MDMs (Fig. 30), but not in monocytes (Fig. 29). These perinuclear factory structures in M2 MDMs exhibited DAPI staining, indicating VV DNA replication (Fig. 30).

CEV virions in cell lines protrude from the cell surface via actin polymerization (111). This process requires certain host factors such as Abl tyrosine kinases (112) and the products of VV genes A36, A33, A34, and B5R (8). We found that VV virions associated with actin tails in MDMs became visible by 3 h post-infection and persisted throughout the course of infection (Fig. 31). Additionally, VV virions were frequently observed to localize inside projections linking neighboring cells together and in areas with lamellipodia-associated protrusions (Fig. 29, white arrows, Fig. 32). Virus-induced branching between cells also occurred (Figs. 29, 32), which is reminiscent of the elongation and branching observed in infected cell lines such as BS-C-1 (113). The VV-associated lamellipodia and branching may represent a strategy for cell-to-cell transmission, which can be visualized by live imaging assays. The increasing presence of multi-nucleated cells was also evident over the course of infection. Macrophages can fuse together to form multi-nucleated cells (giant cells), and this process is associated with granulomas and may occur in response to presence of foreign bodies and certain pathogens. We found that 4.5 ± 1.6% (n =

6) of cells were multi-nucleated at the start of infection, which increased to 19.4 ± 5.0% (n = 6) after 24 h post-infection (Fig. 33). Together, our data indicate that VV factory formation and VV-associated actin tails occur in infected primary MDMs, but not in primary monocytes. Additionally, VV dissemination may occur through routes of cell-to-cell transmission via actin tails, lamellipodia, or branching structures.

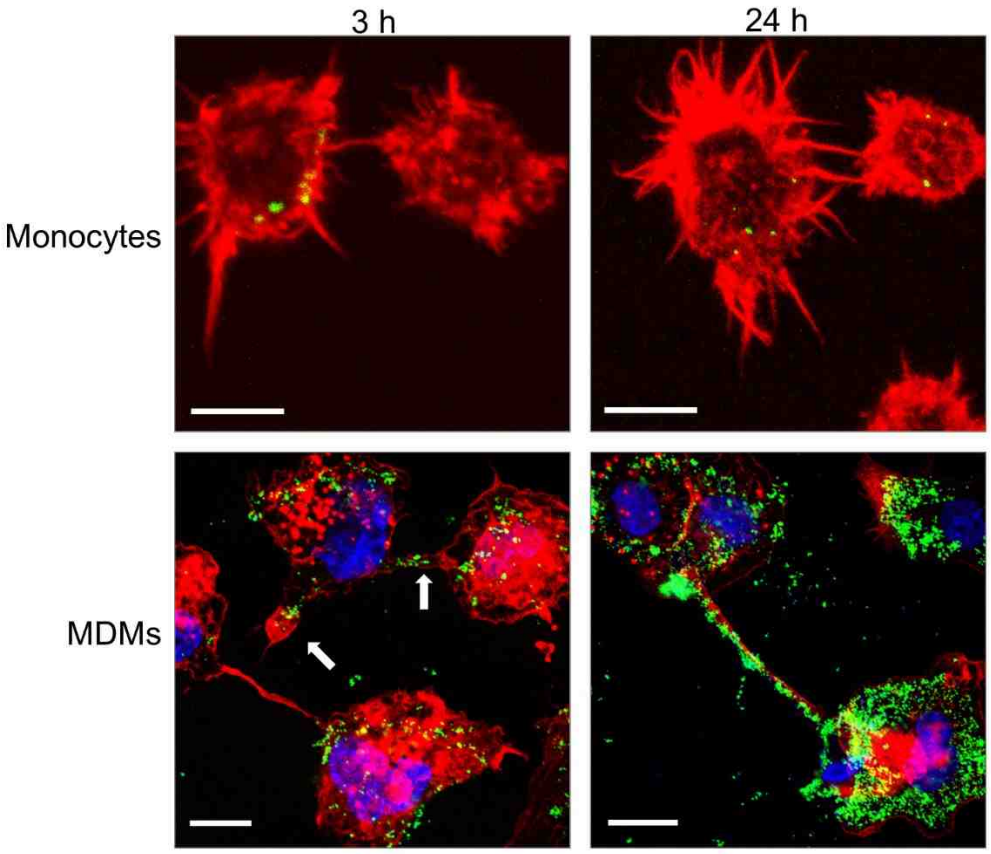

Fig. 29. Virions increase in infected MDMs. Primary monocytes and M2-polarized MDMs were infected with vA5L-YFP (green) at 5 MOI for various time points as indicated and visualized along with F-actin staining with phalloidin (red) and DNA staining with DAPI (blue). Scale bars represent 10 μM. All data are representative of cells derived from five blood donors.

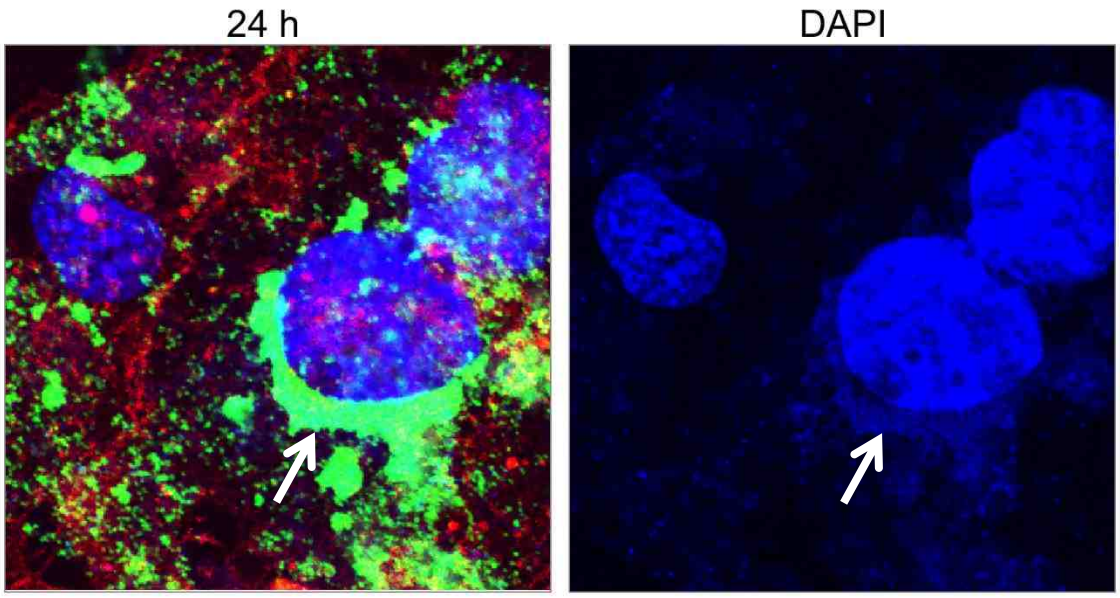

Fig. 30. Virus factories are present in VV-infected MDMs. M2-polarized MDMs were infected with vA5L-YFP (green) at 5 MOI for various time points as indicated and visualized along with F-actin staining with phalloidin (red) and DNA staining with DAPI (blue). Scale bars represent 10 μM. All data are representative of cells derived from five blood donors.

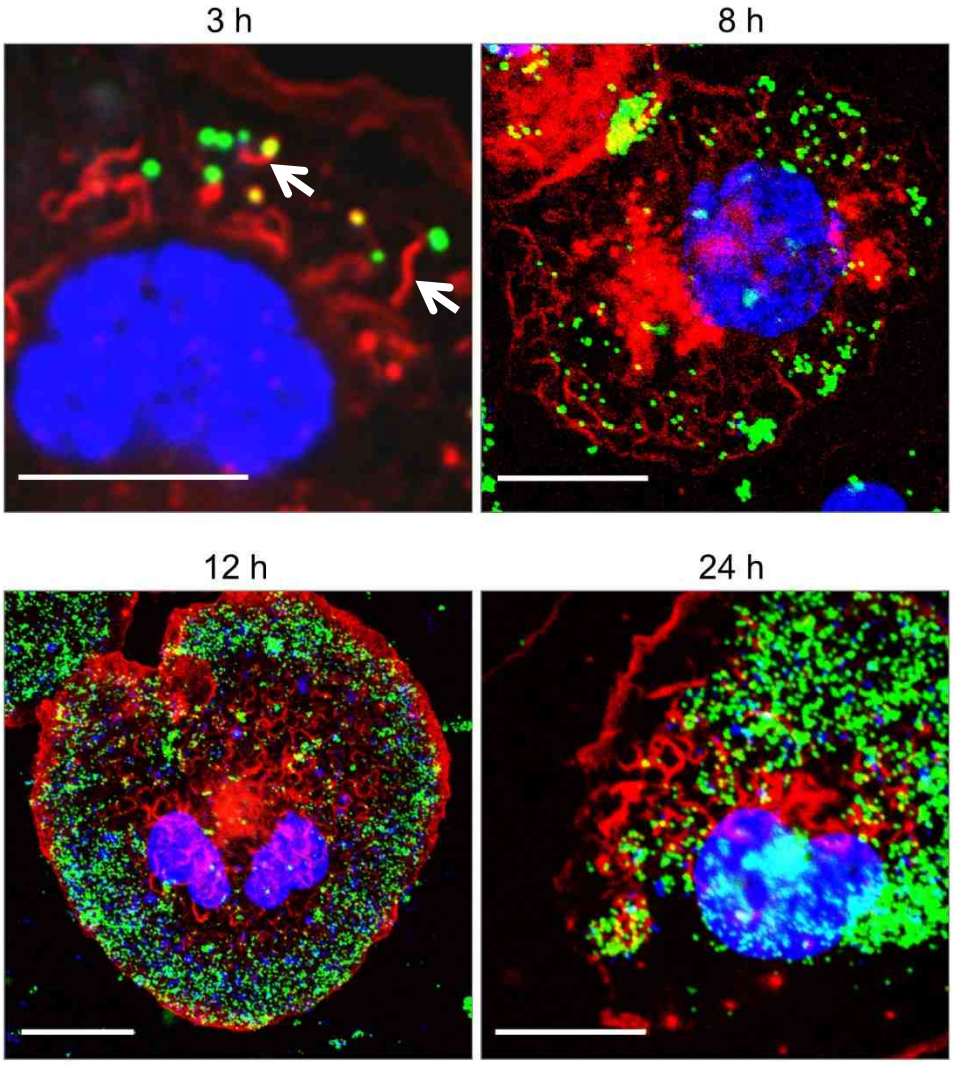

Fig. 31. VV-infected MDMs generate actin tails. M2-polarized MDMs were infected with vA5L-YFP (green) at 5 MOI for the indicated time points and visualized with F-actin staining by phalloidin (red) and DNA staining with DAPI (blue). Scale bars represent 10 μM. All data are representative of cells derived from five blood donors.

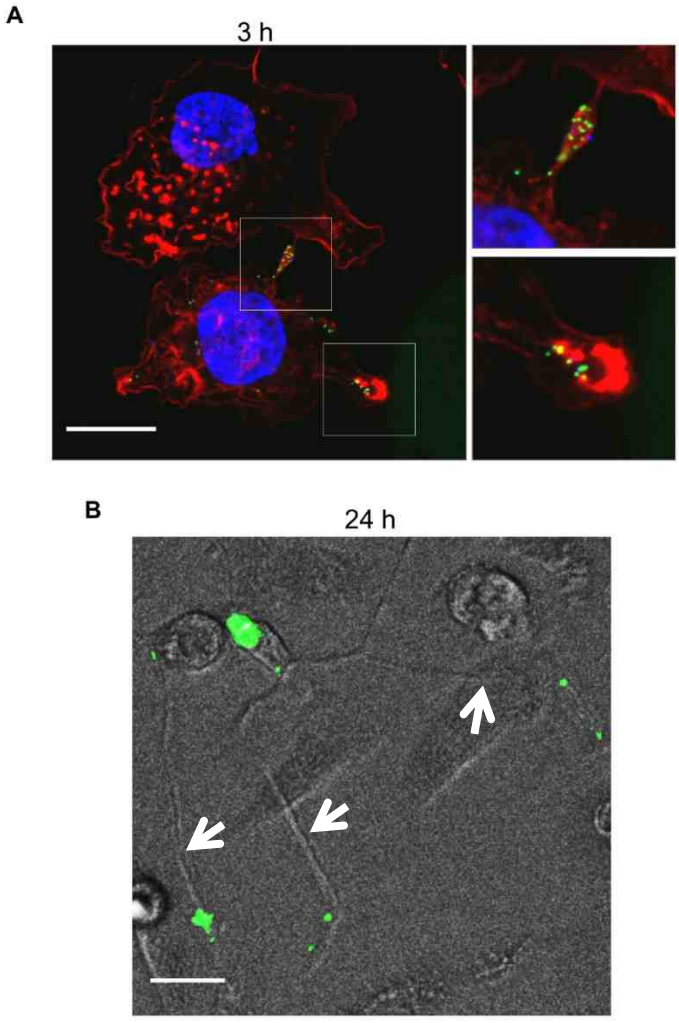

Figure 32. VV associates with cell linking and branching structures. (A) M2-polarized MDMs were infected with vA5L-YFP (green) at 5 MOI for various time points as indicated and visualized along with F-actin staining with phalloidin (red) and DNA staining with DAPI (blue). (B) Transillumination field of A5L-YFP infected M2 MDM. Scale bars represent 10 μM. All data are representative of cells derived from five blood donors.

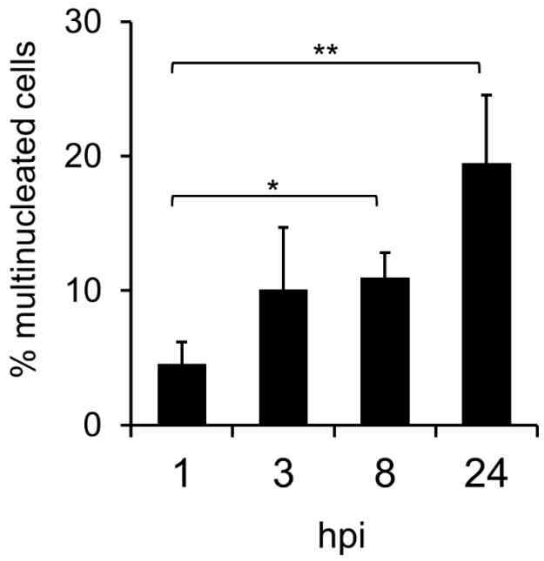

Figure 33. VV-infected MDMs develop giant cells. Giant cell formation throughout VV infection was observed and multinucleated cells counted at various time points. Graph is representative of cells derived from five blood donors. * $p<0.05$, ** $p<0.01$.

MDMs mainly produce enveloped forms of VV

VV titers in culture supernatants and cell pellets from infected M1 and M2-polarized MDMs were analyzed by virus plaque assay, and it was found that supernatants contained more infectious virions than cell lysates (Fig. 34A); specifically, virus titers were 3-fold and 5-fold higher than those from cell lysates of M1 and M2, respectively. Given that a 2-day VV infection did not cause significant cell apoptosis and death that released IMV virions into the culture supernatants, our results suggest that most virions produced in MDMs may be in the form of EEV. The cell-associated virions titrated by the virus plaque assay could either be IMV within the cell, CEV attached to the cell surface, EEV bound to the cell surface, or virus particles from the input of the primary infection. The proportion of intracellular versus extracellular cell-associated virus was determined by confocal microscopy using vA5L-YFP with antibody staining of the VV surface envelope protein L1. By this approach, intact virus particles inside or outside the cells can be visualized with vA5L-YFP, whereas cell surface-attached virions are seen by L1 staining of vA5L-YFP virions. For the first 8 h of infection, 92.8 ± 8.5% of cell-associated virions were extracellular (Fig. 35B, yellow merged from L1 red and YFP green), which was most likely left over from the primary virus input. By 24 h post-infection, the total number of virions was greatly increased and but the percentage of extracellular VV decreased to 45.5 ± 7.0% (Fig. 35B). By 48 h, nearly all of the cell-associated virions were again extracellular, at 87.5 ± 5.2% (Fig. 35B). These data suggest that, by 48 h of infection, nearly all *de novo* cell-associated virus is either CEV or EEV that

reattached to the cell surface. This visualization of cell-associated VV suggests that even the virus derived from cell pellets in Fig. 34A is mostly the double-membraned CEV / EEV form.

To analyze the proportion of double-enveloped forms (CEV and EEV) versus single-enveloped mature forms (IMV), virions were collected from cells and supernatants, purified, combined and separated by a CsCl density-gradient ultracentrifugation. The CsCl density-gradient is able to separate double-enveloped virions (EEV or CEV) that have a lower buoyant density of 1.23-1.24 g/ml from single membrane IMV particles that have a higher buoyant density of 1.27-1.28 g/ml (114). For M2 cells, analysis of fractions from the gradient revealed that most virus particles were enriched in the fraction associated with EEV buoyant density (Fig. 34B), with an estimated 3.8 times the number of VV particles calculated in the IMV form. This is in contrast to VV virions that are produced by the CV-1 cell line (Fig. 34B), with an estimated 4.1 fold higher number of IMV relative to fractions associated with EEV. This result from infected CV-1 cells is typical of most cell lines infected with VV WR. Overall, our results indicate that VV produced in MDMs is mainly EEV released into the supernatant, and that by 48 h of infection most cell-associated VV is on the cell surface.

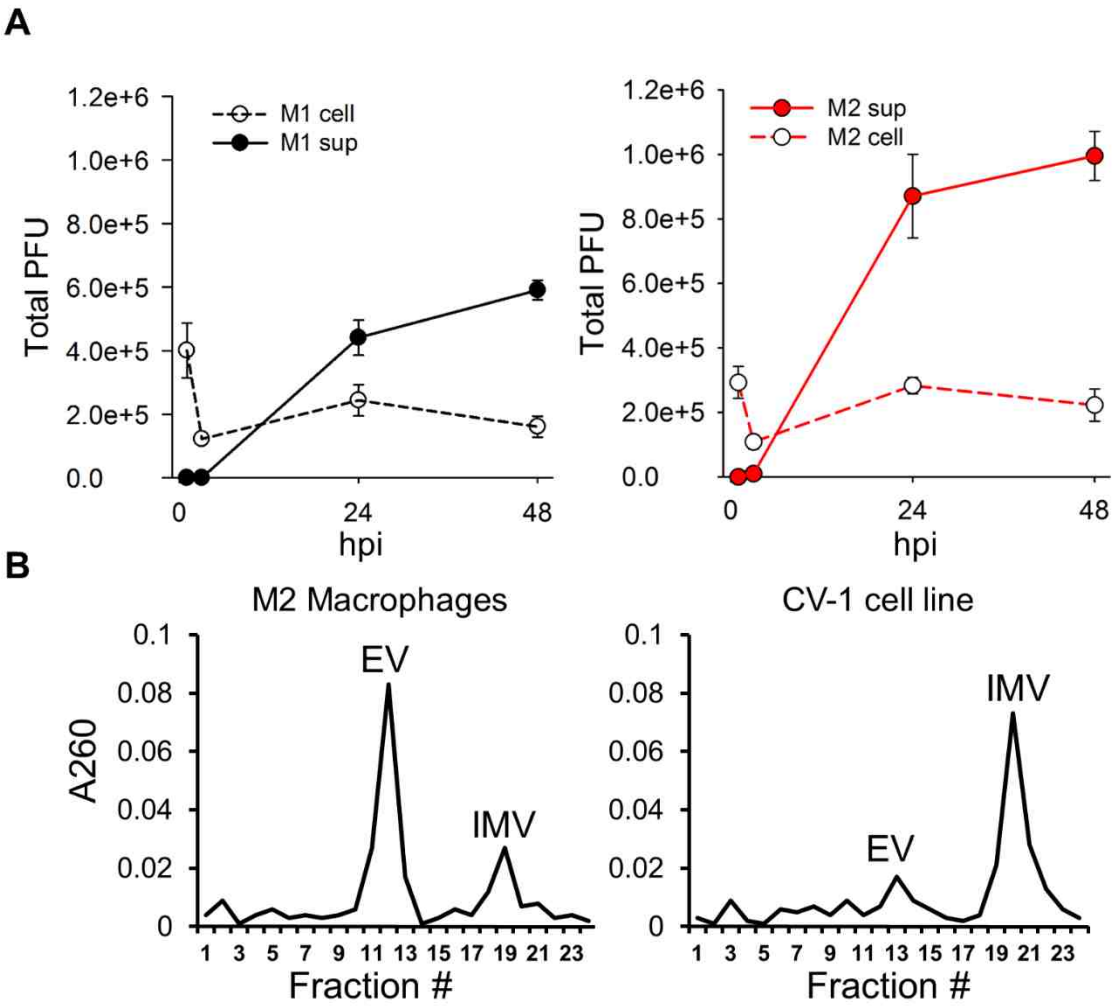

Fig. 34. MDMs mainly produce enveloped forms of VV. (A) M1- and M2-polarized MDMs were infected with VV WR at 5 MOI. Virus was extracted from either cells or culture supernatant at 3, 24, and 48h time points and analyzed by a plaque assay. (B) Purified VV particles from VV WR-infected M2-polarized cells and CV-1 cells were extracted from cell lysates and supernatants and analyzed by separation on a CsCl density gradient. Fractions from the gradients were tested for absorbance at 260 nm to estimate the amount of virus particles corresponding to the buoyant densities of mature or enveloped forms of VV. All data are representative of cells derived from five healthy blood donors. * $p<0.05$.

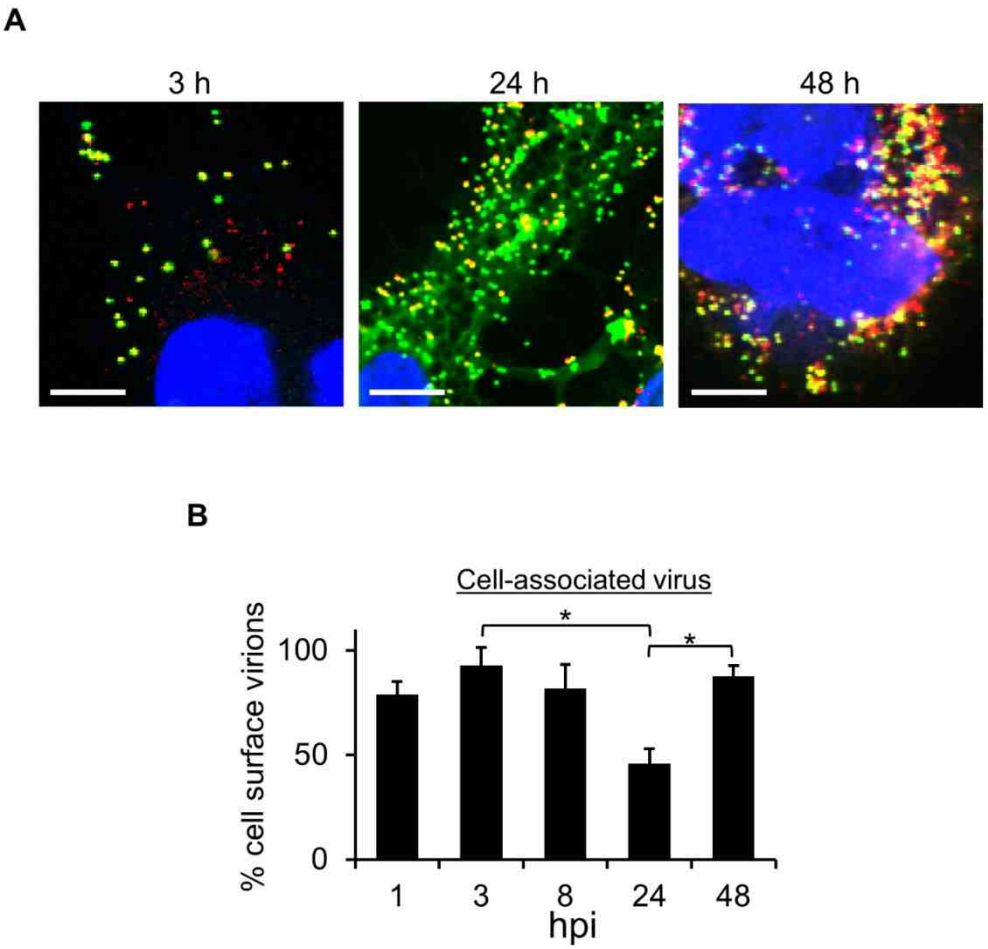

Fig. 35. Cell-associated VV is mainly extracellular 48 h post-infection. (A) M2-polarized cells infected with vA5L-YFP (green) under the same conditions were stained for the VV envelope protein L1 (red) and visualized by confocal microscopy. Scale bars represent 10 μM. (B) The number of extracellular (A5L + L1 staining) and intracellular (A5L alone) cell-associated virions were counted at different time points as indicated. All data are representative of cells derived from five healthy blood donors. * $p<0.05$. hpi, hours post-infection.

VV-associated signaling pathways are required for virus replication in MDMs

VV is dependent on Erk1/2 and Akt signaling pathways for entry and replication (115-118). Additionally, contrasting reports describe the SAPK/JNK pathway as either supportive for VV replication (119) or having no effect (120). VV infection also activates MKK4/7 for the JNK1/2 pathway which is important for changes in host cell motility and branching in mouse embryonic fibroblasts (MEFs) (120). To analyze the dependence of these three pathways on VV replication in MDMs independent of binding and entry, M2-polarized cells were infected with VV at an MOI of 5 for 3 h and then treated with various concentrations of the Akt inhibitor LY294002 and the Erk1/2 inhibitor PD98059. We found that both inhibitors reduced virus replication in a dose-dependent manner, suggesting that Akt and Erk pathways play a critical role in VV replication in MDMs (Fig. 36B), which is in agreement with the results obtained from VV infection in cell lines. Interestingly, the effects of both GM-CSF and M-CSF on MDM differentiation and maturation are partly through activation of the Akt and Erk pathways. We also found that VV replication was markedly inhibited by the JNK1/2 inhibitor SP600125 in a dose-dependent manner (Fig. 36B). SP600125 was previously found to decrease VV and cowpox replication in cell lines, but the same degree of inhibition was observed in JNK1 and JNK2-knockout MEFs (121), which strongly suggests a JNK1/2-independent effect of SP600125.

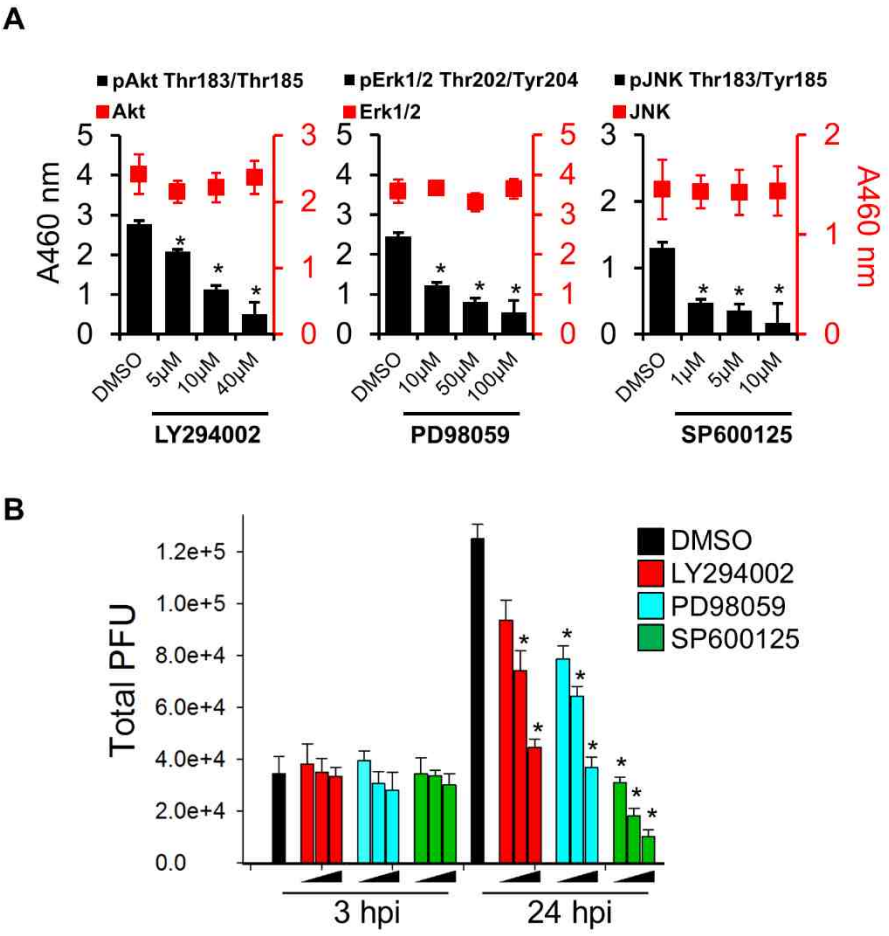

Figure 36. VV-associated signaling pathways are required for VV replication in MDMs. M2-polarized MDMs were infected with 5 MOI of VV WR for 3 h; cells were washed and treated with 5, 10, or 40 μM of LY294002, 1, 10, or 100 μM of PD98059, or 1, 5, or 10 μM of SP600125. Cell lysates were collected at 3 and 24 h post-infection. (A) Lysates were analyzed by a sandwich ELISA coated with anti-Akt, Erk, or JNK antibodies and treated with secondary antibodies against pAkt, pErk, and pJNK and unphosphorylated targets, respectively. (B) VV was extracted from lysates at the different time points as indicated and titrated by a virus plaque assay. All data are representative of cells derived from five blood donors. * $p<0.05$.

Effects of macrophage activation on VV replication

To test the effects of different macrophage activation states on VV replication and to further probe the pathways related to VV replication in MDMs, M1 and M2 activation were induced to observe the effects on VV replication. In general, classical (M1) activation of macrophages in response to IFN-γ and LPS stimulation exhibits an inflammatory phenotype. Alternative (M2) activation of macrophages can be induced via a variety of cytokines and reagents including LPS, immune complexes, glucocorticoids, IL-1β, IL-10, TGF-β and Th2 cytokines like IL-4 and IL-13. These stimuli can produce distinct cell types with unique functions. M1-polarized cells activated by LPS and IFN-γ, and M2-polarized cells activated by either IL-4 (M2a), LPS plus IL-1β (M2b), or IL-10 (M2c), for 2 days were analyzed with RT-PCR for common M1 and M2 activation markers. M1 activation exhibited higher *IL-6* mRNA, whereas M2-activated cells had higher mRNA levels of arginase 1 (*arg-1*), *CD163*, and *IL-10* (Fig. 37A). In addition, surface staining and FACS showed that activated M1 expressed higher levels of the M1 activation marker CD86 on the cell surface (Fig. 37B). M1- or M2-polarized cells were infected with VV WR at an MOI of 5 for 3 h, and then subjected to activation. Activation of M1-polarized cells with LPS plus IFN-γ had no effect on VV replication as VV plaque numbers were not affected (Fig. 38A). Similarly, activation of M2-polarized cells by IL-4 had no effect on VV replication, but treatment with LPS + IL-1β or with IL-10 significantly reduced VV productivity (Fig. 38A). At 48 h of infection, activation of M2b and M2c reduced VV plaques

from 1.22 ± 0.13 $x10^6$ in M2-polarized cells to 0.55 ± 0.06 $x10^6$ and 0.20 ± 0.05 $x10^6$, respectively.

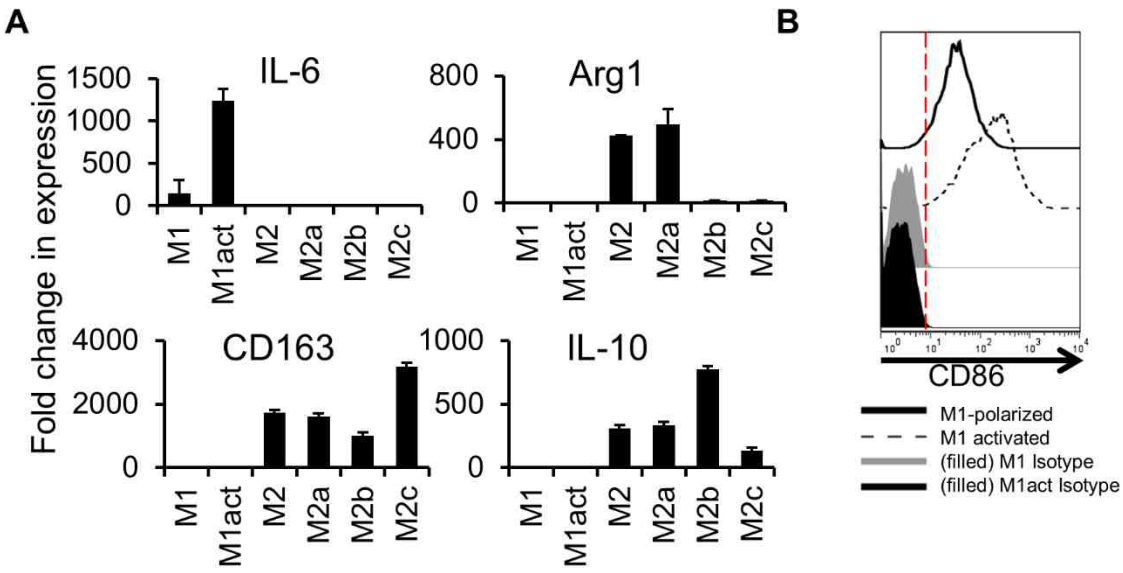

Fig. 37. Verification of macrophage activation markers. M1-polarized cells were stimulated with LPS + IFN-γ, whereas M2-polarized cells were stimulated with IL-4 (M2a), LPS + IL-1β (M2b), or IL-10 (M2c). (A) After 24 h of infection, RNA was extracted from cells and then subjected to cDNA synthesis and RT-PCR to detect M1 (IL-6) and M2 (Arg1, CD163, IL-10) activation-associated genes. (B) M1 cells were surface stained for the activation marker CD86 and analyzed by flow cytometric analysis. All data are representative of cells derived from five blood donors. * $p<0.05$, ** $p<0.01$

In T cells and macrophages, the downstream effects from IL-10 receptor activation largely act through the JAK/STAT pathway, with STAT3 being a prominent transcription factor. We used cucurbitacin I, a specific inhibitor of JAK2/STAT3, to probe the effect of STAT3 activation on VV replication. Compared to untreated M2 cells, M2c cells had significantly higher levels of pSTAT Y705 as determined by FACS, indicating that IL-10 treatment activates STAT3. Both M2-polarized and M2c cells treated with cucurbitacin I had reduced levels of activated STAT3 (Fig. 38B). When M2c cells were infected with VV WR at an MOI of 5 for 3 h, followed by addition of cucurbitacin I, VV production increased to the level of M2 cells without IL-10 stimulation (Fig. 38D). For example, infected M2 cells treated with IL-10 for 48 h produced 0.5 ± 0.2 $x10^6$ PFU, whereas cells treated with IL-10 + 5 uM cucurbitacin I produced 1.4 ± 0.1 $x10^6$ PFU. Surprisingly, M2-polarized cells even without IL-10 treatment produced more VV in response to the inhibitor treatment (Fig. 38C). After 48 h of incubation, untreated M2-polarized cells produced 1.3 ± 0.1 $x10^6$ PFU whereas cells treated with 5 uM cucurbitacin I produced 1.8 ± 0.1 $x10^6$ total PFU. Overall, these data demonstrate that M1 or M2a activation has no effect on VV replication, but M2b and M2c activation markedly reduces virus production. With M2c activation, a JAK2/STAT3 inhibitor rescued levels of virus production to comparable levels to cells without IL-10 treatment.

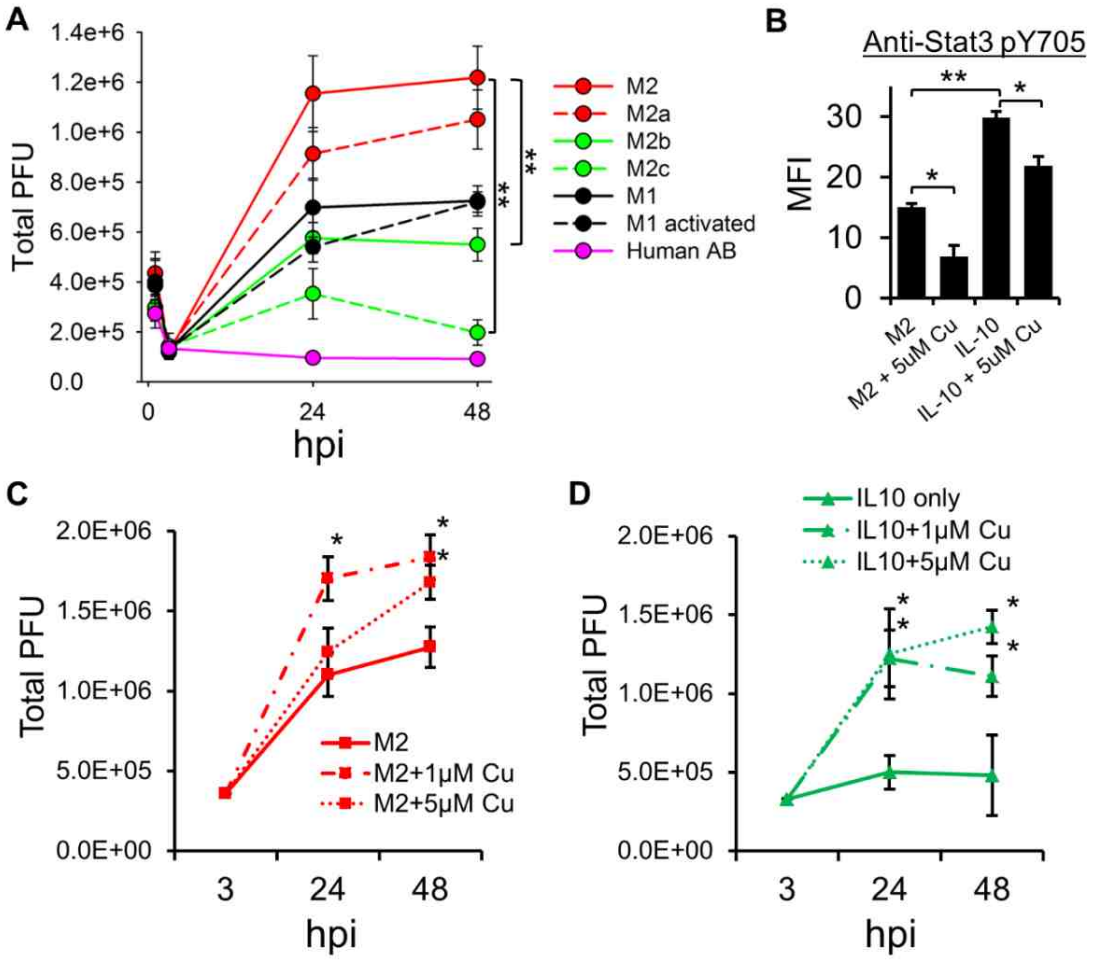

Fig. 38. Alternative activation of MDMs reduces VV production in a STAT3-dependent manner. (A) M1- or M2-polarized cells were infected with 5 MOI of WR VV for 3 h. Cells were washed extensively and treated with M1 or M2 stimulation factors. At 24 and 48 h of infection, virus plaque assays were performed on cell lysates from activated MDMs. (B) M2-polarized cells were stimulated with IL-10 with or without cucurbitacin I and analyzed for STAT3 activation by intracellular staining with anti-pSTAT3 Y705. (C, D) Virus plaque assays were performed on lysates from IL-10 or IL-10 + cucurbitacin I-treated cells after 3, 24, and 48 h of infection. All data are representative of cells derived from five blood donors. * $p<0.05$, ** $p<0.01$. hpi, hours post-infection.

Chapter V - Discussion

Profile of VV binding and infection of PHLs

The discovery of poxvirus receptors will provide a better understanding of the unique effectiveness of live VV-based vaccines that are a focus of several current clinical trials. This knowledge is requisite for the rational development of safer and more effective poxvirus-based vaccines against other infectious pathogens and tumors. Currently, over a dozen viral vaccines based on live poxvirus vectors are licensed in veterinary medicine (122). In humans, a combination of a poxvirus-based HIV-1 vaccine priming with viral envelope (Env) boosting demonstrates a promising protective effect in the HIV-1 vaccine efficacy trial, known as the RV144 clinical trial (123). The success of these poxvirus-based vaccines greatly renews research interest in poxvirus biology and virology. Because VV replication is dependent on epidermal growth factor receptor (EGFR)/Ras pathway signaling, which is commonly active in epithelial cancers (124), VV has been developed as a promising oncolytic agent to kill tumor cells, and been engineered as a vehicle for the intravenous delivery and expression of anti-tumor siRNA and peptides (70, 124, 125). Therefore, characterization of VV binding and infection tropism will also broaden the prospects for engineering live viruses to more specific and dangerous for cancer cells

In this dissertation, we observed the patterns of VV binding to and infection of major PHL subsets including monocytes, B cells, neutrophils, NK cells, and T cells. We found that VV exhibited an extremely strong bias towards

binding to and infecting the monocytes subpopulation of PHLs (Fig. 2, 3) which is in agreement with previous reports (56, 126, 127). VV also bound to primary B cells to a similar degree as that of monocytes, but VV binding to neutrophils was considerably lower (Fig. 2, 3). These results suggest that monocytes not only express VV receptors on the cell surface but also have all pathways necessary for viral uptake, entry, intracellular trafficking and ultimately penetration to the cytoplasm, where the whole process of poxvirus replication takes place. In contrast, primary B cells and neutrophils express VV receptors on their surface, albeit at different degrees, but they likely lack cellular pathways for VV entry or other downstream events. It is also possible that VV may require more than one molecular species as receptors, and monocytes have all these molecular species, whereas B cells and neutrophils have fewer. Many viruses such as poliovirus use a single molecular species as its receptor (128), whereas other viruses such as HIV-1 use more than one molecular species for viral entry (128). Different outcomes of VV binding to monocytes versus B cells or neutrophils imply that these cell types can be used as cell models to dissect the molecular mechanisms of poxvirus binding, penetration, entry, and infection, eventually leading to a better understanding of poxvirus tropism and species specificity, and to the discovery of poxvirus receptors.

HIV-1-infection of monocytic cell lines and VV binding

Interestingly, it was found that monocytic cell lines had a marked reduction in VV binding after HIV-1 infection of these cells. When screening different monocytic cell lines with the VV binding assay, it was noticed that the HIV-1 infected cell line U1 had significantly reduced VV binding relative to its parent cell U937 which is not HIV-1 infected. U1 is a clone from a group of HIV-1-infected U937 cells. U1 was selected because of its phenotype of a latent infection of HIV-1 where the provirus exists in the genome, but can only be induced to produce new virus upon cell activation (129). The latent HIV-1 infection in U1 resulted primarily from a specific mutation in the HIV-1 *tat* gene which induces the virus to mimic a latent phenotype (130). This simulated latency could be reversed by repairing the *tat* mutation or by adding wildtype Tat protein into the cell culture (130). Infection of U937 with the U1-derived HIV-1 virus resulted in a similar reduction in VV binding when comparing U937 to U1. U1 cells, although producing only trace amounts of virus, were shown to express high levels of the HIV-1 regulatory proteins Tat, Rev, and Nef, even before cell activation (131). Nef is known to downregulate surface expression of CD4 (132), CXCR4 (133), and MHC-I (134), and CD1d (135). Thus, a similar mechanism may be involved to selectively downregulate certain VV receptors. Apart from specific viral protein interactions with host membrane proteins to cause their internalization, HIV-1 infection in these cells may also modulate large scale recycling of lipid raft-specific proteins. Lipid rafts are constantly being recycled on the cell surface via raft-specific means of endocytosis like caveolae internalization. Large scale

reabsorption of all surface lipid rafts can occur when certain cell type detach from a surface (136) with storage of raft-enriched membranes in specialized compartments (137, 138). Upon re-attachment to a surface, lipid rafts are released from these compartments and trafficked to the cell surface (137-139). These routes of lipid raft reabsorption may be influenced by HIV-1 infection which can be tested by surface staining for lipid raft-specific factors. Interestingly, the PI3K-dependent Arf6 endocytic pathway regulates both HIV-1 downregulation of MHCI (134) and the internalization of lipid rafts after detachment (138). Thus, candidates for VV receptors may be detected by cataloging the proteins with downregulated surface expression via this pathway.

VV receptor enrichment in PHL lipid rafts

The VV envelope consists of approximately 25 surface membrane proteins and several have been proposed as receptor-binding proteins (140). However, while three envelope proteins have been implicated in binding to highly negatively-charged GAGs, none have been validated as receptor-binding proteins for unique or cell-specific ligands. We found that VV colocalized with lipid rafts on the surface of all major PHL subsets (monocytes, B cells, and neutrophils) that are susceptible to VV binding (Fig. 10, 11, 12, 13). Activated T cells become sensitive to VV binding and infection because VV receptors are induced *de novo* upon T cell activation (56). We found that the VV receptors newly induced on activated T cells also colocalized with lipid rafts (Fig. 12). Strikingly, these receptor molecules move together with lipid rafts, as VV binding

is concentrated in lipid rafts even if they are relocated to the uropods of polarized cells (Fig. 14, 15, 16, 17, 18, 19). While previously VV entry was found to require intact lipid rafts (40), we demonstrate that VV binding is strongly associated with lipid rafts. VV entry is known to be clathrin-independent which is not surprising, as clathrin-formed vesicles are a maximum of 100 nm in diameter (141), while a vaccinia particle is 250 x 400 nm. VV entry is also caveolin-independent, meaning it does not likely use caveolae-related endocytosis (40). Thus, for primary leukocytes, intact lipid rafts may also be required for virus entry but not require caveolin - similar to the entry of HIV-1 (38).

These results differ from prior reports with cell lines in culture (40). In HeLa cells, membrane lipid rafts are important for VV penetration, but not for VV binding, as MβCD treatment significantly inhibits VV uncoating without affecting virion attachment (40). In addition, HeLa cell surface CD29 and CD98, two lipid raft-associated proteins, are important for VV entry (102, 117), but not for VV binding (Fig. 24). These two proteins have no effect on VV binding to and infection of primary human T cells, as knockdown of their expression on the surface of activated T cells does not affect viral binding and infection (Fig. 24), and anti-human CD29 pAbs did not block VV binding to PHLs (Fig. 25). Furthermore, primary human NK cells express high levels of CD29 together with many other adhesion molecules (142), but these cells are resistant to VV binding and infection (56, 57) (also Fig. 2). These data indicate that VV receptors are strongly associated with PHL lipid rafts, but not with CD29 and CD98.

It has been reported that immunosera raised against whole monocytes or activated T cells effectively blocked VV binding to these cells (56). If VV receptors were enriched in lipid rafts, immunosera raised against DRMs would be more effective than immunosera raised against whole cells in blocking VV binding. In fact, anti-DRM immunosera significantly blocked VV binding to the highest degree, whereas immunosera raised against whole cells or CMEs also blocked VV binding but to a much lesser extent (Fig. 21). Blockage of VV binding by these immunosera appears to be specific, as immunosera raised against either DRMs, CMEs, or intact resting T cells did not affect VV binding (Fig. 21). In addition, these immunosera lost their blocking activity if they were depleted against monocytes or activated T cells, but not resting T cells (Fig. 23). Importantly, immunosera raised against monocyte DRMs, CMEs, or whole cells, were able to block VV binding to B cells and activated T cells (Fig. 21). Similarly, immunosera raised against activated T cell DRMs, CMEs, or whole cells were able to crossly block VV binding to B cells and monocytes (Fig. 21). These data strongly suggest that monocytes, B cells, and activated T cells share one or more unique protein receptors for VV. It is pertinent to note that the consequences of VV binding to these cell types have vastly different outcomes.

Activated T cells are permissive to VV binding, infection, and replication. In contrast, primary B cells and neutrophils are only sensitive to VV binding, but not permissive to VV infection. For monocytes, VV binds to and enters cells to initiate virus infection, but the infection is abortive as no viral late gene product has been detected (56) and viral DNA copies are not increased in infected

monocytes (143). This indicates that the state of certain cellular pathways in monocytes is not permissive for VV replication. Monocytes bound with VV may help VV dissemination from initial infected sites to distant organs and tissues as variola virus is disseminated by monocytic cell-associated viremia (42). It is possible that monocytes use the putative viral receptors to grab infectious variola virus particles and then disseminate them to uninfected cells and tissues via filopodial extensions, a major mechanism that HIV-1 uses to disseminate virus from dendritic cells to other cell types (144). Cell-associated VV spread by filopodial extensions greatly reduces the time needed to infect neighboring cells in culture, and this process only requires VV early gene transcription which monocyte-lineage cells are known to express during VV infection (11). It is possible that VV binds to the uropods of phagocytes such as monocytes, macrophages, and neutrophils among PHLs, to spread to tissues and to resist phagocytic activity. A recent report has demonstrated that *Neisseria meningitidis* binds to the uropods of migrating neutrophils to spread the bacteria during cell migration through epithelial cell layers (145). This study found that uropod-bound bacteria were resistant to phagocytosis, which only occurs at the pseudopod end (leading edge) (145). Our results also showed that VV preferentially binds to the uropod ends of phagocytes, which may also provide protection from phagocytosis and assist in viral dissemination leading to a generalized infection.

Permissiveness of primary human cells to VV

The primary human cell types including epithelial cells, keratinocytes, and fibroblasts in the airway, skin, and other tissues have been considered the main cellular sites for orthopoxvirus infection and replication. In one report, primary human dermal microvascular endothelial cells (HMVEC), fibroblasts, and keratinocytes were infected *in vitro* with VV WR at an MOI of 10 for 60 h and produced 197.8, 129.1, 21.8 PFU/cell, respectively (52). This result is comparable to our data where, after 48 h of infection, M1-polarized MDMs produced 15.3 ± 1.2 PFU/cell and M2-polarized cells produced 31.7 ± 3.1 PFU/cell when VV was used at an MOI of 5 (Fig. 26), suggesting that differentiated macrophages may be a significant source of viral load *in vivo*. Previously, the only primary human leukocyte type known to be permissive to VV was activated T cells (56). Among primary human leukocyte subtypes, VV is able to bind to monocytes, activated T cells, B cells, and neutrophils (56, 146, 147), but is only able to express viral genes in monocytes and activated T cells to a significant degree (127, 146, 148). Primary human monocytes and B cells have been shown to express little to no levels of the VV late gene A56 (56), suggesting that these cell types support only an abortive VV infection. We have corroborated this result by showing no virus production in primary human monocytes using a virus plaque assay (Fig. 26D). In contrast to monocytes, MDMs derived from GM-CSF or M-CSF are permissive to VV, but MDMs derived from human AB serum alone are abortive. We observed no differences when comparing VV surface binding and reporter gene expression during early infection between these cell

types. Assuming the reporter gene expression correlates with virus entry, the abortive phenotype in human AB serum-derived cells may be explained by a post-entry mechanism. In comparison to human AB serum alone, it is known that GM-CSF or M-CSF supplementation promotes survival of MDMs (105), increases cell proliferation (149), increases tumoricidal activity (61), and alters the expression of certain cell surface markers (149). However, there are no reports comparing the specific molecular differences or signaling pathways that promote these divergent phenotypes.

VV replication and macrophage signaling

Macrophages display remarkable plasticity and can change their physiology and phenotype in response to environmental cues, e.g., M2 cells reside in the tissues that ubiquitously express M-CSF (150) can be converted to M1 via exposure to bacterial components and GM-CSF (151), or M1 cells associated with inflammation can be converted to M2 with IL-4 or TGF-β exposure (152). M-CSF binds to cell surface colony stimulating factor 1 (c-Fms) to trigger dimerization and subsequent autophosphorylation of tyrosine residues which serve as binding sites for the SH2 domains of specific signaling molecules (153). Ultimately, this leads to the release of ROS which activates Erk1/2, p38 MAPK, and Akt to promote monocyte survival and differentiation (154-159). GM-CSF receptor activation is followed by Jak2 phosphorylation of receptor tyrosines and eventual activation of STAT5 and the MAPK and Akt pathways via Grb2, Shc, and SHP2 (160). Similarly, VV is reported to be dependent on MAPK

signaling (115, 116), and the Akt pathway for replication (118). We observed significantly decreased viral production with treatment of MAPK, Akt, and JNK inhibitors (Fig. 36), although off-target effects of each inhibitor cannot be excluded. It has been previously reported that VV production increases in mouse embryonic fibroblasts (MEFs) from JNK1 or JNK2 knockout mice (119). However, VV production is not altered in MEFs from JNK1/2 double knockout mice (120). Additionally, when MEFs from JNK1/2 double knockout mice are treated with SP600125 (121), VV replication is inhibited. These reports strongly indicate a JNK1/2-independent effect from SP600125 treatment, which has been found to be poorly specific for JNK1/2 and inhibits other kinases (161, 162) and could potentially include VV-encoded kinases critical for infection.

Notably, VV infection itself induces the activation of the Erk1/2, p38 MAPK, and Akt pathways in primary human monocytes (143), and viral protein production is dependent on activation of these pathways (143). Because monocytes are abortive to VV infection, it is likely that the stimulation of these three pathways alone is not sufficient to induce permissiveness in monocytic cells. In primary T cells and T cell lines, tyrosine phosphorylation of CCR5 alone allows cells to become permissive to VV replication (163, 164). This involves the downstream phosphorylation of Grb2, Jak2, and Erk1/2 which are all also directly activated by GM-CSF and M-CSF in monocytic cells. Thus, considering the plasticity of macrophage activation or differentiation and the overlap of signal transduction pathways required by both MDM activation and VV replication, it may be that factors directly downstream of GM-CSF and M-CSF stimulation

induce permissiveness of MDMs, rather than relatively permanent characteristics of cell differentiation.

In vitro activation of MDMs in some ways reflects macrophage activation states *in vivo* in certain diseases (65, 67). Surprisingly, we found that M1 activation resulted in no change to VV production (Fig. 38A). This is counterintuitive because of the many anti-viral factors induced by LPS and IFN-γ stimulation (165). However, poxviruses have evolved dozens of strategies to evade such anti-viral responses (166). Alternative activation with IL-4 treatment had no detectable effect on VV replication (Fig. 38A), which is consistent with similar transcriptional profiles of M-CSF-treated versus IL-4 treated MDMs (167). However, alternative activation with IL-10 or with LPS + IL-1β significantly reduced virus production (Fig. 38A). In different cell types, many of the effects of IL-10 are mediated via the activation of the Jak2/STAT3 pathway, with STAT3 being a crucial factor for alternative activation in macrophages and immune homeostasis. We found that the JAK2/STAT3 inhibitor cucurbitacin I increased VV production in both M2-polarized and M2c activated cells in a manner correlative to STAT3 activation. VV infection does not block STAT3 activity, but does dephosphorylate STAT1 to reduce the effect of IFN-stimulation (168). In general, M1 activation involves STAT1 activation, while much of the effect of M2 activation centers on STAT6 (67). Macrophage-specific STAT3 knockout mice have a phenotype resembling that of IL-10-knockout mice: increased inflammation and susceptibility to endotoxic shock, largely the result of the

effects of IL-10 on macrophages being silenced (169). Therefore, STAT3 activation likely regulates factors that are critical to VV replication.

VV dissemination via macrophages

Our study also provides several lines of evidence that primary macrophages promote VV dissemination: 1) high EEV production, 2) actin tail-associated CEV, and 3) VV-associated cell branching and linkages. IMV is often considered to be the most abundant infectious form of VV produced in most cell types. The CEV form of VV mediates cell-to-cell spreading, and detachment of CEV to become EEV mediates longer-range dissemination (8, 170). We observed that by 48 h of infection with VV WR, EEVs were the dominant virus form produced in MDMs (Fig. 34). This principle of high EEV production is comparable to the rabbit kidney cell line RK_{13} which produces significantly more EEV relative to other cell lines (171). Additionally, the VV strain IHD-J produces high EEV titers in cell lines, especially in RK_{13} (171). When compared to the VV WR strain, IHD-J produces more EEV particles because it releases more CEV into the supernatant while strains like VV WR retain CEV on the cell surface (170). Thus, considering the paradigm in EEV production that exists between WR and IHD-J in cell lines, this anomaly in MDMs will likely be explained by a host cell-related mechanism like that of RK_{13}, rather than a characteristic of the virus strain itself. In cell lines, different factors have been associated with EEV production, including the Abl tyrosine kinases (112, 172) and SH2 domain

containing phosphoinositide 5-phosphatase 2 (SHIP2) (173), which may be involved with the high EEV production seen in MDMs.

Characteristic actin tails were observed associated with MDMs throughout the course of infection (Fig. 31). It is well known that actin-based VV motility is entirely relegated to CEVs on the cell surface, whereas microtubules mediate kinesin transport of intracellular virus particles (110). The formation of actin tails requires the phosphorylation of the VV envelope protein A36 by Src and Abl family kinases (111, 112) which recruit Grb2, Nck, and the Arp2/3 complex to induce the polymerization of actin (174). A36-dependent actin nucleation itself has been implicated in detachment of CEVs from the cell surface (10). The inhibition of actin tails in cell lines dramatically reduces the degree of cell-to-cell infection as seen by shrinking virus plaque formation. Thus, assuming the principle remains the same as in cell lines, the presence of such structures in MDMs is indicative of actin-dependent cell-to-cell transmission. We observed surface-bound virions throughout the first 8 h of infection that could theoretically be carried away from initial infection sites to infect cells contacted by migrating macrophages. The actin polymerization inhibitors cytochalasin D and latrunculin A have been shown to inhibit actin tail formation while not affecting the number of CEVs (9, 175, 176) and could be used in MDMs to test the dependence of actin for cell-to-cell transmission.

Within the first hours of infection, MDMs exhibited VV-associated cell branches and linkages with neighboring cells (Fig. 29, 32). It has been previously found that VV-infected BS-C-1 cells become motile and form branches (113).

These structures are also reminiscent of the cell-to-cell spread of retroviruses via filopodial bridges (177). Additionally, we frequently observed lamellipodia-leading structures containing virus particles in MDMs (Figs. 29, 32). In mouse macrophages, giant cell formation occurs and is preceded by cell branching and lamellipodia formation (178). Interestingly, we observed an increase in giant cell formation throughout the infection (Fig. 33). Macrophage giant cells can be generated via contact with various pathogens and foreign bodies. In this case it is unknown whether giant cell formation is the result of the innate ability of host macrophages to fuse or if it is influenced by VV-induced syncytia. However, syncytia from VV has so far only been observed at low pH (179, 180) or with a mutation or dysfunction in the fusion complex genes A56R (181) and K2L (182, 183).

Chapter VI - Future Directions

Post-binding analysis of VV infection in PHLs

A better understanding of the rate-limiting steps to VV infection of PHLs will provide a better platform to design and test immunotherapies involving VV. What remains a mystery is how to explain the disparity between VV binding and VV gene expression in both primary human leukocytes and monocytic cell lines. Although primary monocytes, B cells, and activated T cells were highly susceptible to VV binding, only monocytes expressed VV reporter gene to a significant degree. Also, whereas U937 was much more susceptible to VV binding, THP-1 expressed higher levels of the VV reporter gene following infection. The answer to this question is most likely found in the differences in VV entry, uncoating, and intracellular signaling by each cell type. Entry of IMV virions can be measured via visualization with confocal microscopy, on either the inside or outside of the cell at different time points. This can be done by cell surface staining for VV envelope proteins to stain extracellular virus and the use of anti-VV core protein antibodies to detect uncoated virus particles intracellularly. Comparing the two conditions for each cell type can reveal differences in the rate of entry. If a different entry rate is observed, various routes of entry can be analyzed by detecting markers of macropinocytosis, or caveolin and dynamin-dependent mechanisms.

Uncoating of the viral core must occur after entry to release virus DNA and enzymes into the cytoplasm to begin viral gene transcription and DNA replication.

Uncoating of poxviruses is known to occur in two stages: 1) host enzymes break away the remaining viral envelope and part of the core; 2) viral DNA within the intact core transcribes most of the early VV genes including enzymes to breakdown the remaining capsid (184). If either stage fails to complete, this can be detected through different observations using a transmission electron microscope to view cross-sections of infection cells. The most obvious sign that uncoat is malfunctioned is if many VV cores are visible within the cell hours after the primary infection. Additionally, cores seen associated with DNA staining are evidence of incomplete uncoating as not only is the core still present, but viral DNA has failed to escape it (185). Such observations are indicative of either a lack of host enzymes to complete the first stage, or a failure of VV early gene transcription or translation to complete the second stage.

If no error in virus uncoating is observed, the infection may be limited by VV gene expression beyond that related to the first stage of uncoating. For example, VV was successfully demonstrated to bind and enter primary human dendritic cells, but only early VV genes were transcribed and no late genes (47, 48) which are critical for virion assembly. Individual genes regulated under early, early/late, intermediate, and late VV promoters can be selected for each infected cell type and analyzed with Northern blotting or RT-PCR to determine at what stage VV gene expression is interrupted. Recently, a microarray with probes for more than 200 VV WR ORFs was developed that successfully profiled VV genes transcribed from human cells (186) which could be used to more specifically locate end points in the VV life cycle.

Enrichment and detection of potential VV receptors

Although several effective anti-viral drugs for poxviruses and DNA viruses exist, the discovery of a specific poxvirus receptor would lead to the development of poxvirus receptor agonists that could be used to quickly treat poxvirus-infected patients to counter viremia. This approach is similar to the CCR5 receptor agonists developed for HIV-1 treatment. Additionally, considering the potential of poxviruses as vaccines and immunotherapies, the identification of the specific receptors that mediate this strict binding tropism will surely lead to better strategies to better engineer poxvirus treatments. Despite the evidence that VV has a strict cell type binding tropism, especially with primary cells, no cell type-specific receptor has ever been discovered. The results presented in this work demonstrate that putative VV receptors can be enriched in DRM fractions from leukocytes. With this knowledge and with the observations of the patterns of VV binding to particular hematopoietic cell types, a study may to designed to specifically enrich and identify putative receptors using liquid chromatography mass spectrometry. Conceivably, surface proteins may be isolated from similar cell types that are known to have an extreme difference in VV binding. This can include naive vs. activated primary T cells, CD16-positive vs. CD16-negative primary monocytes, or HIV-infected or uninfected cells from the U937 cell line.

To use such a method, our data provide critical information about the nature of VV receptors on leukocytes. If a membrane protein is known to be lipid raft or DRM-specific, special methods of isolating membrane protein to avoid the reliance on non-ionic detergents to lyse and solubilize the cell membrane must

be used. Detergent-resistant membrane is known to precipitate out of non-ionic detergent solutions, which leads to the removal of significant portions of DRM-specific proteins during washes and centrifugations. Thus, methods using no detergents or only ionic detergents should be preferred when extracting DRM-enriched proteins. It is interesting to speculate why, after a century of molecular research on poxviruses, a unique VV receptor has not yet been discovered. The insolubility of DRM-enriched proteins may be a contributing factor.

Specific macrophage signaling pathways affecting VV replication

IL-10 produced by T regulatory cells in many types of cancer has been associated with a reduction of Th1 responses that regulate IFN-γ and $CD8^+$ cell anti-tumor immunity (187-189). This role for IL-10 as an anti-inflammatory agent in tumors is significant for the use of VV as an oncolytic agent, as we have found that VV replication in MDMs is sensitive to IL-10 stimulation. IL-10 produced within a tumor may also inhibit VV production in macrophages, which may be a significant source of viral load, and may limit the cell-to-cell spreading via macrophages. Thus, a better understanding of the mechanism of IL-10 inhibition of VV replication should be investigated. We have found that IL-10 reduced VV production mainly through STAT3 activation. In macrophages, STAT3 is a transcription factor that directly regulates the expression of over 100 genes (190), but the pathways leading to VV inhibition are unknown. Activated STAT3 in macrophages is known to downregulate the expression of many pro-inflammatory cytokines, which may somehow be essential for VV replication.

STAT3 also works in macrophages to suppressive the inflammatory response by inducing the transcription of several genes known to be involved in anti-inflammatory pathways (190), and could be potentially inhibitory to VV replication.

Cell-to-cell spread of VV via macrophages

Recently, a report testing oncolytic adenovirus found that delivery of the virus via macrophages was much more effective than other routes of delivery (72). The efficacy of an oncolytic virus is not only determined by its ability to specifically target and kill tumor cells, but also its ability to propagate and spread efficiently between cells with a tumor. Cell-to-cell transmission of VV has been documented in cell lines either by cell elongation and branching (113) or via actin tails (11). We showed that macrophages produce mainly EEV, but numerous micrographs of VV-associated cellular structures were strongly indicative of cell-to-cell transfer. Studying the routes of VV dissemination via macrophage will lead to a better understanding of VV dissemination *in vivo* and may lead to an improved route to deliver oncolytic VV. To further investigate the ability of MDMs to distribute VV via cell-to-cell transmission, live imaging should be carried out to directly view virions crossing from infected MDMs to other uninfected cells. The virions previously viewed as associated with cell-linking structures were most likely cell surface-bound IMV particles left over from the primary. Therefore, anti-EEV neutralizing antibodies could be used to block the infection of newly created extracellular virions to view the infectious nature of surface-bound IMV particles

associated with cell-linking structures. If actin tails are seen mediating cell-to-cell spread, cells could be treated with actin-inhibitors cytochalasin D or latrunculin A (9, 175, 176) to test the effects on actin-dependent dissemination. The role of actin in this process should be visualized using a plasmid or virus vector containing an actin-staining molecule as phalloidin cannot be used for live cell imaging.

Eczema vaccinatum and macrophages

Among the possible negative effects of attenuated VV-based vaccinations, the most dangerous side effect occurs on recipients with a history of atopic dermatitis (AD) or eczema. Although these patients should not be administered the vaccine, they can become exposed from other vaccinated individuals that are shedding the virus (191). VV exposure in these patients leads to eczema vaccinatum (EV), a potentially fatal disease with a widespread rash and smallpox-like patterns of VV-infected skin lesions caused by viremia. EV patients have been successfully treated with anti-VV IgG, DNA replication inhibitor cidofovir, and EEV production-inhibitor tecovirimat (ST-246) resulting in no long term damage and minimal scarring (191). However, precisely how autoimmune diseases in the skin can cause widespread dissemination of attenuated VV is unknown. Skin from AD patients is known to have defective epidermal barriers, and includes mild amounts of keratinocyte hyperplasia and higher amounts of inflammatory cells (192). These hyperplastic keratinocytes may contribute to the high viral load of EV patients, as transformed cells in culture tend to produce

much higher viral titers than primary cells. Additionally, the increased presence of inflammatory cells also suggests a role for enhanced dissemination of the virus which may accommodate the high viremia and dissemination in the skin of EV patients (192). In EV and smallpox patients, variola lesions are strongly associated with areas of healing or inflammation. Similarly, a case study from an autopsy on an EV patient found that virus particles in skin lesions were found mainly in the epidermis but also with high amounts in skin macrophages and neutrophils (193). Thus, macrophages and other inflammatory cells may be associated with the high viral dissemination seen in EV patients.

In AD patients, monocytes much more readily invade sites of inflammation and differentiate into macrophages (194) which explains the high number of macrophages found in AD patient skin (195). These macrophages are highly linked to AD-associated altered expression of cytokines, chemokines, pattern recognition receptors, and aberrant phagocytosis (196). Our results with VV infection of macrophages suggest that MDMs are used by VV to produce virions suitable for long range dissemination, and also seem to contribute to cell-to-cell dissemination. Thus, the widespread dissemination of inflammatory macrophages in AD patients may be an explanation for the high amount of VV dissemination found in EV patients. To test this hypothesis, numerous murine models of AD and EV can be used (192, 197). Mice could be infected with attenuated or non-attenuated strains of VV to induce EV-like symptoms and monocytes/macrophage could be monitored. The route of VV dissemination via viremia could be determined by isolating cell types or serum from the blood and

titering virus on each. The proportion of VV in the circulation could be visualized with live imaging of the blood circulation with staining for VV, monocytes, and other cell types. To find the source of virus entering the skin, histological slides of the skin prior to lesion formation can be prepared with staining for VV antigen and macrophage markers to search for potential associations.

References

1. Morens, D. M., G. K. Folkers, and A. S. Fauci. 2004. The challenge of emerging and re-emerging infectious diseases. *Nature* 430: 242-249.
2. McFadden, G. 2005. Poxvirus tropism. *Nat Rev Microbiol* 3: 201-213.
3. Wilson, I. A., J. J. Skehel, and D. C. Wiley. 1981. Structure of the haemagglutinin membrane glycoprotein of influenza virus at 3 A resolution. *Nature* 289: 366-373.
4. Ibricevic, A., A. Pekosz, M. J. Walter, C. Newby, J. T. Battaile, E. G. Brown, M. J. Holtzman, and S. L. Brody. 2006. Influenza virus receptor specificity and cell tropism in mouse and human airway epithelial cells. *Journal of virology* 80: 7469-7480.
5. Werden, S. J., and G. McFadden. 2008. The role of cell signaling in poxvirus tropism: the case of the M-T5 host range protein of myxoma virus. *Biochim Biophys Acta* 1784: 228-237.
6. Frank Fenner, D. A. H., Isao Arita, Zdeněk Ježek, Ivan Danilovich Ladnyi. 1988. Smallpox and its eradication. *World Health Organization*.
7. Tolonen, N., L. Doglio, S. Schleich, and J. Krijnse Locker. 2001. Vaccinia virus DNA replication occurs in endoplasmic reticulum-enclosed cytoplasmic mini-nuclei. *Molecular biology of the cell* 12: 2031-2046.
8. Smith, G. L., A. Vanderplasschen, and M. Law. 2002. The formation and function of extracellular enveloped vaccinia virus. *The Journal of general virology* 83: 2915-2931.
9. Arakawa, Y., J. V. Cordeiro, S. Schleich, T. P. Newsome, and M. Way. 2007. The release of vaccinia virus from infected cells requires RhoA-mDia modulation of cortical actin. *Cell host & microbe* 1: 227-240.
10. Horsington, J., H. Lynn, L. Turnbull, D. Cheng, F. Braet, R. J. Diefenbach, C. B. Whitchurch, G. Karupiah, and T. P. Newsome. 2013. A36-dependent actin filament nucleation promotes release of vaccinia virus. *PLoS pathogens* 9: e1003239.
11. Doceul, V., M. Hollinshead, L. van der Linden, and G. L. Smith. 2010. Repulsion of superinfecting virions: a mechanism for rapid virus spread. *Science* 327: 873-876.
12. Upton, C., S. Slack, A. L. Hunter, A. Ehlers, and R. L. Roper. 2003. Poxvirus orthologous clusters: toward defining the minimum essential poxvirus genome. *Journal of virology* 77: 7590-7600.
13. Perkus, M. E., S. J. Goebel, S. W. Davis, G. P. Johnson, K. Limbach, E. K. Norton, and E. Paoletti. 1990. Vaccinia virus host range genes. *Virology* 179: 276-286.
14. Gantier, M. P., and B. R. Williams. 2007. The response of mammalian cells to double-stranded RNA. *Cytokine & growth factor reviews* 18: 363-371.
15. Langland, J. O., and B. L. Jacobs. 2002. The role of the PKR-inhibitory genes, E3L and K3L, in determining vaccinia virus host range. *Virology* 299: 133-141.

16. Hsiao, J. C., C. S. Chung, and W. Chang. 1998. Cell surface proteoglycans are necessary for A27L protein-mediated cell fusion: identification of the N-terminal region of A27L protein as the glycosaminoglycan-binding domain. *Journal of virology* 72: 8374-8379.
17. Hsiao, J. C., C. S. Chung, and W. Chang. 1999. Vaccinia virus envelope D8L protein binds to cell surface chondroitin sulfate and mediates the adsorption of intracellular mature virions to cells. *Journal of virology* 73: 8750-8761.
18. Chiu, W. L., C. L. Lin, M. H. Yang, D. L. Tzou, and W. Chang. 2007. Vaccinia virus 4c (A26L) protein on intracellular mature virus binds to the extracellular cellular matrix laminin. *Journal of virology* 81: 2149-2157.
19. Foo, C. H., H. Lou, J. C. Whitbeck, M. Ponce-de-Leon, D. Atanasiu, R. J. Eisenberg, and G. H. Cohen. 2009. Vaccinia virus L1 binds to cell surfaces and blocks virus entry independently of glycosaminoglycans. *Virology* 385: 368-382.
20. Singer, S. J., and G. L. Nicolson. 1972. The fluid mosaic model of the structure of cell membranes. *Science* 175: 720-731.
21. Simons, K., and E. Ikonen. 1997. Functional rafts in cell membranes. *Nature* 387: 569-572.
22. Rodriguez-Boulan, E., K. T. Paskiet, P. J. Salas, and E. Bard. 1984. Intracellular transport of influenza virus hemagglutinin to the apical surface of Madin-Darby canine kidney cells. *The Journal of cell biology* 98: 308-319.
23. Fuller, S., C. H. von Bonsdorff, and K. Simons. 1984. Vesicular stomatitis virus infects and matures only through the basolateral surface of the polarized epithelial cell line, MDCK. *Cell* 38: 65-77.
24. Lisanti, M. P., I. W. Caras, M. A. Davitz, and E. Rodriguez-Boulan. 1989. A glycophospholipid membrane anchor acts as an apical targeting signal in polarized epithelial cells. *The Journal of cell biology* 109: 2145-2156.
25. Nguyen, D. H., and J. E. Hildreth. 2000. Evidence for budding of human immunodeficiency virus type 1 selectively from glycolipid-enriched membrane lipid rafts. *Journal of virology* 74: 3264-3272.
26. Brown, D. A., and J. K. Rose. 1992. Sorting of GPI-anchored proteins to glycolipid-enriched membrane subdomains during transport to the apical cell surface. *Cell* 68: 533-544.
27. Schroeder, R., E. London, and D. Brown. 1994. Interactions between saturated acyl chains confer detergent resistance on lipids and glycosylphosphatidylinositol (GPI)-anchored proteins: GPI-anchored proteins in liposomes and cells show similar behavior. *Proceedings of the National Academy of Sciences of the United States of America* 91: 12130-12134.
28. Krauss, K., and P. Altevogt. 1999. Integrin leukocyte function-associated antigen-1-mediated cell binding can be activated by clustering of membrane rafts. *The Journal of biological chemistry* 274: 36921-36927.

29. Holowka, D., and B. Baird. 2001. Fc(epsilon)RI as a paradigm for a lipid raft-dependent receptor in hematopoietic cells. *Seminars in immunology* 13: 99-105.
30. Takahashi, T., and T. Suzuki. 2011. Function of membrane rafts in viral lifecycles and host cellular response. *Biochemistry research international* 2011: 245090.
31. Marjomaki, V., V. Pietiainen, H. Matilainen, P. Upla, J. Ivaska, L. Nissinen, H. Reunanen, P. Huttunen, T. Hyypia, and J. Heino. 2002. Internalization of echovirus 1 in caveolae. *Journal of virology* 76: 1856-1865.
32. Stuart, A. D., H. E. Eustace, T. A. McKee, and T. D. Brown. 2002. A novel cell entry pathway for a DAF-using human enterovirus is dependent on lipid rafts. *Journal of virology* 76: 9307-9322.
33. Nomura, R., A. Kiyota, E. Suzaki, K. Kataoka, Y. Ohe, K. Miyamoto, T. Senda, and T. Fujimoto. 2004. Human coronavirus 229E binds to CD13 in rafts and enters the cell through caveolae. *Journal of virology* 78: 8701-8708.
34. Pelkmans, L., J. Kartenbeck, and A. Helenius. 2001. Caveolar endocytosis of simian virus 40 reveals a new two-step vesicular-transport pathway to the ER. *Nature cell biology* 3: 473-483.
35. Pelkmans, L., D. Puntener, and A. Helenius. 2002. Local actin polymerization and dynamin recruitment in SV40-induced internalization of caveolae. *Science* 296: 535-539.
36. Kamiyama, H., H. Yoshii, Y. Tanaka, H. Sato, N. Yamamoto, and Y. Kubo. 2009. Raft localization of CXCR4 is primarily required for X4-tropic human immunodeficiency virus type 1 infection. *Virology* 386: 23-31.
37. Carter, G. C., L. Bernstone, D. Sangani, J. W. Bee, T. Harder, and W. James. 2009. HIV entry in macrophages is dependent on intact lipid rafts. *Virology* 386: 192-202.
38. Liao, Z., L. M. Cimakasky, R. Hampton, D. H. Nguyen, and J. E. Hildreth. 2001. Lipid rafts and HIV pathogenesis: host membrane cholesterol is required for infection by HIV type 1. *AIDS Res Hum Retroviruses* 17: 1009-1019.
39. Saifuddin, M., T. Hedayati, J. P. Atkinson, M. H. Holguin, C. J. Parker, and G. T. Spear. 1997. Human immunodeficiency virus type 1 incorporates both glycosyl phosphatidylinositol-anchored CD55 and CD59 and integral membrane CD46 at levels that protect from complement-mediated destruction. *The Journal of general virology* 78 (Pt 8): 1907-1911.
40. Chung, C. S., C. Y. Huang, and W. Chang. 2005. Vaccinia virus penetration requires cholesterol and results in specific viral envelope proteins associated with lipid rafts. *Journal of virology* 79: 1623-1634.
41. Prevention, C. f. D. C. a. 2004. Smallpox Fact Sheet.
42. Jahrling, P. B., L. E. Hensley, M. J. Martinez, J. W. Leduc, K. H. Rubins, D. A. Relman, and J. W. Huggins. 2004. Exploring the potential of variola virus infection of cynomolgus macaques as a model for human smallpox. *Proceedings of the National Academy of Sciences of the United States of America* 101: 15196-15200.

43. Wahl-Jensen, V., J. A. Cann, K. H. Rubins, J. W. Huggins, R. W. Fisher, A. J. Johnson, F. de Kok-Mercado, T. Larsen, J. L. Raymond, L. E. Hensley, and P. B. Jahrling. 2011. Progression of pathogenic events in cynomolgus macaques infected with variola virus. *PloS one* 6: e24832.
44. Hickman, H. D., G. V. Reynoso, B. F. Ngudiankama, E. J. Rubin, J. G. Magadan, S. S. Cush, J. Gibbs, B. Molon, V. Bronte, J. R. Bennink, and J. W. Yewdell. 2013. Anatomically restricted synergistic antiviral activities of innate and adaptive immune cells in the skin. *Cell host & microbe* 13: 155-168.
45. Broder, C. C., P. E. Kennedy, F. Michaels, and E. A. Berger. 1994. Expression of foreign genes in cultured human primary macrophages using recombinant vaccinia virus vectors. *Gene* 142: 167-174.
46. Drillien, R., D. Spehner, A. Bohbot, and D. Hanau. 2000. Vaccinia virus-related events and phenotypic changes after infection of dendritic cells derived from human monocytes. *Virology* 268: 471-481.
47. Engelmayer, J., M. Larsson, M. Subklewe, A. Chahroudi, W. I. Cox, R. M. Steinman, and N. Bhardwaj. 1999. Vaccinia virus inhibits the maturation of human dendritic cells: a novel mechanism of immune evasion. *Journal of immunology* 163: 6762-6768.
48. Jenne, L., C. Hauser, J. F. Arrighi, J. H. Saurat, and A. W. Hugin. 2000. Poxvirus as a vector to transduce human dendritic cells for immunotherapy: abortive infection but reduced APC function. *Gene therapy* 7: 1575-1583.
49. Subklewe, M., A. Chahroudi, A. Schmaljohn, M. G. Kurilla, N. Bhardwaj, and R. M. Steinman. 1999. Induction of Epstein-Barr virus-specific cytotoxic T-lymphocyte responses using dendritic cells pulsed with EBNA-3A peptides or UV-inactivated, recombinant EBNA-3A vaccinia virus. *Blood* 94: 1372-1381.
50. Bronte, V., M. W. Carroll, T. J. Goletz, M. Wang, W. W. Overwijk, F. Marincola, S. A. Rosenberg, B. Moss, and N. P. Restifo. 1997. Antigen expression by dendritic cells correlates with the therapeutic effectiveness of a model recombinant poxvirus tumor vaccine. *Proceedings of the National Academy of Sciences of the United States of America* 94: 3183-3188.
51. Chahroudi, A., D. A. Garber, P. Reeves, L. Liu, D. Kalman, and M. B. Feinberg. 2006. Differences and similarities in viral life cycle progression and host cell physiology after infection of human dendritic cells with modified vaccinia virus Ankara and vaccinia virus. *Journal of virology* 80: 8469-8481.
52. Liu, L., Z. Xu, R. C. Fuhlbrigge, V. Pena-Cruz, J. Lieberman, and T. S. Kupper. 2005. Vaccinia virus induces strong immunoregulatory cytokine production in healthy human epidermal keratinocytes: a novel strategy for immune evasion. *Journal of virology* 79: 7363-7370.
53. Gomez, C. E., B. Perdiguero, J. Garcia-Arriaza, and M. Esteban. 2012. Poxvirus vectors as HIV/AIDS vaccines in humans. *Human vaccines & immunotherapeutics* 8: 1192-1207.

54. Thorne, S. H. 2012. Next-generation oncolytic vaccinia vectors. *Methods in molecular biology* 797: 205-215.
55. Guse, K., V. Cerullo, and A. Hemminki. 2011. Oncolytic vaccinia virus for the treatment of cancer. *Expert opinion on biological therapy* 11: 595-608.
56. Chahroudi, A., R. Chavan, N. Kozyr, E. K. Waller, G. Silvestri, and M. B. Feinberg. 2005. Vaccinia virus tropism for primary hematolymphoid cells is determined by restricted expression of a unique virus receptor. *Journal of virology* 79: 10397-10407.
57. Yu, Q., Hu, N., Ostrowski, M. 2009. Poxvirus tropism for primary human leukocytes and hematopoietic cells. *Methods in molecular biology* 515: 309-328.
58. Yu, Q., Jones, B., Hu, N., Chang, H., Ahmad, S., Liu, J., Parrington, M., Ostrowski, M. 2006. Comparative analysis of tropism between canarypox (ALVAC) and vaccinia viruses reveals a more restricted and preferential tropism of ALVAC for human cells of the monocytic lineage. *Vaccine* 24: 6376-6391.
59. Musson, R. A. 1983. Human serum induces maturation of human monocytes in vitro. Changes in cytolytic activity, intracellular lysosomal enzymes, and nonspecific esterase activity. *The American journal of pathology* 111: 331-340.
60. Eischen, A., F. Vincent, J. P. Bergerat, B. Louis, A. Faradji, A. Bohbot, and F. Oberling. 1991. Long term cultures of human monocytes in vitro. Impact of GM-CSF on survival and differentiation. *Journal of immunological methods* 143: 209-221.
61. Suzu, S., H. Yokota, M. Yamada, N. Yanai, M. Saito, T. Kawashima, M. Saito, F. Takaku, and K. Motoyoshi. 1989. Enhancing effect of human monocytic colony-stimulating factor on monocyte tumoricidal activity. *Cancer research* 49: 5913-5917.
62. Helinski, E. H., K. L. Bielat, G. M. Ovak, and J. L. Pauly. 1988. Long-term cultivation of functional human macrophages in Teflon dishes with serum-free media. *Journal of leukocyte biology* 44: 111-121.
63. Vogel, S. N., P. Y. Perera, M. M. Hogan, and J. A. Majde. 1988. Use of serum-free, compositionally defined medium for analysis of macrophage differentiation in vitro. *Journal of leukocyte biology* 44: 136-142.
64. Jaguin, M., N. Houlbert, O. Fardel, and V. Lecureur. 2013. Polarization profiles of human M-CSF-generated macrophages and comparison of M1-markers in classically activated macrophages from GM-CSF and M-CSF origin. *Cellular immunology* 281: 51-61.
65. Loke, P., M. G. Nair, J. Parkinson, D. Guiliano, M. Blaxter, and J. E. Allen. 2002. IL-4 dependent alternatively-activated macrophages have a distinctive in vivo gene expression phenotype. *BMC immunology* 3: 7.
66. Ghassabeh, G. H., P. De Baetselier, L. Brys, W. Noel, J. A. Van Ginderachter, S. Meerschaut, A. Beschin, F. Brombacher, and G. Raes. 2006. Identification of a common gene signature for type II cytokine-associated myeloid cells elicited in vivo in different pathologic conditions. *Blood* 108: 575-583.

67. Sica, A., and A. Mantovani. 2012. Macrophage plasticity and polarization: in vivo veritas. *The Journal of clinical investigation* 122: 787-795.
68. Park, B. H., T. Hwang, T. C. Liu, D. Y. Sze, J. S. Kim, H. C. Kwon, S. Y. Oh, S. Y. Han, J. H. Yoon, S. H. Hong, A. Moon, K. Speth, C. Park, Y. J. Ahn, M. Daneshmand, B. G. Rhee, H. M. Pinedo, J. C. Bell, and D. H. Kirn. 2008. Use of a targeted oncolytic poxvirus, JX-594, in patients with refractory primary or metastatic liver cancer: a phase I trial. *Lancet Oncol* 9: 533-542.
69. Heo, J., C. J. Breitbach, A. Moon, C. W. Kim, R. Patt, M. K. Kim, Y. K. Lee, S. Y. Oh, H. Y. Woo, K. Parato, J. Rintoul, T. Falls, T. Hickman, B. G. Rhee, J. C. Bell, D. H. Kirn, and T. H. Hwang. Sequential therapy with JX-594, a targeted oncolytic poxvirus, followed by sorafenib in hepatocellular carcinoma: preclinical and clinical demonstration of combination efficacy. *Mol Ther* 19: 1170-1179.
70. Liu, T. C., T. Hwang, B. H. Park, J. Bell, and D. H. Kirn. 2008. The targeted oncolytic poxvirus JX-594 demonstrates antitumoral, antivascular, and anti-HBV activities in patients with hepatocellular carcinoma. *Mol Ther* 16: 1637-1642.
71. Heo, J., T. Reid, L. Ruo, C. J. Breitbach, S. Rose, M. Bloomston, M. Cho, H. Y. Lim, H. C. Chung, C. W. Kim, J. Burke, R. Lencioni, T. Hickman, A. Moon, Y. S. Lee, M. K. Kim, M. Daneshmand, K. Dubois, L. Longpre, M. Ngo, C. Rooney, J. C. Bell, B. G. Rhee, R. Patt, T. H. Hwang, and D. H. Kirn. Randomized dose-finding clinical trial of oncolytic immunotherapeutic vaccinia JX-594 in liver cancer. *Nature medicine* 19: 329-336.
72. Muthana, M., A. Giannoudis, S. D. Scott, H. Y. Fang, S. B. Coffelt, F. J. Morrow, C. Murdoch, J. Burton, N. Cross, B. Burke, R. Mistry, F. Hamdy, N. J. Brown, L. Georgopoulos, P. Hoskin, M. Essand, C. E. Lewis, and N. J. Maitland. 2011. Use of macrophages to target therapeutic adenovirus to human prostate tumors. *Cancer research* 71: 1805-1815.
73. Kirn, D. H., Y. Wang, W. Liang, C. H. Contag, and S. H. Thorne. 2008. Enhancing poxvirus oncolytic effects through increased spread and immune evasion. *Cancer research* 68: 2071-2075.
74. Mooij, P., S. S. Balla-Jhagjhoorsingh, G. Koopman, N. Beenhakker, P. van Haaften, I. Baak, I. G. Nieuwenhuis, I. Kondova, R. Wagner, H. Wolf, C. E. Gomez, J. L. Najera, V. Jimenez, M. Esteban, and J. L. Heeney. 2008. Differential CD4+ versus CD8+ T-cell responses elicited by different poxvirus-based human immunodeficiency virus type 1 vaccine candidates provide comparable efficacies in primates. *Journal of virology* 82: 2975-2988.
75. Norbury, C. C., D. Malide, J. S. Gibbs, J. R. Bennink, and J. W. Yewdell. 2002. Visualizing priming of virus-specific CD8+ T cells by infected dendritic cells in vivo. *Nature immunology* 3: 265-271.
76. Katsafanas, G. C., and B. Moss. 2007. Colocalization of transcription and translation within cytoplasmic poxvirus factories coordinates viral expression and subjugates host functions. *Cell host & microbe* 2: 221-228.

77. Law, M., and G. L. Smith. 2004. Studying the binding and entry of the intracellular and extracellular enveloped forms of vaccinia virus. *Methods in molecular biology* 269: 187-204.
78. Ambarus, C. A., S. Krausz, M. van Eijk, J. Hamann, T. R. Radstake, K. A. Reedquist, P. P. Tak, and D. L. Baeten. 2012. Systematic validation of specific phenotypic markers for in vitro polarized human macrophages. *Journal of immunological methods* 375: 196-206.
79. Vicente-Manzanares, M., M. Rey, D. R. Jones, D. Sancho, M. Mellado, J. M. Rodriguez-Frade, M. A. del Pozo, M. Yanez-Mo, A. M. de Ana, A. C. Martinez, I. Merida, and F. Sanchez-Madrid. 1999. Involvement of phosphatidylinositol 3-kinase in stromal cell-derived factor-1 alpha-induced lymphocyte polarization and chemotaxis. *J Immunol* 163: 4001-4012.
80. Yeh, J. H., S. S. Sidhu, and A. C. Chan. 2008. Regulation of a late phase of T cell polarity and effector functions by Crtam. *Cell* 132: 846-859.
81. Okamoto, N., Y. Nukada, K. Tezuka, K. Ohashi, K. Mizuno, and T. Tsuji. 2004. AILIM/ICOS signaling induces T-cell migration/polarization of memory/effector T-cells. *Int Immunol* 16: 1515-1522.
82. Schmitt, M., and C. G. Cochrane. 1987. Cell-dependent chemiluminescence. Modulation of the N-formyl chemotactic peptide (FNLPNTL) mediated oxidative burst in human polymorphonuclear leukocytes (PMNL) by murine monoclonal antibody NMS-1. *Free radical research communications* 2: 359-368.
83. Foster, L. J., C. L. De Hoog, and M. Mann. 2003. Unbiased quantitative proteomics of lipid rafts reveals high specificity for signaling factors. *Proceedings of the National Academy of Sciences of the United States of America* 100: 5813-5818.
84. de Gassart, A., C. Geminard, B. Fevrier, G. Raposo, and M. Vidal. 2003. Lipid raft-associated protein sorting in exosomes. *Blood* 102: 4336-4344.
85. Livak, K. J., and T. D. Schmittgen. 2001. Analysis of relative gene expression data using real-time quantitative PCR and the 2(-Delta Delta C(T)) Method. *Methods* 25: 402-408.
86. Herrera, E., M. M. Lorenzo, R. Blasco, and S. N. Isaacs. 1998. Functional analysis of vaccinia virus B5R protein: essential role in virus envelopment is independent of a large portion of the extracellular domain. *Journal of virology* 72: 294-302.
87. Payne, L. G., and E. Norrby. 1976. Presence of haemagglutinin in the envelope of extracellular vaccinia virus particles. *The Journal of general virology* 32: 63-72.
88. Janes, P. W., S. C. Ley, and A. I. Magee. 1999. Aggregation of lipid rafts accompanies signaling via the T cell antigen receptor. *The Journal of cell biology* 147: 447-461.
89. Senkevich, T. G., B. M. Ward, and B. Moss. 2004. Vaccinia virus A28L gene encodes an essential protein component of the virion membrane with intramolecular disulfide bonds formed by the viral cytoplasmic redox pathway. *Journal of virology* 78: 2348-2356.

90. Chung, C. S., J. C. Hsiao, Y. S. Chang, and W. Chang. 1998. A27L protein mediates vaccinia virus interaction with cell surface heparan sulfate. *Journal of virology* 72: 1577-1585.
91. Chang, W., J. C. Hsiao, C. S. Chung, and C. H. Bair. 1995. Isolation of a monoclonal antibody which blocks vaccinia virus infection. *Journal of virology* 69: 517-522.
92. Altmann, S. E., J. C. Jones, S. Schultz-Cherry, and C. R. Brandt. 2009. Inhibition of Vaccinia virus entry by a broad spectrum antiviral peptide. *Virology* 388: 248-259.
93. Rajendran, L., J. Beckmann, A. Magenau, E. M. Boneberg, K. Gaus, A. Viola, B. Giebel, and H. Illges. 2009. Flotillins are involved in the polarization of primitive and mature hematopoietic cells. *PloS one* 4: e8290.
94. Gomez-Mouton, C., J. L. Abad, E. Mira, R. A. Lacalle, E. Gallardo, S. Jimenez-Baranda, I. Illa, A. Bernad, S. Manes, and A. C. Martinez. 2001. Segregation of leading-edge and uropod components into specific lipid rafts during T cell polarization. *Proceedings of the National Academy of Sciences of the United States of America* 98: 9642-9647.
95. Rossy, J., D. Schlicht, B. Engelhardt, and V. Niggli. 2009. Flotillins interact with PSGL-1 in neutrophils and, upon stimulation, rapidly organize into membrane domains subsequently accumulating in the uropod. *PloS one* 4: e5403.
96. Vicente-Manzanares, M., M. C. Montoya, M. Mellado, J. M. Frade, M. A. del Pozo, M. Nieto, M. O. de Landazuri, A. C. Martinez, and F. Sanchez-Madrid. 1998. The chemokine SDF-1alpha triggers a chemotactic response and induces cell polarization in human B lymphocytes. *European journal of immunology* 28: 2197-2207.
97. Sanchez-Madrid, F., and M. A. del Pozo. 1999. Leukocyte polarization in cell migration and immune interactions. *The EMBO journal* 18: 501-511.
98. Li, N., A. Mak, D. P. Richards, C. Naber, B. O. Keller, L. Li, and A. R. Shaw. 2003. Monocyte lipid rafts contain proteins implicated in vesicular trafficking and phagosome formation. *Proteomics* 3: 536-548.
99. Ancuta, P., K. Y. Liu, V. Misra, V. S. Wacleche, A. Gosselin, X. Zhou, and D. Gabuzda. 2009. Transcriptional profiling reveals developmental relationship and distinct biological functions of CD16+ and CD16- monocyte subsets. *BMC genomics* 10: 403.
100. Birzele, F., T. Fauti, H. Stahl, M. C. Lenter, E. Simon, D. Knebel, A. Weith, T. Hildebrandt, and D. Mennerich. Next-generation insights into regulatory T cells: expression profiling and FoxP3 occupancy in Human. *Nucleic Acids Res* 39: 7946-7960.
101. Izmailyan, R., J. C. Hsao, C. S. Chung, C. H. Chen, P. W. Hsu, C. L. Liao, and W. Chang. Integrin beta1 mediates vaccinia virus entry through activation of PI3K/Akt signaling. *Journal of virology* 86: 6677-6687.
102. Schroeder, N., C. S. Chung, C. H. Chen, C. L. Liao, and W. Chang. The lipid raft-associated protein CD98 is required for vaccinia virus endocytosis. *Journal of virology* 86: 4868-4882.

103. Raju, B., C. F. Tung, D. Cheng, N. Yousefzadeh, R. Condos, W. N. Rom, and D. B. Tse. 2001. In situ activation of helper T cells in the lung. *Infection and immunity* 69: 4790-4798.
104. Dominique, S., F. Bouchonnet, J. M. Smiejan, and A. J. Hance. 1990. Expression of surface antigens distinguishing "naive" and previously activated lymphocytes in bronchoalveolar lavage fluid. *Thorax* 45: 391-396.
105. Young, D. A., L. D. Lowe, and S. C. Clark. 1990. Comparison of the effects of IL-3, granulocyte-macrophage colony-stimulating factor, and macrophage colony-stimulating factor in supporting monocyte differentiation in culture. Analysis of macrophage antibody-dependent cellular cytotoxicity. *Journal of immunology* 145: 607-615.
106. Humlova, Z., M. Vokurka, M. Esteban, and Z. Melkova. 2002. Vaccinia virus induces apoptosis of infected macrophages. *The Journal of general virology* 83: 2821-2832.
107. Bzowska, M., K. Guzik, K. Barczyk, M. Ernst, H. D. Flad, and J. Pryjma. 2002. Increased IL-10 production during spontaneous apoptosis of monocytes. *European journal of immunology* 32: 2011-2020.
108. Mercer, J., and A. Helenius. 2008. Vaccinia virus uses macropinocytosis and apoptotic mimicry to enter host cells. *Science* 320: 531-535.
109. Jemielity, S., J. J. Wang, Y. K. Chan, A. A. Ahmed, W. Li, S. Monahan, X. Bu, M. Farzan, G. J. Freeman, D. T. Umetsu, R. H. Dekruyff, and H. Choe. 2013. TIM-family proteins promote infection of multiple enveloped viruses through virion-associated phosphatidylserine. *PLoS pathogens* 9: e1003232.
110. Rietdorf, J., A. Ploubidou, I. Reckmann, A. Holmstrom, F. Frischknecht, M. Zettl, T. Zimmermann, and M. Way. 2001. Kinesin-dependent movement on microtubules precedes actin-based motility of vaccinia virus. *Nature cell biology* 3: 992-1000.
111. Frischknecht, F., V. Moreau, S. Rottger, S. Gonfloni, I. Reckmann, G. Superti-Furga, and M. Way. 1999. Actin-based motility of vaccinia virus mimics receptor tyrosine kinase signalling. *Nature* 401: 926-929.
112. Reeves, P. M., B. Bommarius, S. Lebeis, S. McNulty, J. Christensen, A. Swimm, A. Chahroudi, R. Chavan, M. B. Feinberg, D. Veach, W. Bornmann, M. Sherman, and D. Kalman. 2005. Disabling poxvirus pathogenesis by inhibition of Abl-family tyrosine kinases. *Nature medicine* 11: 731-739.
113. Sanderson, C. M., M. Way, and G. L. Smith. 1998. Virus-induced cell motility. *Journal of virology* 72: 1235-1243.
114. Boulter, E. A., and G. Appleyard. 1973. Differences between extracellular and intracellular forms of poxvirus and their implications. *Progress in medical virology. Fortschritte der medizinischen Virusforschung. Progres en virologie medicale* 16: 86-108.
115. de Magalhaes, J. C., A. A. Andrade, P. N. Silva, L. P. Sousa, C. Ropert, P. C. Ferreira, E. G. Kroon, R. T. Gazzinelli, and C. A. Bonjardim. 2001. A mitogenic signal triggered at an early stage of vaccinia virus infection:

implication of MEK/ERK and protein kinase A in virus multiplication. *The Journal of biological chemistry* 276: 38353-38360.
116. Andrade, A. A., P. N. Silva, A. C. Pereira, L. P. De Sousa, P. C. Ferreira, R. T. Gazzinelli, E. G. Kroon, C. Ropert, and C. A. Bonjardim. 2004. The vaccinia virus-stimulated mitogen-activated protein kinase (MAPK) pathway is required for virus multiplication. *The Biochemical journal* 381: 437-446.
117. Izmailyan, R., J. C. Hsao, C. S. Chung, C. H. Chen, P. W. Hsu, C. L. Liao, and W. Chang. 2012. Integrin beta1 mediates vaccinia virus entry through activation of PI3K/Akt signaling. *Journal of virology* 86: 6677-6687.
118. Soares, J. A., F. G. Leite, L. G. Andrade, A. A. Torres, L. P. De Sousa, L. S. Barcelos, M. M. Teixeira, P. C. Ferreira, E. G. Kroon, T. Souto-Padron, and C. A. Bonjardim. 2009. Activation of the PI3K/Akt pathway early during vaccinia and cowpox virus infections is required for both host survival and viral replication. *Journal of virology* 83: 6883-6899.
119. Hu, W., W. Hofstetter, W. Guo, H. Li, A. Pataer, H. H. Peng, Z. S. Guo, D. L. Bartlett, A. Lin, S. G. Swisher, and B. Fang. 2008. JNK-deficiency enhanced oncolytic vaccinia virus replication and blocked activation of double-stranded RNA-dependent protein kinase. *Cancer gene therapy* 15: 616-624.
120. Pereira, A. C., F. G. Leite, B. S. Brasil, J. A. Soares-Martins, A. A. Torres, P. F. Pimenta, T. Souto-Padron, P. Traktman, P. C. Ferreira, E. G. Kroon, and C. A. Bonjardim. 2012. A vaccinia virus-driven interplay between the MKK4/7-JNK1/2 pathway and cytoskeleton reorganization. *Journal of virology* 86: 172-184.
121. Pereira, A. C., J. A. Soares-Martins, F. G. Leite, A. F. Da Cruz, A. A. Torres, T. Souto-Padron, E. G. Kroon, P. C. Ferreira, and C. A. Bonjardim. 2012. SP600125 inhibits Orthopoxviruses replication in a JNK1/2 - independent manner: Implication as a potential antipoxviral. *Antiviral research* 93: 69-77.
122. Gerdts, V., G. K. Mutwiri, S. K. Tikoo, and L. A. Babiuk. 2006. Mucosal delivery of vaccines in domestic animals. *Veterinary research* 37: 487-510.
123. Rerks-Ngarm, S., P. Pitisuttithum, S. Nitayaphan, J. Kaewkungwal, J. Chiu, R. Paris, N. Premsri, C. Namwat, M. de Souza, E. Adams, M. Benenson, S. Gurunathan, J. Tartaglia, J. G. McNeil, D. P. Francis, D. Stablein, D. L. Birx, S. Chunsuttiwat, C. Khamboonruang, P. Thongcharoen, M. L. Robb, N. L. Michael, P. Kunasol, and J. H. Kim. 2009. Vaccination with ALVAC and AIDSVAX to prevent HIV-1 infection in Thailand. *The New England journal of medicine* 361: 2209-2220.
124. Breitbach, C. J., J. Burke, D. Jonker, J. Stephenson, A. R. Haas, L. Q. Chow, J. Nieva, T. H. Hwang, A. Moon, R. Patt, A. Pelusio, F. Le Boeuf, J. Burns, L. Evgin, N. De Silva, S. Cvancic, T. Robertson, J. E. Je, Y. S. Lee, K. Parato, J. S. Diallo, A. Fenster, M. Daneshmand, J. C. Bell, and D. H. Kirn. 2011. Intravenous delivery of a multi-mechanistic cancer-targeted oncolytic poxvirus in humans. *Nature* 477: 99-102.

125. Breitbach, C. J., R. Arulanandam, N. De Silva, S. H. Thorne, R. Patt, M. Daneshmand, A. Moon, C. Ilkow, J. Burke, T. H. Hwang, J. Heo, M. Cho, H. Chen, F. A. Angarita, C. Addison, J. A. McCart, J. C. Bell, and D. H. Kirn. Oncolytic vaccinia virus disrupts tumor-associated vasculature in humans. *Cancer research* 73: 1265-1275.
126. Yu, Q., B. Jones, N. Hu, H. Chang, S. Ahmad, J. Liu, M. Parrington, and M. Ostrowski. 2006. Comparative analysis of tropism between canarypox (ALVAC) and vaccinia viruses reveals a more restricted and preferential tropism of ALVAC for human cells of the monocytic lineage. *Vaccine* 24: 6376-6391.
127. Sanchez-Puig, J. M., L. Sanchez, G. Roy, and R. Blasco. 2004. Susceptibility of different leukocyte cell types to Vaccinia virus infection. *Virology journal* 1: 10.
128. Grove, J., and M. Marsh. 2011. The cell biology of receptor-mediated virus entry. *The Journal of cell biology* 195: 1071-1082.
129. Folks, T. M., J. Justement, A. Kinter, S. Schnittman, J. Orenstein, G. Poli, and A. S. Fauci. 1988. Characterization of a promonocyte clone chronically infected with HIV and inducible by 13-phorbol-12-myristate acetate. *Journal of immunology* 140: 1117-1122.
130. Emiliani, S., W. Fischle, M. Ott, C. Van Lint, C. A. Amella, and E. Verdin. 1998. Mutations in the tat gene are responsible for human immunodeficiency virus type 1 postintegration latency in the U1 cell line. *Journal of virology* 72: 1666-1670.
131. Ranki, A., A. Lagerstedt, V. Ovod, E. Aavik, and K. J. Krohn. 1994. Expression kinetics and subcellular localization of HIV-1 regulatory proteins Nef, Tat and Rev in acutely and chronically infected lymphoid cell lines. *Archives of virology* 139: 365-378.
132. Lundquist, C. A., M. Tobiume, J. Zhou, D. Unutmaz, and C. Aiken. 2002. Nef-mediated downregulation of CD4 enhances human immunodeficiency virus type 1 replication in primary T lymphocytes. *Journal of virology* 76: 4625-4633.
133. Venzke, S., N. Michel, I. Allespach, O. T. Fackler, and O. T. Keppler. 2006. Expression of Nef downregulates CXCR4, the major coreceptor of human immunodeficiency virus, from the surfaces of target cells and thereby enhances resistance to superinfection. *Journal of virology* 80: 11141-11152.
134. Blagoveshchenskaya, A. D., L. Thomas, S. F. Feliciangeli, C. H. Hung, and G. Thomas. 2002. HIV-1 Nef downregulates MHC-I by a PACS-1- and PI3K-regulated ARF6 endocytic pathway. *Cell* 111: 853-866.
135. Chen, N., C. McCarthy, H. Drakesmith, D. Li, V. Cerundolo, A. J. McMichael, G. R. Screaton, and X. N. Xu. 2006. HIV-1 down-regulates the expression of CD1d via Nef. *European journal of immunology* 36: 278-286.
136. del Pozo, M. A., N. B. Alderson, W. B. Kiosses, H. H. Chiang, R. G. Anderson, and M. A. Schwartz. 2004. Integrins regulate Rac targeting by internalization of membrane domains. *Science* 303: 839-842.

137. Gauthier, N. C., O. M. Rossier, A. Mathur, J. C. Hone, and M. P. Sheetz. 2009. Plasma membrane area increases with spread area by exocytosis of a GPI-anchored protein compartment. *Molecular biology of the cell* 20: 3261-3272.
138. Balasubramanian, N., D. W. Scott, J. D. Castle, J. E. Casanova, and M. A. Schwartz. 2007. Arf6 and microtubules in adhesion-dependent trafficking of lipid rafts. *Nature cell biology* 9: 1381-1391.
139. del Pozo, M. A., N. Balasubramanian, N. B. Alderson, W. B. Kiosses, A. Grande-Garcia, R. G. Anderson, and M. A. Schwartz. 2005. Phospho-caveolin-1 mediates integrin-regulated membrane domain internalization. *Nature cell biology* 7: 901-908.
140. Laliberte, J. P., A. S. Weisberg, and B. Moss. 2011. The membrane fusion step of vaccinia virus entry is cooperatively mediated by multiple viral proteins and host cell components. *PLoS pathogens* 7: e1002446.
141. Stoorvogel, W., V. Oorschot, and H. J. Geuze. 1996. A novel class of clathrin-coated vesicles budding from endosomes. *The Journal of cell biology* 132: 21-33.
142. Maenpaa, A., J. Jaaskelainen, O. Carpen, M. Patarroyo, and T. Timonen. 1993. Expression of integrins and other adhesion molecules on NK cells; impact of IL-2 on short- and long-term cultures. *Int J Cancer* 53: 850-855.
143. Hu, N., R. Yu, C. Shikuma, B. Shiramizu, M. A. Ostrwoski, and Q. Yu. 2009. Role of cell signaling in poxvirus-mediated foreign gene expression in mammalian cells. *Vaccine* 27: 2994-3006.
144. Aggarwal, A., T. L. Iemma, I. Shih, T. P. Newsome, S. McAllery, A. L. Cunningham, and S. G. Turville. 2012. Mobilization of HIV spread by diaphanous 2 dependent filopodia in infected dendritic cells. *PLoS pathogens* 8: e1002762.
145. Soderholm, N., K. Vielfort, K. Hultenby, and H. Aro. 2011. Pathogenic Neisseria hitchhike on the uropod of human neutrophils. *PloS one* 6: e24353.
146. Byrd, D., T. Amet, N. Hu, J. Lan, S. Hu, and Q. Yu. 2013. Primary human leukocyte subsets differentially express vaccinia virus receptors enriched in lipid rafts. *Journal of virology* 87: 9301-9312.
147. Chan, W. M., E. C. Bartee, J. S. Moreb, K. Dower, J. H. Connor, and G. McFadden. 2013. Myxoma and vaccinia viruses bind differentially to human leukocytes. *Journal of virology* 87: 4445-4460.
148. Yu, Q., N. Hu, and M. Ostrowski. 2009. Poxvirus tropism for primary human leukocytes and hematopoietic cells. *Methods in molecular biology* 515: 309-328.
149. Finnin, M., J. A. Hamilton, and S. T. Moss. 1999. Characterization of a CSF-induced proliferating subpopulation of human peripheral blood monocytes by surface marker expression and cytokine production. *Journal of leukocyte biology* 66: 953-960.
150. Stanley, E. R., K. L. Berg, D. B. Einstein, P. S. Lee, F. J. Pixley, Y. Wang, and Y. G. Yeung. 1997. Biology and action of colony--stimulating factor-1. *Molecular reproduction and development* 46: 4-10.

151. Gabrilove, J. L., and A. Jakubowski. 1990. Hematopoietic growth factors: biology and clinical application. *Journal of the National Cancer Institute. Monographs*: 73-77.
152. Mantovani, A., S. K. Biswas, M. R. Galdiero, A. Sica, and M. Locati. 2013. Macrophage plasticity and polarization in tissue repair and remodelling. *The Journal of pathology* 229: 176-185.
153. Downing, J. R., C. W. Rettenmier, and C. J. Sherr. 1988. Ligand-induced tyrosine kinase activity of the colony-stimulating factor 1 receptor in a murine macrophage cell line. *Molecular and cellular biology* 8: 1795-1799.
154. Hamilton, J. A. 1997. CSF-1 signal transduction. *Journal of leukocyte biology* 62: 145-155.
155. Wang, Y., M. M. Zeigler, G. K. Lam, M. G. Hunter, T. D. Eubank, V. V. Khramtsov, S. Tridandapani, C. K. Sen, and C. B. Marsh. 2007. The role of the NADPH oxidase complex, p38 MAPK, and Akt in regulating human monocyte/macrophage survival. *American journal of respiratory cell and molecular biology* 36: 68-77.
156. Bhatt, N. Y., T. W. Kelley, V. V. Khramtsov, Y. Wang, G. K. Lam, T. L. Clanton, and C. B. Marsh. 2002. Macrophage-colony-stimulating factor-induced activation of extracellular-regulated kinase involves phosphatidylinositol 3-kinase and reactive oxygen species in human monocytes. *Journal of immunology* 169: 6427-6434.
157. Sengupta, A., W. K. Liu, Y. G. Yeung, D. C. Yeung, A. R. Frackelton, Jr., and E. R. Stanley. 1988. Identification and subcellular localization of proteins that are rapidly phosphorylated in tyrosine in response to colony-stimulating factor 1. *Proceedings of the National Academy of Sciences of the United States of America* 85: 8062-8066.
158. Platanias, L. C. 2003. Map kinase signaling pathways and hematologic malignancies. *Blood* 101: 4667-4679.
159. Cross, M., T. Nguyen, V. Bogdanoska, E. Reynolds, and J. A. Hamilton. 2005. A proteomics strategy for the enrichment of receptor-associated complexes. *Proteomics* 5: 4754-4763.
160. Guthridge, M. A., F. C. Stomski, D. Thomas, J. M. Woodcock, C. J. Bagley, M. C. Berndt, and A. F. Lopez. 1998. Mechanism of activation of the GM-CSF, IL-3, and IL-5 family of receptors. *Stem cells* 16: 301-313.
161. Bogoyevitch, M. A., and P. G. Arthur. 2008. Inhibitors of c-Jun N-terminal kinases: JuNK no more? *Biochimica et biophysica acta* 1784: 76-93.
162. Bain, J., L. Plater, M. Elliott, N. Shpiro, C. J. Hastie, H. McLauchlan, I. Klevernic, J. S. Arthur, D. R. Alessi, and P. Cohen. 2007. The selectivity of protein kinase inhibitors: a further update. *The Biochemical journal* 408: 297-315.
163. Rahbar, R., T. T. Murooka, and E. N. Fish. 2009. Role for CCR5 in dissemination of vaccinia virus in vivo. *Journal of virology* 83: 2226-2236.
164. Rahbar, R., T. T. Murooka, A. A. Hinek, C. L. Galligan, A. Sassano, C. Yu, K. Srivastava, L. C. Platanias, and E. N. Fish. 2006. Vaccinia virus activation of CCR5 invokes tyrosine phosphorylation signaling events that support virus replication. *Journal of virology* 80: 7245-7259.

165. Yanguez, E., A. Garcia-Culebras, A. Frau, C. Llompart, K. P. Knobeloch, S. Gutierrez-Erlandsson, A. Garcia-Sastre, M. Esteban, A. Nieto, and S. Guerra. 2013. ISG15 regulates peritoneal macrophages functionality against viral infection. *PLoS pathogens* 9: e1003632.
166. Perdiguero, B., and M. Esteban. 2009. The interferon system and vaccinia virus evasion mechanisms. *Journal of interferon & cytokine research : the official journal of the International Society for Interferon and Cytokine Research* 29: 581-598.
167. Martinez, F. O., S. Gordon, M. Locati, and A. Mantovani. 2006. Transcriptional profiling of the human monocyte-to-macrophage differentiation and polarization: new molecules and patterns of gene expression. *Journal of immunology* 177: 7303-7311.
168. Mann, B. A., J. H. Huang, P. Li, H. C. Chang, R. B. Slee, A. O'Sullivan, M. Anita, N. Yeh, M. J. Klemsz, R. R. Brutkiewicz, J. S. Blum, and M. H. Kaplan. 2008. Vaccinia virus blocks Stat1-dependent and Stat1-independent gene expression induced by type I and type II interferons. *Journal of interferon & cytokine research : the official journal of the International Society for Interferon and Cytokine Research* 28: 367-380.
169. Takeda, K., B. E. Clausen, T. Kaisho, T. Tsujimura, N. Terada, I. Forster, and S. Akira. 1999. Enhanced Th1 activity and development of chronic enterocolitis in mice devoid of Stat3 in macrophages and neutrophils. *Immunity* 10: 39-49.
170. Blasco, R., and B. Moss. 1992. Role of cell-associated enveloped vaccinia virus in cell-to-cell spread. *Journal of virology* 66: 4170-4179.
171. Payne, L. G. 1979. Identification of the vaccinia hemagglutinin polypeptide from a cell system yielding large amounts of extracellular enveloped virus. *Journal of virology* 31: 147-155.
172. Reeves, P. M., S. K. Smith, V. A. Olson, S. H. Thorne, W. Bornmann, I. K. Damon, and D. Kalman. 2011. Variola and monkeypox viruses utilize conserved mechanisms of virion motility and release that depend on abl and SRC family tyrosine kinases. *Journal of virology* 85: 21-31.
173. McNulty, S., K. Powell, C. Erneux, and D. Kalman. 2011. The host phosphoinositide 5-phosphatase SHIP2 regulates dissemination of vaccinia virus. *Journal of virology* 85: 7402-7410.
174. Scaplehorn, N., A. Holmstrom, V. Moreau, F. Frischknecht, I. Reckmann, and M. Way. 2002. Grb2 and Nck act cooperatively to promote actin-based motility of vaccinia virus. *Current biology : CB* 12: 740-745.
175. Payne, L. G., and K. Kristensson. 1982. The effect of cytochalasin D and monensin on enveloped vaccinia virus release. *Archives of virology* 74: 11-20.
176. Hollinshead, M., G. Rodger, H. Van Eijl, M. Law, R. Hollinshead, D. J. Vaux, and G. L. Smith. 2001. Vaccinia virus utilizes microtubules for movement to the cell surface. *The Journal of cell biology* 154: 389-402.
177. Sherer, N. M., M. J. Lehmann, L. F. Jimenez-Soto, C. Horensavitz, M. Pypaert, and W. Mothes. 2007. Retroviruses can establish filopodial

bridges for efficient cell-to-cell transmission. *Nature cell biology* 9: 310-315.
178. Jay, S. M., E. Skokos, F. Laiwalla, M. M. Krady, and T. R. Kyriakides. 2007. Foreign body giant cell formation is preceded by lamellipodia formation and can be attenuated by inhibition of Rac1 activation. *The American journal of pathology* 171: 632-640.
179. Gong, S. C., C. F. Lai, and M. Esteban. 1990. Vaccinia virus induces cell fusion at acid pH and this activity is mediated by the N-terminus of the 14-kDa virus envelope protein. *Virology* 178: 81-91.
180. Doms, R. W., R. Blumenthal, and B. Moss. 1990. Fusion of intra- and extracellular forms of vaccinia virus with the cell membrane. *Journal of virology* 64: 4884-4892.
181. Ichihashi, Y., and S. Dales. 1971. Biogenesis of poxviruses: interrelationship between hemagglutinin production and polykaryocytosis. *Virology* 46: 533-543.
182. Turner, P. C., and R. W. Moyer. 1992. An orthopoxvirus serpinlike gene controls the ability of infected cells to fuse. *Journal of virology* 66: 2076-2085.
183. Zhou, J., X. Y. Sun, G. J. Fernando, and I. H. Frazer. 1992. The vaccinia virus K2L gene encodes a serine protease inhibitor which inhibits cell-cell fusion. *Virology* 189: 678-686.
184. Pedersen, K., E. J. Snijder, S. Schleich, N. Roos, G. Griffiths, and J. K. Locker. 2000. Characterization of vaccinia virus intracellular cores: implications for viral uncoating and core structure. *Journal of virology* 74: 3525-3536.
185. Mallardo, M., E. Leithe, S. Schleich, N. Roos, L. Doglio, and J. Krijnse Locker. 2002. Relationship between vaccinia virus intracellular cores, early mRNAs, and DNA replication sites. *Journal of virology* 76: 5167-5183.
186. Rubins, K. H., L. E. Hensley, G. W. Bell, C. Wang, E. J. Lefkowitz, P. O. Brown, and D. A. Relman. 2008. Comparative analysis of viral gene expression programs during poxvirus infection: a transcriptional map of the vaccinia and monkeypox genomes. *PloS one* 3: e2628.
187. Klages, K., C. T. Mayer, K. Lahl, C. Loddenkemper, M. W. Teng, S. F. Ngiow, M. J. Smyth, A. Hamann, J. Huehn, and T. Sparwasser. 2010. Selective depletion of Foxp3+ regulatory T cells improves effective therapeutic vaccination against established melanoma. *Cancer research* 70: 7788-7799.
188. Teng, M. W., S. F. Ngiow, B. von Scheidt, N. McLaughlin, T. Sparwasser, and M. J. Smyth. 2010. Conditional regulatory T-cell depletion releases adaptive immunity preventing carcinogenesis and suppressing established tumor growth. *Cancer research* 70: 7800-7809.
189. Teng, M. W., J. B. Swann, B. von Scheidt, J. Sharkey, N. Zerafa, N. McLaughlin, T. Yamaguchi, S. Sakaguchi, P. K. Darcy, and M. J. Smyth. 2010. Multiple antitumor mechanisms downstream of prophylactic regulatory T-cell depletion. *Cancer research* 70: 2665-2674.

190. Hutchins, A. P., S. Poulain, and D. Miranda-Saavedra. 2012. Genome-wide analysis of STAT3 binding in vivo predicts effectors of the anti-inflammatory response in macrophages. *Blood* 119: e110-119.
191. Vora, S., I. Damon, V. Fulginiti, S. G. Weber, M. Kahana, S. L. Stein, S. I. Gerber, S. Garcia-Houchins, E. Lederman, D. Hruby, L. Collins, D. Scott, K. Thompson, J. V. Barson, R. Regnery, C. Hughes, R. S. Daum, Y. Li, H. Zhao, S. Smith, Z. Braden, K. Karem, V. Olson, W. Davidson, G. Trindade, T. Bolken, R. Jordan, D. Tien, and J. Marcinak. 2008. Severe eczema vaccinatum in a household contact of a smallpox vaccinee. *Clin Infect Dis* 46: 1555-1561.
192. Reed, J. L., D. E. Scott, and M. Bray. 2012. Eczema vaccinatum. *Clin Infect Dis* 54: 832-840.
193. Shirasawa, K., K. Akai, Y. Kawaguchi, S. Maeda, S. Nagahara, H. Toyoda, and T. Kurata. 1979. Widespread eczema vaccinatum acquired by contacts. A report of an autopsy case. *Acta pathologica japonica* 29: 435-455.
194. Vestergaard, C., H. Just, J. Baumgartner Nielsen, K. Thestrup-Pedersen, and M. Deleuran. 2004. Expression of CCR2 on monocytes and macrophages in chronically inflamed skin in atopic dermatitis and psoriasis. *Acta dermato-venereologica* 84: 353-358.
195. Kiekens, R. C., T. Thepen, A. J. Oosting, I. C. Bihari, J. G. Van De Winkel, C. A. Bruijnzeel-Koomen, and E. F. Knol. 2001. Heterogeneity within tissue-specific macrophage and dendritic cell populations during cutaneous inflammation in atopic dermatitis. *The British journal of dermatology* 145: 957-965.
196. Kasraie, S., and T. Werfel. 2013. Role of macrophages in the pathogenesis of atopic dermatitis. *Mediators of inflammation* 2013: 942375.
197. Oyoshi, M. K., N. Ramesh, and R. S. Geha. 2012. Vaccinia Ig ameliorates eczema vaccinatum in a murine model of atopic dermatitis. *The Journal of investigative dermatology* 132: 1299-1301.

CURRICULUM VITAE

Daniel James Byrd

Education

Western Kentucky University	B.S., Recombinant Genetics, B.S., Chemistry
	2004-2008
Indiana University	Ph.D., Microbiology and Immunology
	2008-2014

Honors, Awards, Fellowships

2008	Indiana University Fellowship Travel Grant
2011-2013	NIH T32 Infectious Disease Training Grant

Presentations

1. Yu Q., Amet T., **Byrd D.,** Lan J., "T-cell senescence and monocyte activation in HCV/HIV-1 coinfection". 31th Annual Meeting of the American Society for Virology. July 21 – 25, 2012, Madison, WI (*oral*).
2. **Byrd D.,** Hu N., Amet T., Hu S., Grantham A., Yu Q., "Vaccinia virus uses a common receptor to bind to and infect primary human monocytes, B cells and activated T cells". 31th Annual Meeting of the American Society for Virology. July 21 – 25, 2012, Madison, WI (*oral*).

3. Amet T., Grantham A., **Byrd D**., Hu S., Yu Q., "CD317/BST-2 restricts hepatitis C virus infection". 31th Annual Meeting of the American Society for Virology. July 21 – 25, 2012, Madison, WI (*oral*).
4. Amet T., Grantham A., **Byrd D**., Hu S., Yu Q., "Interferon-α-mediated suppression of hepatitis C virus production correlates with upregulation of BST-2/tetherin expression". The 7th International Symposium on Alcoholic Liver and Pancreatic Diseases and Cirrhosis (ISALPD/C). September 6-7, 2012, Beijing, China (*poster*)
5. Hu S., Ghabril M., Amet T., Hu., N., **Byrd D.**, Vuppalanchi R., Saxena R., Gupta S., Johnson R., Chalasani N., Yu Q., "HIV-1 coinfection alters intrahepatic inflammatory profiles in HCV-infected subjects". The 7th International Symposium on Alcoholic Liver and Pancreatic Diseases and Cirrhosis (ISALPD/C). September 6-7, 2012, Beijing, China (*poster*) *(#Dr. Yu received a travel grant from this meeting organizer)*.
6. Lan J., **Byrd D**., Amet T., Yu Q., "Protease inhibitor-containing antiretroviral therapy is comparable with provirus stimulants to purge latently HIV-1-infected cells". Strategies for an HIV Cure Conference. November 20 - 30, 2012, Washington DC (*poster*).
7. Meng Z., Amet T., **Byrd D**., Lan J., Yu Q., "Antiretrovial therapy changes circulating autoantibody profiles in patients chronically infected with human immunodeficiency virus 1". 100th Annual Meeting of the American Association of Immunologists. May 3 – 7, 2013, Honolulu, HI (*poster*).
8. Lan J., **Byrd D.,** Amet T., Yu Q., "A combination of provirus stimulants with

blockers of regulators of complement activation represents a novel approach for purging HIV-1 latently infected cells". 100th Annual Meeting of the American Association of Immunologists. May 3 – 7, 2013, Honolulu, HI (*poster*).

9. **Byrd D.,** Amet T., Hu S., Lan J., Yu Q., "Vaccinia virus preferentially binds to protein enriched in lipid rafts on the surface of leukocytes". 100th Annual Meeting of the American Association of Immunologists. May 3 – 7, 2013, Honolulu, HI (*poster*).
10. Lan J., **Byrd D**., Amet T., Meng Z., Yu Q. Romidespin effectively reactivates proviruses in latently HIV-1-infected cells. 32th Annual Meeting of the American Society for Virology. July 20 - 24, 2013, University Park, PA (*poster*).
11. Amet T., Meng Z., **Byrd D.**, Lan J., Yu Q. HIV-1 virions incorporate host proteins into viral envelope from the surface of infected cells. 32th Annual Meeting of the American Society for Virology. July 20 - 24, 2013, University Park, PA (*poster*).
12. Yu Q., Ghabril M., Meng M., Hu S., Amet T., **Byrd D**., Lan J., Chalasani N. Intrahepatic CXCR3-associated chemokines and circulating autoantibody profiles in patients chronically infected with hepatitis C virus. International Congress of Immunology. 2013, August 22 – 27, Milan, Italy (*poster*).

Publications

1. Hu W., Yu Q., Hu N., **Byrd D**., Shikuma C., Shiramizu B., Halperin JA., Qin X. A high-affinity inhibitor of human CD59 enhances antibody-dependent complement-mediated virolysis of HIV-1. *The Journal of Immunology*, 2010; 184: 359–368 PMID: 19955519
2. Chi X., Amet T., **Byrd D.**, Shah K., Hu S, Grantham A., Duan J., Yu Q. Direct effects of HIV-1 Tat protein on excitability and survival of primary dorsal root ganglion neurons: possible contribution to HIV-1-associated pain. *PLoS ONE*, 2011, 6(9): e24412. PMCID: PMC3166319
3. Amet T., Ghabril M., Chalasani N., **Byrd D.**, Hu N., Grantham A., Liu Z., Qin X., He JJ., Yu Q. CD59 incorporation protects hepatitis C virus from complement-mediated destruction. *HEPATOLOGY*, 2012, 55 (2): 354-363. PMID: 21932413.
4. Yu Q., Chow E. McCaw SE. Hu N., **Byrd D.**, Amet T., Hu S., Ostrowski M., Gray-Owen S. Association of *Neisseria gonorrhoeae* Opa_{CEA} proteins with dendritic cells decreases HIV-1 $CD8^+$ T cell memory responses. *PLoS ONE* 2013, 8(2):e56705.doi:10.1371/journal.pone.0056705
5. **Byrd D.**, Amet T., Hu N., Lan J., Hu S., Yu Q. Primary human leukocyte subsets differentially express vaccinia virus receptors enriched in lipid rafts. *The Journal of Virology*, 2013, 87(16):9301. DOI: 10.1128/JVI.01545-13.

6. Amet T., **Byrd D.**, Hu N., Sun Q., Li F., Zhao Y., Hu S., Grantham A., Yu Q. BST-2 expression in human hepatocytes is inducible by all three types of interferons and restricts production of hepatitis C Virus. *Current Molecular Medicine,* 2014, 14: 1-13.
7. Hu S., Ghabril M., Amet T., Hu N., **Byrd D.**, Vuppalanchi R., Saxena R., Desai M., Lan J, Johnson R., Gupta S., Chalasani N., Yu Q. HIV-1 coinfection profoundly alters intrahepatic chemokine but not inflammatory cytokine profiles in HCV-infected subjects. *PLoS ONE*, 2014, 9(2): e86964. doi:10.1371/journal.pone.0086964
8. Lan J., **Byrd D.**, Hu N., Amet T., Shepherd N., Desai M., Yang K., Gupta S., Yu Q. Provirus activation plus CD59 blockage triggers antibody-dependent complement-mediated lysis of latently HIV-1-infected cells. *The Journal of Immunology*, in revision.
9. **Byrd D.**, Shepherd N., Lan J., Hu N., Amet T., Yang K., Desai M., Yu Q., Primary human macrophages serve as vehicles for vaccinia virus replication and dissemination. *The Journal of Virology*, 2013, doi: 10.1128/JVI.03726-13

Book (2012)

Book Title: Apoptosis

Book Editor: Justine Rudner, Ph.D**.**

Chapter Authors: Desai M., Hu N., **Byrd D.**, Yu Q.

Publisher: InTech (www.intechopen.com)